

**Study of Z_N symmetry in $SU(N)$ gauge theories
in the presence of matter fields**

By
SABIAR SHAIKH
PHYS10201604001

The Institute of Mathematical Sciences, Chennai

A thesis submitted to the
Board of Studies in Physical Sciences
In partial fulfilment of requirements
For the Degree of
DOCTOR OF PHILOSOPHY
of
HOMI BHABHA NATIONAL INSTITUTE



September, 2022

Homi Bhabha National Institute

Recommendations of the Viva Voce Board

As members of the Viva Voce Board, we certify that we have read the dissertation prepared by Sabiar Shaikh entitled “Study of Z_N symmetry in $SU(N)$ gauge theories in the presence of matter fields” and recommend that it may be accepted as fulfilling the dissertation requirement for the Degree of Doctor of Philosophy.



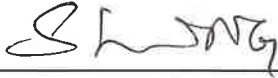
Date: 17.04.2023

Chair - V. Ravindran



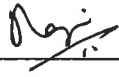
Date: 17.04.2023

Guide/Convener - Sanatan Digal



Date: 17.04.2023

Member 1 - Shrihari Gopalakrishna



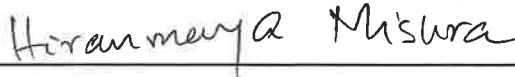
Date: 17/4/2023

Member 2 - Rajesh Ravindran



Date: 17/04/2023

Member 3 - Syed R. Hassan



Date: 17.04.2023

External Examiner - Hiranmaya Mishra

Final approval and acceptance of this dissertation is contingent upon the candidate's submission of the final copies of the dissertation to HBNI.

I hereby certify that I have read this dissertation prepared under my direction and recommend that it may be accepted as fulfilling the dissertation requirement.

Date: 17.04.2023

Place: IMSc, Chennai



Guide - Sanatan Digal

STATEMENT BY AUTHOR

This dissertation has been submitted in partial fulfilment of requirements for an advanced degree at Homi Bhabha National Institute (HBNI) and is deposited in the Library to be made available to borrowers under rules of the HBNI.

Brief quotations from this dissertation are allowable without special permission, provided that accurate acknowledgement of source is made. Requests for permission for extended quotation from or reproduction of this manuscript in whole or in part may be granted by the Competent Authority of HBNI when in his or her judgment the proposed use of the material is in the interests of scholarship. In all other instances, however, permission must be obtained from the author.

Sabiar Shaikh

Sabiar Shaikh

DECLARATION

I, hereby declare that the investigation presented in the thesis has been carried out by me.
The work is original and has not been submitted earlier as a whole or in part for a degree
/ diploma at this or any other Institution / University.

Sabiar Shaikh
Sabiar Shaikh

List of Publications arising from the thesis

Journal

1. “ Z_N symmetry in $SU(N)$ gauge theories”,
Minati Biswal, Sanatan Digal, Vinod Mamale, Sabiar Shaikh,
Int. J. Mod. Phys. A **37** (2022) no.09, 2250047,
[arXiv:2102.12935 \[hep-lat\]](#).
2. “Confinement-deconfinement transition and Z_2 symmetry in Z_2 +Higgs theory”,
Minati Biswal, Sanatan Digal, Vinod Mamale, Sabiar Shaikh,
Mod. Phys. Lett. A **36** (2021) no.30, 2150218,
[arXiv:2102.11091 \[hep-lat\]](#).

Manuscript under communication

1. “The Confinement-deconfinement transition in $SU(3)$ +Higgs theory”,
Sanatan Digal, Vinod Mamale, Sabiar Shaikh,
[arXiv:2211.06586 \[hep-lat\]](#).

Conference Proceedings

1. “ Z_2 symmetry in Z_2 +Higgs theory”,
Minati Biswal, Sanatan Digal, Vinod Mamale, Sabiar Shaikh,
PoS LATTICE 2021, vol 396 (2022), 505.

Sabiar Shaikh

Sabiar Shaikh

Conferences and workshops attended

1. “A Virtual Tribute to Quark Confinement and the Hadron Spectrum 2021” organized by University of Stavanger, Stavanger, Norway from 2-6 August 2021.
2. “The 38th International Symposium on Lattice Field Theory” conducted by Massachusetts Institute of Technology, Cambridge, United States from 26-30 July 2021.
3. “The 9th Annual Conference (online) on Large Hadron Collider Physics” by CERN from 7-12 June 2021.
4. “The 19th International Conference on Strangeness in Quark Matter” conducted by Brookhaven National Laboratory, New York, United States from 17-22 May 2021.
5. “24th DAE BRNS High Energy Physics Symposium” organized by National Institute of Science Education and Research, Bhubaneswar, India from 14-18 December 2020.
6. “32nd International (online) Workshop on High Energy Physics (Hot Problems of Strong Interactions)” from 9-13 November 2020.
7. “Extreme Non-equilibrium QCD” at International Centre for Theoretical Sciences, Bengaluru, India from 5-9 October 2020.
8. “Virtual Meeting on Compact Stars and QCD” at International Centre for Theoretical Sciences, Bengaluru, India from 17-21 August 2020.
9. “16th Workshop on High Energy Physics Phenomenology” held at Indian Institute of Technology, Guwahati, India from 1-10 December 2019.

10. “1st IMSc Discussion Meeting on Extreme QCD matter” held at The Institute of Mathematical Sciences, Chennai, India from 16-21 September 2019.

11. “23rd DAE BRNS High Energy Physics Symposium” held at Indian Institute of Technology, Madras, India from 10-14 December 2018.

Presentation and poster

1. “*Confinement-deconfinement transition and Z_2 symmetry in Z_2 +Higgs theory*”, talk given at “65th DAE-BRNS Symposium on Nuclear Physics ” at Bhabha Atomic Research Center, Mumbai, India from 1-5 December 2021.
2. “ *Z_N symmetry in $SU(N)$ gauge theories*”, talk given at “Anomalies 2021” at Indian Institute of Technology, Hyderabad, India on 10-12 November 2021.
3. “ *Z_N symmetry in $SU(N)$ gauge theories*”, talk given at “The XXV International Scientific Conference of Young Scientists and Specialists (AYSS-2021)” at Joint Institute for Nuclear Research, Dubna, Russia on 11-15 October 2021.
4. “*Confinement-deconfinement transition and Z_2 symmetry in Z_2 +Higgs theory*”, talk given at “The 38th International Symposium on Lattice Field Theory” at Massachusetts Institute of Technology, Cambridge, United States on 26-30 July 2021.

To My Parents

ACKNOWLEDGEMENTS

First of all, I would like to express my deepest gratitude to my supervisor Prof. Sanatan Digal for his guidance, support, and encouragement throughout the rigorous journey of my Ph.D. I am grateful to him for considering my mistakes and helping me to overcome my limitations. He always motivated me in my research work for the last couple of years. I thank him for being so friendly and kind to me.

I would also like to thank my other doctoral committee members Prof. V. Ravindran, Prof. Shrihari Gopalakrishna, Prof. Rajesh Ravindran, and Prof. Syed R. Hassan for their support, guidance, and necessary help.

I wish to thank my collaborators Dr. Minati Biswal and Vinod Mamale for their intense collaborations and discussions. I am especially thankful to Minati for the wonderful collaboration, and illuminating discussions. I am grateful to her for all the necessary help I have received several times. I am also thankful to Vinod for being an amazing friendly collaborator.

It has been a great pleasure for me to discuss physics with Dr. Shreyansh and I have learned a lot from him as well. I thank Sumit for being an amazing friend and it's fun to discuss physics with him. I would also like to thank Dr. Mridupawan and Dr. Saumia for their useful suggestions and discussions.

I am extremely thankful to the IMSc office staff, for being so kind and helpful. I am also thankful to the library staff, canteen staff, cleaning staff, security guards, electrician staff, and computer staff for being so helpful and friendly. I wish to thank G. Srinivasan and Mr. Mangalapandi for helping me out with any issues related to the system and cluster.

I am grateful to have had an amazing bunch of friends during all these years. I wish to thank my officemate Atanu da, Arnab da, Rupam da, Tanmoy, and Vinod for the amazing discussion and fun we had together. It has been a wonderful memory to spend a few years with these amazing friends.

I would like to thank Sujoy, Ramit, Soumya, Gourav, Semanti, Subhankar, Ujjal, Ajjath,

Pritam, Arpan, Shabbir, Rakesh, Amir, Sumit and many more for all the enlighting conversations, outings, trips, and the beautiful memories.

Finally, I convey my heartfelt gratitude to my parents and sisters for their continual and unconditional love, support, encouragement, patience, and sacrifices, without them it would not have been possible for me to pursue and sustain this long journey of Ph.D.

Abstract

In this thesis, we study the confinement-deconfinement (CD) transition and the Z_3 symmetry in SU(3)+Higgs theory in 3 + 1 dimensions, using non-perturbative lattice Monte Carlo simulations. In particular, we study the cut-off effects on the CD transition and the Z_3 symmetry by varying the number of lattice sites in the temporal direction (N_τ). The Higgs field is considered to be in the fundamental representation. It is found that for $N_\tau = 2$ the CD transition is a continuous, along with a large explicit breaking of the Z_3 symmetry. With the increase in N_τ the strength of the CD transition increases, while the strength of explicit breaking decreases. Our results suggest that the explicit breaking is vanishingly small in the $N_\tau \rightarrow \infty$ limit. In this limit, the CD transition is first order as that in the case of pure SU(3) gauge theory. Similar results were also observed in SU(2)+Higgs. These results are rather surprising since as long as the masses of the matter fields are finite, the Euclidean action breaks the Z_3 symmetry.

To understand the realization of Z_N symmetry in the $N_\tau \rightarrow \infty$, we consider a one-dimensional gauged chain of matter fields. As in SU(N) gauge theories with matter fields in the fundamental representation in 3 + 1 dimensions, the action breaks Z_N symmetry explicitly. The analytic calculation of the partition function shows that the Z_N symmetry is realized in the continuum limit for a gauged chain of bosonic matter fields. To further probe the reason behind the realisation of Z_N symmetry we consider a simple model of Z_2 +Higgs theory in both 3+1 and 0+1 dimensions where it is shown that the density of states (DoS) exhibits Z_2 symmetry. As the DoS dominate the thermodynamics over the Boltzmann factor in the partition function, for a large number of temporal lattice sites and in the Higgs symmetric phase, the Z_2 symmetry is realized.

Contents

Synopsis	1
1 Motivation and Introduction	25
2 Z_N symmetry in $SU(N)$ gauge theories	33
2.1 Z_N symmetry in pure $SU(N)$ gauge theories	33
2.2 Z_N symmetry in $SU(N)$ gauge theories in the presence of matter fields in the fundamental representation	36
2.2.1 Z_N symmetry in $SU(N)$ gauge theories with Higgs	36
2.2.2 Z_N symmetry in $SU(N)$ gauge theories with fermion	38
3 Confinement deconfinement transition and Z_3 symmetry in $SU(3)$+Higgs theory	41
3.1 Numerical simulations of the CD transition and the Z_3 symmetry	42
3.2 The CD transition vs N_τ	51
3.3 Z_3 symmetry vs N_τ	57
4 Gauged 1 – d chain of $SU(N)$ in presence of matter fields	65

4.1	Gauged 1 – d chain of $SU(N)$ – Higgs	66
4.2	Gauged 1 – d chain of $SU(N)$ – fermion	72
5	Study of Z_2 symmetry, CD transition and density of states in Z_2+Higgs theory	83
5.1	Z_2 symmetry in Z_2 +Higgs gauge theory	84
5.2	Numerical technique and Monte Carlo simulation results	86
5.3	The partition function and density of states in 0 + 1 dimensions	96
6	Conclusion	103

Synopsis

Motivation and Introduction

At high temperatures, hadrons melt into quark-gluon plasma (QGP). Theoretical studies in Quantum Chromodynamics (QCD) show that this melting proceeds via a transition known as the confinement-deconfinement (CD) transition. In pure $SU(N)$ gauge theories, the CD transition is described by the center $Z_N \in SU(N)$ symmetry and the Polyakov loop (L) which plays the role of an order parameter. This symmetry is spontaneously broken at high temperatures for pure $SU(N)$ gauge theories. In the confined phase the Polyakov loop average vanishes which leads to the Z_N symmetric phase. In the deconfined phase, the Polyakov loop acquires a non-zero thermal average value which leads to the spontaneous symmetry breaking (SSB) of the Z_N symmetry, hence it plays the role of an order parameter [1, 2] for the confinement-deconfinement (CD) transition. The Z_N symmetry of pure $SU(N)$ gauge theory is spoiled when matter fields are included. Since the matter fields satisfy either periodic (boson) or anti-periodic (fermion) boundary conditions so the gauge transformations which do not satisfy the required boundary condition in temporal directions can not act on the matter fields [3–5]. These may act only on the gauge fields but in the process, the action does not remain invariant. There are several studies of explicit breaking of Z_N symmetry due to matter fields over the years. Perturbative loop calculations of the Polyakov loop effective potential show that this symmetry is explicitly broken by matter fields in the fundamental representation and this explicit breaking

increases with a decrease in mass of the matter fields [3, 6]. Similarly, non-perturbative computations find that the strength of explicit breaking vanishes only in the limit of infinitely massive matter fields [7]. There are some recent non-perturbative Monte Carlo simulations of SU(2)+Higgs theory, that shows the strength of Z_2 explicit breaking depends on the Higgs condensate [5]. These studies find that the CD transition exhibits critical behaviour in the Higgs symmetric phase for a large number of temporal sites (N_τ). The distributions of the Polyakov loop are found to be Z_2 symmetric, albeit within statistical errors, suggesting the realisation of Z_2 symmetry in the Higgs symmetric phase.

We plan to investigate the effect of matter fields on Z_3 symmetry. For this, we consider SU(3)+Higgs theory in 3+1 dimensions. With the Higgs field in the fundamental representation, the Z_3 symmetry is explicitly broken. Our numerical results show that the CD transition becomes first order in the Higgs symmetric phase at large N_τ . The distribution of the phase of the Polyakov loop exhibits Z_3 symmetry which indicates the realization of Z_3 symmetry in the Higgs symmetric phase. It is highly desirable to obtain such results through analytic calculation, where the partition function exhibits the Z_N symmetry even though the action breaks it explicitly. However, the exact calculation of the partition function in 3 + 1 dimensional theories is extremely difficult. Therefore, we consider a one-dimensional chain of fermionic/bosonic matter fields which are in the fundamental representation of the SU(N) gauge group. From these calculations, the free energy for the Polyakov loop is obtained. The results show that, in the case of the Higgs (bosonic) field, the explicit breaking of Z_N rapidly decreases with the number of temporal sites (N_τ) vanishing in the “continuum” limit ($N_\tau \rightarrow \infty$). In the case of fermions, the explicit breaking initially decreases rapidly with N_τ but seems to approach a limiting value which is non-zero. To understand the reason behind the realization of Z_N symmetry we have numerically studied the simple model of Z_2 + Higgs theory [8, 9] in both 3+1 and 0+1 dimensions. The effects of the Higgs field on both the CD transition and Z_2 symmetry are studied in lattice Z_2 +Higgs theory in 3 + 1 dimensional space. It is observed from our 3 + 1 dimensional simulation results that the Z_2 symmetry breaks explicitly in presence

of matter fields for small N_τ . But it is realized at a large N_τ limit in the Higgs symmetric phase. Our 0 + 1 dimensional results suggest that with the increase in N_τ the density of states (DoS) dominates the thermodynamics. Further, since the DoS turns out to be Z_2 symmetric, thus the partition function exhibits the Z_2 symmetry. The free energy calculation in one dimension also suggests that the free energy difference between the two Polyakov loop sectors vanishes at a large N_τ limit, which leads to the realization of Z_2 symmetry due to the dominance of the density of states.

Z_N symmetry in $SU(N)$ gauge theories

In this section, we discuss the effect of matter fields on the Z_N symmetry in $SU(N)$ gauge theories. The total partition function of $SU(N)$ gauge theory of fermions and bosons in 3 + 1 dimensional Euclidean space is given by

$$\mathcal{Z} = \int [DA][D\Phi][D\Phi^\dagger][D\Psi][D\bar{\Psi}] \text{Exp}[-S], \quad (1)$$

where the Euclidean action is

$$S = \int_V d^3x \int_0^\beta d\tau \left[\frac{1}{2} \left\{ \text{Tr} (F^{\mu\nu} F_{\mu\nu}) + |D_\mu \Phi|^2 + m_b^2 \Phi^\dagger \Phi \right\} + \bar{\Psi} (\not{D} + m_f) \Psi \right], \quad (2)$$

$$F_{\mu\nu} = \partial_\mu A_\nu - \partial_\nu A_\mu + g[A_\mu, A_\nu], \quad D_\mu \Phi = (\partial_\mu + igA_\mu)\Phi, \quad \not{D}\Psi = (\not{\partial} + ig\not{A})\Psi.$$

Here A_μ , Φ and Ψ are the gauge, Higgs and the fermion fields respectively. Φ and Ψ are in the fundamental representation. g is the gauge coupling strength, $m_b(m_f)$ is the mass of $\Phi(\Psi)$ fields and β is the inverse of temperature, i.e. $\beta = 1/T$. At finite temperature, the gauge fields are required to be periodic and all gauge transformations are allowed as long as they preserve the periodicity of the gauge fields in the temporal direction, i.e. $A_\mu(\tau = 0) = A_\mu(\tau = \beta)$.

The matter fields on the other hand satisfy the following temporal boundary conditions:

$$\Phi(\tau = 0) = \Phi(\tau = \beta), \quad \Psi(\tau = 0) = -\Psi(\tau = \beta). \quad (3)$$

These fields transform under a gauge transformation $V \in \text{SU}(N)$ as

$$A_\mu \longrightarrow VA_\mu V^{-1} + \frac{1}{g}(\partial_\mu V)V^{-1}, \quad \Phi \longrightarrow V\Phi, \quad \Psi \longrightarrow V\Psi. \quad (4)$$

In the absence of the matter fields, one can consider V which is not necessarily periodic but satisfies

$$V(\tau = 0) = zV(\tau = \beta), \quad (5)$$

where z is an element of the center Z_N of $\text{SU}(N)$. Though the pure gauge action is invariant under this transformation, the Polyakov loop,

$$L(\vec{x}) = \frac{1}{N} \text{Tr} \left[\text{P} \left\{ \text{Exp} \left(-ig \int_0^\beta A_0 d\tau \right) \right\} \right], \quad (6)$$

transforms as $L \rightarrow zL$. In the deconfined phase, the Polyakov loop acquires some non-zero thermal average value and the Z_N symmetry is broken spontaneously. As a result, there are N degenerate states in the deconfined phase characterized by the elements of Z_N .

In the presence of the matter fields (Φ, Ψ) , the boundary conditions in Eq. 3, restrict the gauge transformations to be periodic in τ . Non-periodic gauge transformations can not act on the matter fields, hence two configurations of the Polyakov loop, $L(\vec{x})$ and $zL(\vec{x})$, do not necessarily contribute equally to the partition function in Eq. 1. Hence the Z_N symmetry is explicitly broken. In presence of Higgs as matter fields, One can consider these gauge transformations with $z \neq \mathbb{1}$ but acting only on the gauge fields. But any gauge transformations acting only on the gauge fields will likely result in a change in the action. For example we make a transformation, $(A_\mu, \Phi) \rightarrow (A'_\mu, \Phi)$, where A'_μ is gauge transform of A_μ with $V(\tau = 0) = zV(\tau = \beta)$. The action for two configurations (A_μ, Φ) and (A'_μ, Φ) will be different, i.e. $S(A'_\mu, \Phi) > S(A_\mu, \Phi)$. Now keeping A'_μ fixed we can vary Φ . It may

be possible that there exists some Φ' for which $S(A'_\mu, \Phi') = S(A_\mu, \Phi)$. This then can lead to the realization of the Z_N symmetry [5].

CD transition and Z_3 symmetry in SU(3)+Higgs theory

In this section, we study the effect of the Higgs field on the CD transition and Z_3 symmetry in SU(3)+Higgs theory. To simplify the problem we consider vanishing bare Higgs mass (m) and Higgs quartic coupling (λ). The total discretized lattice action for SU(3)+Higgs theory in 3+1 dimensional space ($N_s^3 \times N_\tau$) can be written as [5],

$$S = \beta_g \sum_P \text{Tr} \left(1 - \frac{U_P + U_P^\dagger}{2} \right) - \frac{1}{8} \sum_{n,\mu} \text{Re} (\Phi_{n+\hat{\mu}}^\dagger U_{n,\mu} \Phi_n) + \frac{1}{2} \sum_n (\Phi_n^\dagger \Phi_n). \quad (7)$$

The Higgs field Φ_n is defined only on the lattice site n and $U_{n,\hat{\mu}}$ is the gauge link which connects site n and $n + \hat{\mu}$. Here $n = (n_1, n_2, n_3, n_4)$ represents a point on the lattice with $1 \leq n_1, n_2, n_3 \leq N_s$ and $1 \leq n_4 \leq N_\tau$. β_g is the gauge interaction strength and $\kappa = (m^2 + 8)^{-1}$ is gauge-Higgs interaction coupling. For vanishing bare Higgs mass, the coupling $\kappa = 0.125$. The plaquette U_P is the path ordered product of links $U_{n,\mu}$ along an elementary square. The first term in Eq. 7, is the pure gauge action and the second term is the gauge-Higgs interaction. On the discrete lattice, the Polyakov loop is defined as the path order product of gauge links along the temporal direction, i.e.

$$L(\vec{n}) = \prod_{n_4=1}^{N_\tau} U_{(\vec{n}, n_4), \hat{4}}. \quad (8)$$

Here $\vec{n} \equiv n_1, n_2, n_3$ are the spatial and n_4 is the temporal coordinates. Under the non-periodic gauge transformations, the Polyakov loop transforms as

$$L(\vec{n}) \rightarrow zL(\vec{n}). \quad (9)$$

The pure gauge part of the action is always invariant under the gauge transformation. But as mentioned above, the Φ fields cannot be transformed under nonperiodic gauge transformations, so the second term does not remain invariant under this transformation and the Z_N symmetry is broken explicitly. The above action is used in the Monte Carlo simulation and a sequence of statistically independent configurations of $(U_{n,\mu}, \Phi_n)$ are generated. A new configuration is generated by repeatedly updating an arbitrary initial configuration using standard heat bath algorithms [10, 11]. Initially pure gauge simulations for SU(3) are performed to understand the nature of CD transition for $N_\tau = 2$ and 4. Then the Higgs fields Φ are added and the CD transition is studied again to observe the effects of matter fields on the transition. From the Monte Carlo simulations for the pure SU(3) study, the distribution of the Polyakov loop clearly shows there is a coexistence of both confined and deconfined phases at $N_\tau = 2$. The coexistence of the confined and deconfined phases and the jump in the order parameter L provide evidence that the transition is of the first order and the Z_3 symmetry is broken spontaneously in the deconfined phase.

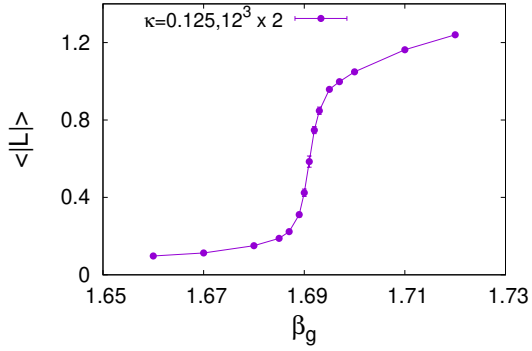


Figure 1: Average of L vs β_g for $N_\tau = 2$.

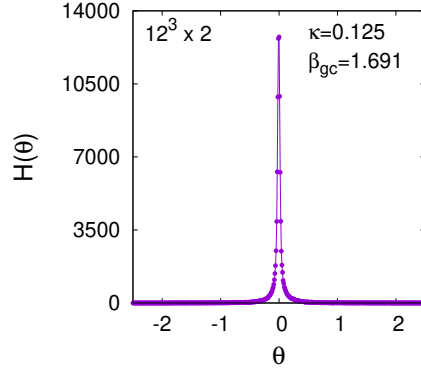


Figure 2: Distribution of phase of L .

Now to observe the effects of Higgs (Φ) as matter fields on the CD transition and the Z_3 symmetry, the Polyakov loop average is plotted with respect to coupling β_g for gauge-Higgs interaction strength $\kappa = 0.125$ in Fig. 1. The sharp variation of the Polyakov loop around $\beta_{gc} \sim 1.691$ for $N_\tau = 2$ only suggests a crossover for the CD transition. This change in the nature of the transition from first order to crossover suggests that the Z_3 symmetry is broken explicitly in presence of Higgs fields for $N_\tau = 2$. To study the Z_3

symmetry at $\kappa = 0.125$, we compute the distribution of phase of the Polyakov loop $H(\theta)$ on the complex plane. In Fig. 2 we show $H(\theta)$ vs θ for $\beta_g = 1.691$. It is clear that there is only one peak at $\theta = 0$. Even for different values of β_g , only one peak appears here which indicates that the Z_3 symmetry is broken explicitly.

To check how the nature of CD transition depends on N_τ at $\kappa = 0.125$, the distribution of the Polyakov loop are studied for $N_\tau = 4$ with different values of β_g . From Fig. 3, it is observed that at the critical point there is a coexistence of confined and deconfined phases which indicates the CD transition is first order at $N_\tau = 4$ even in the presence of Higgs. This change of the nature of transition from crossover for $N_\tau = 2$ to first order for $N_\tau = 4$ clearly suggests that the explicit breaking of Z_3 is reducing for higher N_τ for $\kappa = 0.125$. We show $H(\theta)$ vs θ for $\beta_g = 1.903$ in Fig. 4. For this value of β_g the distribution of

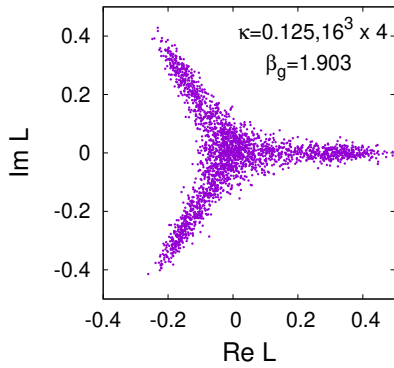


Figure 3: Distribution of L for $N_\tau = 4$.

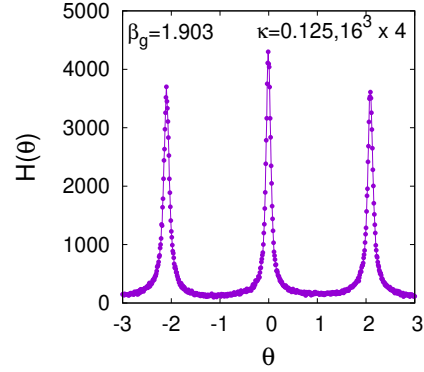


Figure 4: Distribution of phase of L .

the phase of the Polyakov loop shows almost three degenerate peaks. These higher N_τ studies show a monotonic decrease in the explicit breaking of Z_3 suggesting that it will be vanishingly small for $N_\tau \rightarrow \infty$.

Gauged 1 – d chain of $SU(N)$ in presence of matter fields

In this section, we calculate the free energy corresponding to the Polyakov loop analytically in a 0+1 dimensional model for $SU(N)$ gauge theories in presence of matter fields.

Gauged 1 – d chain of $SU(N)$ – Higgs

The $SU(N)$ +Higgs action in 3+1 Euclidean lattice is [5]

$$S = \beta_g \sum_p \left[1 - \frac{1}{2} \text{Tr}(U_p + U_p^\dagger) \right] - b \sum_{n,\mu} (\Phi_n^\dagger U_{n,\mu} \Phi_{n+\hat{\mu}} + h.c.) + a \sum_n \Phi_n^\dagger \Phi_n . \quad (10)$$

β_g is the gauge coupling constant, $a = \frac{1}{2}$ and the coupling $b = (m_b^2 + 8)^{-1}$, the Higgs mass m_b is expressed in lattice units [5]. The part of the action which breaks the Z_N symmetry explicitly is given by

$$S' = -b \sum_n (\Phi_n^\dagger U_{n,\hat{4}} \Phi_{n+\hat{4}} + h.c.) . \quad (11)$$

One can start from a continuum 1-dimensional toy model whose lattice discretization will result in the action in Eq. 11. The action for the one-dimensional chain is given by considering a fixed spatial site and including the last term of Eq. 10

$$S = a \sum_{i=1}^{N_\tau} \Phi_i^\dagger \Phi_i - b \sum_{i=1}^{N_\tau} (\Phi_i^\dagger U_i \Phi_{i+1} + h.c.) . \quad (12)$$

Here the Φ field does not interact with nearest neighbors in the spatial direction. Φ satisfies periodic boundary condition, i.e. $\Phi_{N_\tau+1} = \Phi_1$. The Polyakov loop is $L = \frac{1}{N} \text{Tr} \left(\prod_{i=1}^{N_\tau} U_i \right)$. We consider a gauge choice in which $U_i = \mathbb{1}$ for $i = 1, 2, \dots, N_\tau - 1$ and $U_{N_\tau} = U$. Note that this gauge choice preserves the Polyakov loop ($\text{Tr}(U)$). To derive the free energy $V(L)$,

only the Φ_i fields in the partition function \mathcal{Z}_L are to be integrated out

$$\mathcal{Z}_L = \int \prod_{i=1}^{N_\tau} d\Phi_i^\dagger d\Phi_i \text{Exp}[-S], \quad S = S_1 + S_2, \quad (13)$$

where

$$\begin{aligned} S_1 &= a\Phi_1^\dagger\Phi_1 - b(\Phi_{N_\tau}^\dagger U\Phi_1 + h.c.), \\ S_2 &= a \sum_{i=2}^{N_\tau} \Phi_i^\dagger\Phi_i - b \sum_{i=1}^{N_\tau-1} (\Phi_i^\dagger\Phi_{i+1} + h.c.). \end{aligned} \quad (14)$$

At first, the fields Φ_2 to $\Phi_{N_\tau-1}$ are integrated out sequentially using Gaussian integration, i.e.

$$\mathcal{Z} = \int \prod_{i=2}^{N_\tau-1} d\Phi_i^\dagger d\Phi_i \text{Exp}[-S_2], \quad (15)$$

$$\mathcal{Z}_L = \int d\Phi_1^\dagger d\Phi_1 d\Phi_{N_\tau}^\dagger d\Phi_{N_\tau} (\mathcal{Z} \times \text{Exp}[-S_1]). \quad (16)$$

The partition function after integrating out Φ_2 to $\Phi_{N_\tau-1}$ is

$$\mathcal{Z}_L = Q \int d\Phi_1^\dagger d\Phi_1 d\Phi_{N_\tau}^\dagger d\Phi_{N_\tau} \times \text{Exp} \left[-A_{N_\tau} \Phi_{N_\tau}^\dagger \Phi_{N_\tau} - C_{N_\tau} \Phi_1^\dagger \Phi_1 + (\Phi_{N_\tau}^\dagger (B_{N_\tau} \mathbb{1} + bU)\Phi_1 + h.c.) \right]. \quad (17)$$

$Q = \prod_{k=2}^{N_\tau} I_k^n$, $n = 2N$, n is number of components of the Φ field and $C_{N_\tau} = a - E_{N_\tau}$. The coefficients A_{N_τ} to E_{N_τ} can be obtained by recursion formula

$$I_{k+1} = \sqrt{\frac{\pi}{A_k}}, \quad A_{k+1} = a - \frac{b^2}{A_k}, \quad B_{k+1} = \frac{bB_k}{A_k}, \quad E_{k+1} = E_k + \frac{B_k^2}{A_k}, \quad (18)$$

with $I_2 = 1$, $A_2 = a$, $B_2 = b$ and $E_2 = 0$. After the integration of the remaining fields, Φ_1 and Φ_{N_τ} the partition function takes the form

$$\mathcal{Z}_L = Q \sqrt{\frac{\pi^8}{\text{Det}(M)}}. \quad (19)$$

Here the matrix M is $(4N \times 4N)$ given by

$$\begin{pmatrix} A_{N_\tau} & B_{N_\tau} + bU \\ B_{N_\tau} + bU^\dagger & C_{N_\tau} \end{pmatrix}.$$

We consider $N = 2$ and evaluate \mathcal{Z}_L explicitly for an arbitrary U

$$U = \alpha_0 + i\alpha \cdot \sigma, \quad \alpha = (\alpha_1, \alpha_2, \alpha_3), \quad (20)$$

where σ_i 's are the Pauli matrices. The determinant of M is

$$\text{Det } M = \left(B_{N_\tau}^2 - A_{N_\tau} C_{N_\tau} + 2bB_{N_\tau}\alpha_0 + b^2 \right)^4. \quad (21)$$

Z_2 rotation of the Polyakov loop ($L = \alpha_0$) changes $\alpha_0 \rightarrow -\alpha_0$. So in the determinant, the

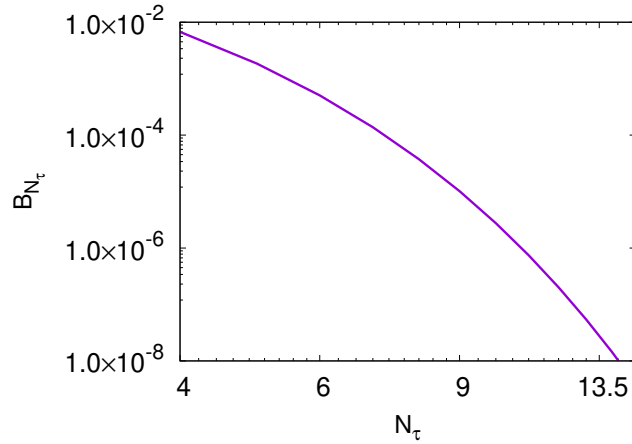


Figure 5: B_{N_τ} versus N_τ for Higgs mass parameter $m_b \propto 1/N_\tau$.

explicit symmetry breaking term of Z_2 is $2bB_{N_\tau}\alpha_0$. For a fixed temperature and physical Higgs mass parameter, it is observed that B_{N_τ} rapidly decreases, vanishing in the larger N_τ limit restoring the Z_2 symmetry. This happens even when the lattice Higgs mass parameter scales as $m_b \propto 1/N_\tau$. Even for higher N one can see the realisation of Z_N symmetry as the off-diagonal elements of the matrix M turn out to be just U and U^\dagger due to the vanishing of B_{N_τ} . Effecting a Z_N transformation, i.e. $U \rightarrow zU$, the factor z in U will cancel with z^* in U^\dagger leaving the determinant unchanged. Fig. 5, shows B_{N_τ} versus N_τ for $m_b \propto 1/N_\tau$. In the log-log scale, it is clear that B_{N_τ} decreases faster than exponential decay. In the following,

we consider the effects of staggered fermion fields on the Z_N symmetry.

Gauged 1 – d chain of $SU(N)$ – fermion

The lattice action for $SU(N)$ staggered fermions is given by [12]

$$S = \beta_g \sum_p \left[1 - \frac{1}{2} \text{Tr}(U_p + U_p^\dagger) \right] + 2m_f \sum_n \bar{\Psi}_n \Psi_n + \sum_{n,\mu} \eta_{n,\mu} \left[\bar{\Psi}_n U_{n,\mu} \Psi_{n+\mu} - \bar{\Psi}_n U_{n-\mu,\mu}^\dagger \Psi_{n-\mu} \right]. \quad (22)$$

Here the fermion mass, as well as the fields, are expressed in lattice unit. The analog of Eq. 12 in this case turns out to be

$$S = 2m_f \sum_{i=1}^{N_\tau} \bar{\Psi}_i \Psi_i + \sum_{i=1}^{N_\tau-1} \left(\bar{\Psi}_i \Psi_{i+1} - \bar{\Psi}_{i+1} \Psi_i \right) - \bar{\Psi}_{N_\tau} U \Psi_1 + \bar{\Psi}_1 U^\dagger \Psi_{N_\tau}, \quad (23)$$

Here we have considered the KS phase η_0 to be +1 [13,14], however the results/conclusions do not depend on η_0 . To find out the free energy $V(L)$ we need to integrate out only the fermion fields using standard Grassman integration. Before we integrate out, for convenience we write $S = S_1 + S_2$, where

$$S_1 = 2m_f \bar{\Psi}_1 \Psi_1 - \bar{\Psi}_{N_\tau} U \Psi_1 + \bar{\Psi}_1 U^\dagger \Psi_{N_\tau}, \quad (24)$$

$$S_2 = 2m_f \sum_{i=2}^{N_\tau} \bar{\Psi}_i \Psi_i + \sum_{i=1}^{N_\tau-1} \left(\bar{\Psi}_i \Psi_{i+1} - \bar{\Psi}_{i+1} \Psi_i \right). \quad (25)$$

Initially we integrate the fields $\Psi_2, \bar{\Psi}_2$ to $\Psi_{N_\tau-1}, \bar{\Psi}_{N_\tau-1}$ sequentially as in the previous section using Grassman integration. Afterwards $\Psi_1, \bar{\Psi}_1$ and $\Psi_{N_\tau}, \bar{\Psi}_{N_\tau}$ are integrated out to obtain the partition function

$$\mathcal{Z}_L = \int d\bar{\Psi}_1 d\Psi_1 d\bar{\Psi}_{N_\tau} d\Psi_{N_\tau} \text{Exp}[-S_1] \mathcal{Z}, \quad (26)$$

where

$$\mathcal{Z} = \int \prod_{i=2}^{N_\tau-1} d\bar{\Psi}_i d\Psi_i \text{Exp}[-S_2].$$

The partition function can be written as

$$\begin{aligned}
\mathcal{Z}_L = & \int d\bar{\Psi}_1 d\Psi_1 d\bar{\Psi}_{N_\tau} d\Psi_{N_\tau} \text{Exp} \left[\bar{\Psi}_{N_\tau} U \Psi_1 - \bar{\Psi}_1 U^\dagger \Psi_{N_\tau} \right] \\
& \times \prod_r \left(1 - 2m_f \bar{\psi}_1^r \psi_1^r - 2m_f \bar{\psi}_{N_\tau}^r \psi_{N_\tau}^r + 4m_f^2 \bar{\psi}_1^r \psi_1^r \bar{\psi}_{N_\tau}^r \psi_{N_\tau}^r \right) \\
& \times \left(A_{N_\tau} - B_{N_\tau} \bar{\psi}_1^r \psi_1^r - C_{N_\tau} \bar{\psi}_{N_\tau}^r \psi_{N_\tau}^r + \bar{\psi}_{N_\tau}^r \psi_1^r + D_{N_\tau} \bar{\psi}_1^r \psi_{N_\tau}^r + E_{N_\tau} \bar{\psi}_{N_\tau}^r \psi_{N_\tau}^r \bar{\psi}_1^r \psi_1^r \right) .
\end{aligned} \tag{27}$$

Note that ψ_i^r denotes the colour r of the field Ψ_i at the temporal site i . The coefficients A_{N_τ} to E_{N_τ} can be obtained by recursion as

$$A_{k+1} = 2m_f A_k + C_k, \quad B_{k+1} = 2m_f B_k + E_k, \quad C_{k+1} = A_k, \quad D_{k+1} = (-1)^k, \quad E_{k+1} = B_k, \tag{28}$$

with $A_4 = (1 + 4m_f^2)$, $B_4 = 2m_f$, $C_4 = 2m_f$, $E_4 = 1$.

The simplified partition function is

$$\begin{aligned}
\mathcal{Z}_L = & \int d\bar{\Psi}_1 d\Psi_1 d\bar{\Psi}_{N_\tau} d\Psi_{N_\tau} \text{Exp} \left[\bar{\Psi}_{N_\tau} U \Psi_1 - \bar{\Psi}_1 U^\dagger \Psi_{N_\tau} \right] \\
& \times \prod_r \left(\tilde{A} - \tilde{B} \bar{\psi}_1^r \psi_1^r - \tilde{C} \bar{\psi}_{N_\tau}^r \psi_{N_\tau}^r + \bar{\psi}_{N_\tau}^r \psi_1^r + \tilde{D} \bar{\psi}_1^r \psi_{N_\tau}^r + \tilde{E} \bar{\psi}_{N_\tau}^r \psi_{N_\tau}^r \bar{\psi}_1^r \psi_1^r \right) ,
\end{aligned} \tag{29}$$

where $\tilde{A} = A_{N_\tau}$, $\tilde{B} = (2m_f A_{N_\tau} + B_{N_\tau})$, $\tilde{C} = (2m_f A_{N_\tau} + C_{N_\tau})$, $\tilde{D} = D_{N_\tau}$ and $\tilde{E} = E_{N_\tau} + 2m_f C_{N_\tau} + 2m_f B_{N_\tau} + 4m_f^2 A_{N_\tau}$.

For $N = 2$, integration of the rest of the fields in Eq. 29 leads to

$$\begin{aligned}
\mathcal{Z}_L = & \tilde{E}^2 + 2\tilde{E}\tilde{A}|U_{11}|^2 + \tilde{A}^2 + 2\tilde{B}\tilde{C}|U_{12}|^2 + 2 \left[1 - \tilde{D} \text{Re}(U_{11}^2) \right] \\
& + (\tilde{E} + \tilde{A})(1 - \tilde{D}) \text{Tr}(U) .
\end{aligned} \tag{30}$$

The Z_2 explicit breaking term turns out to be linear in $\tilde{E} + \tilde{A}$ in Eq. 30. For higher N it is difficult to evaluate \mathcal{Z}_L for a general U . To proceed further we assume the U to be

$U_{rs} = \lambda_r \delta_{rs}$. After the exponential term in the partition function is written as a polynomial

$$\mathcal{Z}_L = \int d\bar{\Psi}_1 d\Psi_1 d\bar{\Psi}_{N_\tau} d\Psi_{N_\tau} \times \prod_r \left(A - B\bar{\psi}'_1 \psi'_1 - C\bar{\psi}'_{N_\tau} \psi'_{N_\tau} + F_r \bar{\psi}'_{N_\tau} \psi'_1 + D_r \bar{\psi}'_1 \psi'_{N_\tau} + E_r \bar{\psi}'_{N_\tau} \psi'_{N_\tau} \bar{\psi}'_1 \psi'_1 \right), \quad (31)$$

where $A = \tilde{A}$, $B = \tilde{B}$, $C = \tilde{C}$, $D_r = \tilde{D} - \lambda_r^* \tilde{A}$, $E_r = \tilde{E} - \lambda_r \tilde{D} + \lambda_r^* + \tilde{A}$ and $F_r = (1 + \lambda_r \tilde{A})$.

The partition function for higher N is

$$\mathcal{Z}_L = \prod_r E_r. \quad (32)$$

The corresponding free energy is

$$V(L) = -T \sum_r \left\{ \log(\tilde{E} + \tilde{A}) + \log\left(1 - \frac{\lambda_r \tilde{D} - \lambda_r^*}{\tilde{E} + \tilde{A}}\right) \right\}. \quad (33)$$

The second term in Eq. 33, breaks the Z_N symmetry explicitly. If the lattice spacing is

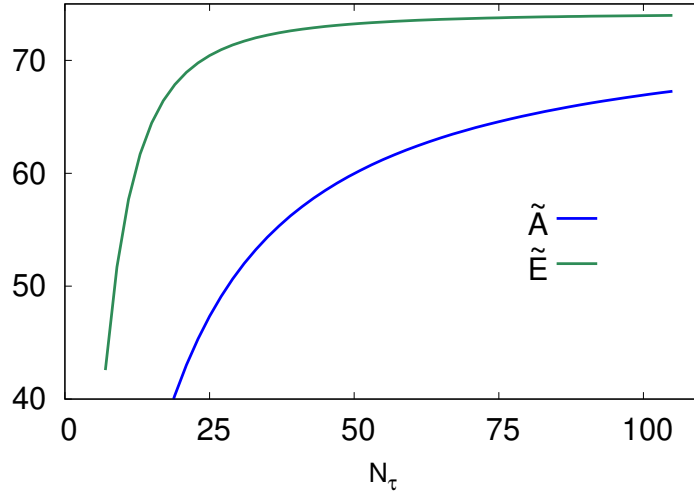


Figure 6: \tilde{A} and \tilde{E} versus N_τ for fermion mass parameter $m_f \propto 1/N_\tau$.

fixed, then $\tilde{E} + \tilde{A}$ diverges in the limit $N_\tau \rightarrow \infty$. The second term vanishes in this limit, and so does the temperature. In order to study the explicit breaking at a fixed nonzero

temperature, the behavior of \tilde{E} and \tilde{A} must be studied in the limit $N_\tau \rightarrow \infty$ while scaling the fermion mass parameter (in lattice units) as $m_f \propto 1/N_\tau$. We have numerically checked that \tilde{E} and \tilde{A} increase rapidly with N_τ initially, but seem to approach a finite limiting value for $N_\tau \rightarrow \infty$. For $m_f \propto 1/N_\tau$, Fig. 6 shows the N_τ dependence \tilde{E} and \tilde{A} . These results suggest that for the one-dimensional fermion chain the explicit breaking of Z_N vanishes only at zero temperature.

Study of Z_2 symmetry, CD transition and density of states in Z_2 +Higgs theory

In this section, we study the Monte Carlo simulation results of Z_2 +Higgs theory in the 3+1 dimension. We also analytically calculate the free energy of the Polyakov loop and the density of states of this theory in 0+1 dimensions. The lattice action for the Z_2 +Higgs theory in 3 + 1 dimensional space is given by

$$S = -\beta_g \sum_P U_P - \kappa \sum_{n,\hat{\mu}} \Phi_{n+\hat{\mu}} U_{n,\hat{\mu}} \Phi_n . \quad (34)$$

β_g is the gauge coupling constant and κ is the strength of gauge Higgs interaction. Here both the $U_{n,\hat{\mu}}$ and Φ_n take values ± 1 . For this theory, under the Z_2 gauge transformations, the gauge links $U_{n,\hat{\mu}}$ transform as

$$U_{n,\hat{\mu}} \rightarrow V_n U_{n,\hat{\mu}} V_{n+\hat{\mu}}^{-1} . \quad (35)$$

The matter fields (Φ_n), transform as, $\Phi_n \rightarrow V_n \Phi_n$. Here V_n and $V_{n+\hat{\mu}}$ are the elements of Z_2 gauge group and they can take values ± 1 . The V_n 's satisfy the following equation

$$V(\vec{n}, n_4 = 1) = z V(\vec{n}, n_4 = N_\tau) , \quad (36)$$

where $z \in Z_2$ with $z = \pm 1$. The pure gauge part of the action, in Eq. 34, is invariant under the Z_2 gauge transformations of the gauge links, i.e. Z_2 symmetry is always there for pure gauge theory which is just spontaneously broken at high β_g values. The Polyakov loop, $L(\vec{n})$ is the order parameter of this theory and transforms non-trivially under Z_2 gauge transformations, [2] i.e.

$$L(\vec{n}) \rightarrow zL(\vec{n}) . \quad (37)$$

Now since the Higgs fields are periodic, they satisfy the boundary condition, $\Phi(\vec{n}, n_4 = 1) = \Phi(\vec{n}, n_4 = N_\tau)$. Z_2 gauge transformations spoil this boundary condition. Therefore, in the presence of Higgs fields (Φ_n), the Z_2 symmetry is broken explicitly.

For $\kappa \neq 0$ case, $S(U, \Phi) \neq S(U_g, \Phi)$, where $U_g = VUV^{-1}$ with $V(0) = zV(\beta)$. So these pair of configurations will not contribute equally to the partition function. The change in the action due to Z_2 "rotation" of gauge links can be compensated by changing the Higgs field appropriately. This was numerically tested by updating the Higgs field using Monte Carlo steps after Z_2 rotating the gauge links.

In the following Metropolis algorithm [15] is used to update the gauge links $U_{n,\hat{\mu}}$ and Higgs fields Φ_n in the lattice Monte Carlo simulations. The nature of CD transition is studied for both pure Z_2 gauge theory ($\kappa = 0$) and in presence of Higgs field ($\kappa = 0.13$) for different values of N_τ . In Fig. 7, We show the plot of Polyakov loop vs β_g for $N_\tau = 8$.

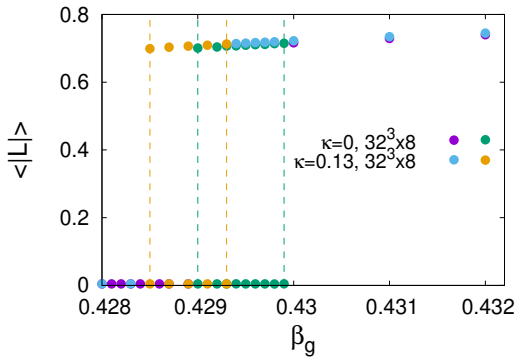


Figure 7: Average of L vs β_g for $N_\tau = 8$.

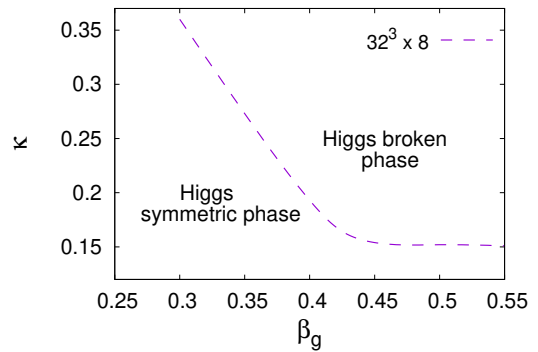


Figure 8: Phase diagram for $N_\tau = 8$.

The results of $\kappa = 0$ suggest that there is a range of β_g over which two separated states

(green line) are present. This indicates that the CD transition is first order. It is observed that the CD transition is first order also for $N_\tau = 4$ but it is a crossover one for $N_\tau = 2$.

In order to study the effect of Φ field on the CD transition and Z_2 symmetry, phase diagram is studied in $\beta_g - \kappa$ plane [16, 17] in Fig. 8. In the Higgs symmetric phase ($\kappa < \kappa_c$), the distribution of the interaction term, in other words, the entropy, dominates over the action or the Boltzmann factor. In this phase, there is a possibility for the realization of Z_2 symmetry. In the Higgs broken phase ($\kappa > \kappa_c$), i.e. large κ , the interaction term dominates over the entropy and Z_2 symmetry is badly broken in this phase. Our study is mostly focused on studying the CD transition and Z_2 symmetry in the Higgs symmetric phase.

To observe the effect of the Φ field on the CD transition, in Fig. 7 we have shown how the order parameter behaves with β_g for $\kappa = 0.13$. We can see the CD transition is still first order as two states (yellow line) clearly appear here as well for a given range of β_g but the range of β_g over which two states appear moves towards smaller values of β_g , i.e. the critical β_g decreases.

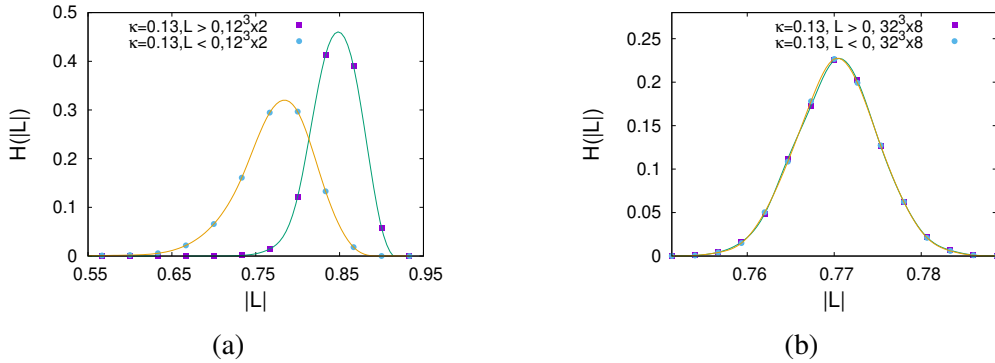


Figure 9: (a) $H(|L|)$ vs $|L|$ in deconfined phase for $N_\tau = 2$, (b) $H(|L|)$ vs $|L|$ in deconfined phase for $N_\tau = 8$.

In Figs. 9a and 9b, the histograms of the Polyakov loop $H(|L|)$ is studied numerically for $\kappa = 0.13$ to see the effect of N_τ on Z_2 symmetry. Here $\kappa = 0.13$ corresponds to Higgs symmetric phase. This study is done in the deconfined phase for the two Polyakov loop sectors at $N_\tau = 2, 8$. We plot $H(|L|)$ but present $L > 0$ and $L < 0$ sectors as separate data. For $N_\tau = 2$, the histograms of the two Polyakov loop sectors do not agree with each

other which indicates the Z_2 symmetry is explicitly broken here. But for $N_\tau = 8$, the two distributions corresponding to the two Polyakov loop sectors agree well which leads to almost realization of Z_2 symmetry at higher N_τ . For larger κ in the Higgs broken phase, Z_2 symmetry is badly broken.

To study how Z_2 symmetry depends on κ , the thermal average of the temporal components of interaction, $sk_4 = \sum_n \Phi_n U_{n,\hat{4}} \Phi_{n+\hat{4}}^\dagger$ and the corresponding susceptibility $\chi_{sk_4} = \langle sk_4^2 \rangle - \langle sk_4 \rangle^2$ are computed in the deconfined phase at $\beta_g = 0.435$. The results for $(\langle sk_4 \rangle, \chi_{sk_4})$ are shown in Figs. 10a and 10b for $N_\tau = 16$. It is observed that $\kappa < 0.154$ corresponds to the Higgs symmetric phase and for $\kappa > 0.154$ the system is in Higgs broken phase. In the Higgs symmetric phase, for larger N_τ , the κ value up to which sk_4 and χ_{sk_4} of the two Polyakov sectors match (within numerical errors) is higher. But in the Higgs broken phase, the Z_2 symmetry is not observed even at higher N_τ .

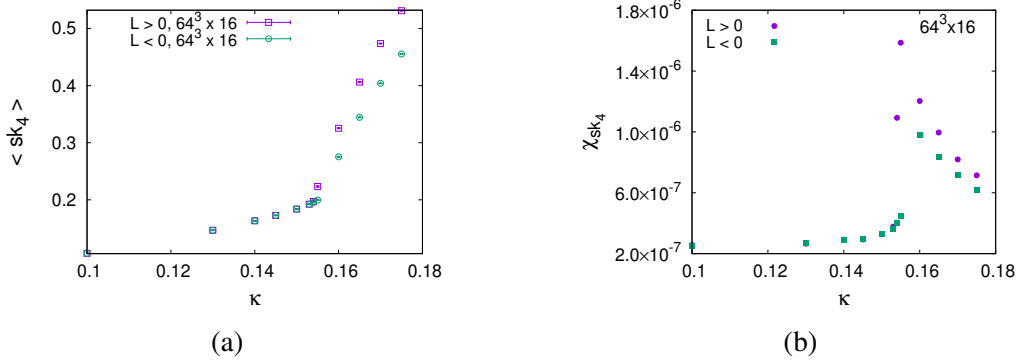


Figure 10: (a) $\langle sk_4 \rangle$ vs κ for $\beta_g = 0.435$ on $64^3 \times 16$ lattice, (b) χ_{sk_4} vs κ for $\beta_g = 0.435$ on $64^3 \times 16$ lattice.

To understand the realization of Z_2 symmetry in this theory, we consider a simple temporal one-dimensional model for a given spatial site. The gauge Higgs interaction action for this 0 + 1 dimensional model which breaks the Z_2 symmetry is

$$S_{1D} = -\kappa sk_4, \quad sk_4 = \sum_{n=1}^{N_\tau} \Phi_n U_n \Phi_{n+1}. \quad (38)$$

n denotes the temporal lattice site, i.e. $1 \leq n \leq N_\tau$ and Φ_{N_τ} satisfies periodic boundary condition $\Phi_{N_\tau+1} = \Phi_1$. To see the N_τ dependence of the Z_2 symmetry we calculate the

free energy $V(L, N_\tau)$ analytically. To simplify the calculation we have considered a gauge choice in which all the gauge links are set to unity except the last one, i.e. $U_i = 1$ for $i = 1, 2, \dots, N_\tau - 1$ and $U_{N_\tau} = L$. With this gauge choice, for $L = 1$ this model behaves like a one-dimensional Ising model. The Z_2 rotated part of it, i.e. $L = -1$ can be obtained by making the coupling between the fields Φ_{N_τ} and Φ_1 as anti-ferromagnetic. The exact partition functions for the two Polyakov loop sectors are given by

$$\mathcal{Z}(L = 1) = \lambda_1^{N_\tau} + \lambda_2^{N_\tau}, \quad \mathcal{Z}(L = -1) = \lambda_1^{N_\tau} - \lambda_2^{N_\tau}, \quad (39)$$

where $\lambda_1 = e^\kappa + e^{-\kappa}$ and $\lambda_2 = e^\kappa - e^{-\kappa}$. The free energies corresponding to the partition function in the large N_τ limit are given by

$$V(L = 1) = V(L = -1) = -TN_\tau \log(\lambda_1). \quad (40)$$

It is clear that the free energies for the two Polyakov loop sectors are equal at the large N_τ limit in this 0 + 1 dimensional model. This clearly indicates that the Z_2 symmetry realization happens at a large N_τ limit even in the presence of Φ .

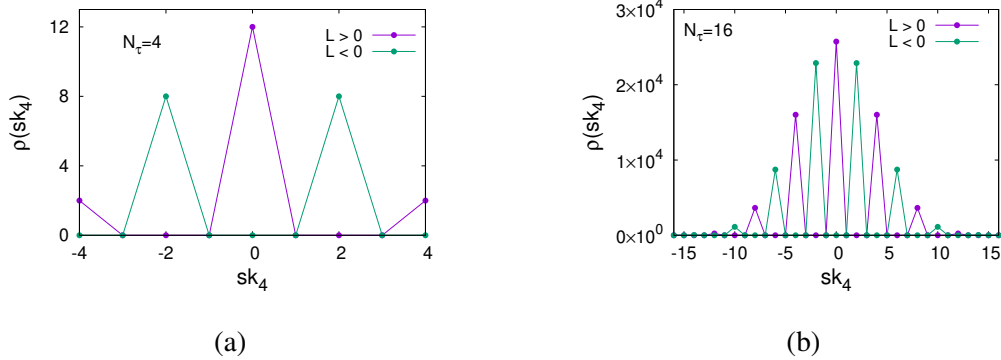


Figure 11: (a) $\rho(sk_4)$ for $\kappa = 0$ in 0+1 dimensions, (b) $\rho(sk_4)$ for $\kappa = 0$ in 0+1 dimensions.

The entropy or the DoS, i.e. $\rho(sk_4)$ corresponding to sk_4 are shown in Figs. 11a and 11b. For smaller N_τ ($N_\tau = 4$), the DoS or $\rho(sk_4)$ for the two Polyakov loop sectors are not described by a single function which indicates there is no Z_2 symmetry. But for large N_τ ($N_\tau = 16$), the distribution of sk_4 for the two Polyakov loop sectors are well described by

a single Gaussian function whose peak is at $sk_4 = 0$ and $\sqrt{N_\tau}$ as standard deviation. So the peak height and the distribution of sk_4 around this peak dominate the thermodynamics at a large N_τ limit where Z_2 symmetry is observed even in the presence of Higgs fields. It is also clear from the 1 + 1 dimensional numerical study that the interaction along the spatial directions does not affect the 0 + 1 dimensional results of Z_2 symmetry realization.

Conclusion

In this thesis, we study the Z_N symmetry in $SU(N)$ gauge theories in the presence of matter fields. The matter fields are in the fundamental representation of the $SU(N)$ gauge group. Our numerical study of $SU(3)$ +Higgs in 3+1 dimension shows that in presence of Higgs as matter fields, the CD transition becomes a crossover for small N_τ and the Z_3 symmetry is broken explicitly. With the increase in N_τ , the CD transition becomes a first order which is accompanied by the effective realization of the Z_3 symmetry in the Higgs symmetric phase. In order to calculate the free energy analytically, a 0+1 dimensional model is considered for $SU(N)$ gauge theories in presence of matter fields. The action for the gauged chains can be obtained by considering the terms of the corresponding 3+1 gauge theories which break the Z_N symmetry explicitly. The matter fields are integrated out, in the partition function, which results in an analytic form of the Polyakov loop free energy and it suggests that the explicit breaking of Z_N decreases with an increase in N_τ . In the study of Z_2 +Higgs, it is argued that the dependence of explicit breaking on N_τ is possibly due to the enhancement of density of states [18]. At the large N_τ limit, the density of states dominates the thermodynamics which results in the realization of Z_N symmetry. It is also observed that in the phase diagram where the action dominates over the entropy or the density of states, the Z_N symmetry is explicitly broken. Hence the Z_N symmetry is explicitly broken in the Higgs broken phase even for large N_τ but in the Higgs symmetric phase, it is realized in the large N_τ limit. It would be interesting to find numerically if there is a realization of Z_N symmetry in presence of fermions.

Plan of the thesis

In this thesis, we study the Z_N symmetry in $SU(N)$ gauge theories in the presence of matter fields.

- Chapter 1 will provide a general introduction and motivation for studying Z_N symmetry in $SU(N)$ gauge theories.
- Chapter 2 will discuss Z_N symmetry in $SU(N)$ gauge theories.
- Chapter 3 will study CD transition and Z_3 symmetry in $SU(3)$ +Higgs theory.
- Chapter 4 will study gauged 1-d chain of $SU(N)$ in presence of matter fields.
- Chapter 5 will Study the Z_2 symmetry, CD transition and density of states in Z_2 +Higgs theory.
- Chapter 6 will conclude with a discussion of the results as well as open problems.

List of Figures

1	Average of L vs β_g for $N_\tau = 2$	6
2	Distribution of phase of L	6
3	Distribution of L for $N_\tau = 4$	7
4	Distribution of phase of L	7
5	B_{N_τ} versus N_τ for Higgs mass parameter $m_b \propto 1/N_\tau$	10
6	\tilde{A} and \tilde{E} versus N_τ for fermion mass parameter $m_f \propto 1/N_\tau$	13
7	Average of L vs β_g for $N_\tau = 8$	15
8	Phase diagram for $N_\tau = 8$	15
9	(a) $H(L)$ vs $ L $ in deconfined phase for $N_\tau = 2$, (b) $H(L)$ vs $ L $ in deconfined phase for $N_\tau = 8$	16
10	(a) $\langle sk_4 \rangle$ vs κ for $\beta_g = 0.435$ on $64^3 \times 16$ lattice, (b) χ_{sk_4} vs κ for $\beta_g = 0.435$ on $64^3 \times 16$ lattice.	17
11	(a) $\rho(sk_4)$ for $\kappa = 0$ in 0+1 dimensions, (b) $\rho(sk_4)$ for $\kappa = 0$ in 0+1 dimensions.	18
3.1	Sketch of an elementary plaquette U_P	43
3.2	Position of gauge links U and Higgs fields Φ on the lattice.	45

3.3	$H(L)$ for $N_\tau = 2$ at $\beta_g = 1.698$ and $\kappa = 0$.	51
3.4	$H(L)$ for $N_\tau = 4$ at $\beta_g = 1.897$ and $\kappa = 0$.	51
3.5	$\langle L \rangle$ vs β_g for $N_\tau = 2$.	52
3.6	$\langle L \rangle$ vs β_g for $N_\tau = 4$.	52
3.7	Confined phase.	53
3.8	Near critical point.	53
3.9	Deconfined phase.	53
3.10	Polyakov loop vs β_g for $\kappa = 0.125$.	54
3.11	Susceptibility vs β_g for $\kappa = 0.125$.	54
3.12	$H(L)$ for $N_\tau = 3$ at $\beta_g = 1.854$ and $\kappa = 0.125$.	55
3.13	$H(L)$ for $N_\tau = 4$ at $\beta_g = 1.904$ and $\kappa = 0.125$.	55
3.14	$\langle L \rangle$ vs β_g for $N_\tau = 3$.	56
3.15	$\langle L \rangle$ vs β_g for $N_\tau = 4$.	56
3.16	Distribution of L in the confined phase for $N_\tau = 4$.	57
3.17	Distribution of L in the deconfined phase for $N_\tau = 4$.	58
3.18	Distribution of phase of the Polyakov loop for $\langle L \rangle = 0.584874$.	59
3.19	L on the complex plane for $12^3 \times 2$ lattice.	59
3.20	Distribution of phase of the Polyakov loop.	60
3.21	L on the complex plane for $16^3 \times 4$ lattice.	60
3.22	Difference of S_K between $\theta = 0$ and $2\pi/3$ in the deconfined phase.	61
3.23	Difference of S_g between $\theta = 0$ and $2\pi/3$ in the deconfined phase.	61

3.24	S_K for different N_τ near β_{gc}	62
4.1	one-dimensional temporal chain.	67
4.2	B_{N_τ} versus N_τ for Higgs mass parameter $m_b \propto 1/N_\tau$	72
4.3	N_τ dependence for fermion mass parameter $m_f = \text{constant}$	79
4.4	N_τ dependence for fermion mass parameter $m_f \propto 1/N_\tau$	79
4.5	\tilde{A} and \tilde{E} versus N_τ for fermion mass parameter $m_f = \text{constant}$	81
4.6	\tilde{A} and \tilde{E} versus N_τ for fermion mass parameter $m_f \propto 1/N_\tau$	81
5.1	The average of the Polyakov loop vs β_g for $N_\tau = 2$	87
5.2	The average of the Polyakov loop vs β_g for $N_\tau = 4$	88
5.3	The average of the Polyakov loop vs β_g for $N_\tau = 8$	88
5.4	Monte Carlo history of Polyakov loop for $N_\tau = 4$	89
5.5	Monte Carlo history of Polyakov loop for $N_\tau = 8$	89
5.6	Phase diagram.	90
5.7	$\langle sk \rangle$ vs κ for $\beta_g = 0.3$	90
5.8	$\langle sk \rangle$ vs κ for $\beta_g = 0.35$	91
5.9	$\langle sk \rangle$ vs κ for $\beta_g = 0.45$	91
5.10	The average of the Polyakov loop vs β_g for $N_\tau = 2$	92
5.11	The average of the Polyakov loop vs β_g for $N_\tau = 4$	92
5.12	The average of the Polyakov loop vs β_g for $N_\tau = 8$	93
5.13	Histogram of L in the confined phase.	93

5.14	Histogram of L in the deconfined phase.	93
5.15	Histogram of L in the confined phase.	94
5.16	Histogram of L in the deconfined phase.	94
5.17	Histogram of L in the confined phase.	94
5.18	Histogram of L in the deconfined phase.	94
5.19	sk_4 average vs κ for $\beta_g = 0.435$ on $16^3 \times 4$ lattice.	95
5.20	sk_4 fluctuation vs κ for $\beta_g = 0.435$ on $16^3 \times 4$ lattice.	95
5.21	sk_4 average vs κ for $\beta_g = 0.435$ on $64^3 \times 16$ lattice.	95
5.22	sk_4 fluctuation vs κ for $\beta_g = 0.435$ on $64^3 \times 16$ lattice.	95
5.23	$\rho(sk_4)$ for $\kappa = 0$ in 0+1 dimensions.	99
5.24	$\rho(sk_4)$ for $\kappa = 0$ in 0+1 dimensions.	99
5.25	$\rho(sk_4)$ for $\kappa = 0$ in 0+1 dimensions.	99
5.26	$\rho(sk_4)$ for $\kappa = 0$ in 0+1 dimensions.	99
5.27	$\rho(sk)$ for $\kappa = 0$ in 0+1 dimensions.	100
5.28	$\rho(sk)$ for $\kappa = 0$ in 0+1 dimensions.	100
5.29	$H(sk_4)$ for $\kappa = 0.1$, $\beta_g = 0.435$ for 3 + 1 dimension.	101
5.30	$H(sk_4)$ for $\kappa = 0.1$, $\beta_g = 0.435$ for 3 + 1 dimension.	101
5.31	$H(sk_4)$ fitted with 0 + 1 density of states with a Boltzmann factor.	102

Chapter 1

Motivation and Introduction

The study of confinement-deconfinement (CD) transition is an important part of understanding matter at extreme temperatures and/or densities. These extreme conditions are believed to exist in the early Universe, in extreme dense stars, the quark-gluon plasma (QGP) formed in relativistic heavy-ion collisions etc. Most of the theories in this context, of which non-abelian gauge fields are a part, undergo the CD transition. These fields are described by Yang-Mill's $SU(N)$ gauge theories and are responsible for interaction between matter fields in theories such as quantum chromodynamics (QCD), electroweak theory (EWT) etc. The basic constituents of QCD are quarks and gluons that are confined inside hadrons in the hadronic matter. At high temperatures and/or densities hadrons melt into quark-gluon plasma (QGP), in which the quarks and gluons are deconfined [19–22]. The detailed phase diagram study of QCD shows that this melting of hadrons proceeds via a transition known as confinement-deconfinement (CD) transition. The nature of this transition depends on the masses and the number of quark flavours [23–28]. The CD transition also occurs in the EWT, apart from the Higgs transition. The gauge sector background is taken to be in the deconfined state during the Higgs transition. The nature of CD transition in EWT is also affected by the Higgs field [29, 30]. Given that the CD transition is an integral part of theories such as QCD, EWT etc., it is necessary to

understand in detail the effects of the matter field for smaller lattice cut-off.

In pure $SU(N)$ gauge theory, the confined and deconfined phases are characterized by the free energy of an isolated static charge. In the confined phase the free energy diverges, as a consequence static charges can occur only in color singlet pairs. In the string model of confinement, the static charges are connected by a string of non-zero tension. The string picture of confinement is supported by lattice gauge theory calculations which show that the free energy of static charges rises linearly with distance [31]. The melting of this string leads to the liberation of the static charges and the onset of deconfinement in the deconfined phase. The Euclidean formulation of thermodynamics relates the free energy of an isolated static charge, in units of temperature, to the negative logarithm of the Polyakov loop average [32, 33]. The Polyakov loop average vanishes in the confined phase and acquires a non-zero value in the deconfined phase, thus acting as an order parameter for the CD transition. The Euclidean action is found to be symmetric under gauge transformations, which are classified by the center Z_N of the gauge group $SU(N)$. The Polyakov loop transforms like a Z_N -spin under these gauge transformations. Since the Polyakov loop acquires a non-zero average value in the deconfined phase, the Z_N symmetry is spontaneously broken (SSB) [1, 34–36]. The SSB leads to N degenerate states in the deconfined phase and global topological defects such as strings and domain walls in physical space [3, 37–40]. The N degenerate states are characterized by each element of Z_N . Non-perturbative studies show that the CD transition is second order [33, 41] for $N = 2$ and first order [34, 35] for $N \geq 3$.

The Z_N symmetry of pure $SU(N)$ gauge theory is spoiled when matter fields in the fundamental representation, as in QCD, EWT etc., are included. The matter fields in the fundamental representation, satisfy either periodic(boson) or anti-periodic(fermion) boundary conditions. However, the Z_N gauge transformations are not compatible with these boundary conditions. The requirement that the matter fields satisfy either periodic or anti-periodic boundary conditions in the temporal direction forces the gauge transformations

to be periodic [3–5, 42–44]. It is necessary to consider the Z_N transformations on the gauge fields, as it is expected that the Polyakov loop configurations belonging to different Z_N sectors will contribute to the partition function. Thus the Z_N gauge transformations may act only on the gauge fields but in the process, the action does not remain invariant. Therefore the Z_N symmetry is explicitly broken. As a consequence, in the presence of dynamical matter fields in the fundamental representation, the string connecting the static particle and anti-particle pair breaks due to excitations of dynamical charges. The free energy of isolated static charges remains finite. The Polyakov loop average, as a result, is expected to become non-zero even in the confined phase. Studies of spin systems show that the strength of a phase transition and explicit breaking of the associated symmetry are correlated. A strong first-order phase transition can turn to a crossover for large explicit breaking. So, it is expected that the explicit breaking of Z_N symmetry will soften the CD transition. There are several studies of explicit breaking of Z_N symmetry due to matter fields over the years [3, 7, 9, 40, 42, 43, 45–47]. In lattice gauge theories in the strong coupling limit, mean-field calculations show that the explicit breaking increases with a decrease in quark masses [42, 48]. Similarly, in the perturbative limit, one loop calculations find that with the decrease in the mass of dynamical fields, the explicit breaking increases [1, 48]. Recently, there are extensions of loop calculations to higher order which show a similar trend [6]. Further, the free energy difference between different Z_N states, in the deconfined phase, increases with temperature. Note that these perturbative calculations on Z_N symmetry in $SU(N)$ gauge theories are reliable at high temperatures and away from the CD transition point. As the fluctuations and gauge coupling are expected to grow if the temperature is lowered towards the CD transition point. Thus, non-perturbative effects are expected to dominate near the CD transition point.

The effect of dynamical fields near the CD transition is studied mostly in non-perturbative lattice simulations. Previously, the lattices in these studies have a small number of temporal lattice sites ($N_\tau \leq 4$). Early lattice studies in $SU(2)$ with dynamical quarks find a sharp crossover CD transition [49]. In $SU(3)$ with dynamical quarks, the explicit break-

ing of Z_3 increases for smaller masses [44], in the heavy-quark region. For small enough masses, the explicit breaking is so large that the CD transition becomes a crossover. Similar results were also observed in SU(2)+Higgs theory [50]. It was observed that the CD transition becomes sharper for $N_\tau = 4$ than for $N_\tau = 2$. Recent studies of Z_2 symmetry in SU(2)+Higgs theory suggests that the explicit breaking is vanishingly small even before the pure gauge limit [4]. The explicit breaking decrease in the Higgs symmetric phase suggests the Higgs condensate could be playing the role of the symmetry breaking field. In further studies, for vanishing bare Higgs mass and quartic coupling, the CD transition shows critical behaviour. This critical behaviour was observed only in the continuum limit, i.e. for $N_\tau \rightarrow \infty$ or cut-off approaching zero [5]. These results suggest that the interaction between the gauge and matter fields depends on N_τ . Also, the explicit breaking is vanishingly small, for vanishing bare Higgs mass, where it is least expected.

It is important to study, whether in SU(N)+Higgs theories for higher $N \geq 3$, explicit breaking of Z_N decreases with N_τ . Also if this leads to any changes in the nature of CD transition in SU(N)+Higgs theory *vs* N_τ . As an extension of the previous study in SU(2)+Higgs theory, in the present thesis work, we study the CD transition in SU(3)+Higgs theory and the explicit breaking of Z_3 symmetry near the transition point. For simplicity, we consider vanishing bare Higgs mass ($m = 0$) and quartic coupling ($\lambda = 0$). For this choice of parameters, the system is found to be in the Higgs symmetric phase around the CD transition point. As in the case of SU(2)+Higgs, the CD transition is found to depend on the lattice cut-off. The distribution of the Polyakov loop shows that the strength of explicit breaking decreases with N_τ . Also, the CD transition becomes stronger with N_τ . It is found that for $N_\tau = 2$ the transition is a continuous and the Z_3 symmetry is badly broken. For $N_\tau > 2$ the transition is first order. The Z_N asymmetry in the distribution of the Polyakov loop decreases monotonically with N_τ .

The exact calculation of the partition function in 3 + 1 dimensional theories is extremely difficult. In this case, the evidence of Z_N symmetry in the results is valid only up to an

error. Hence, it is highly desirable to obtain the above results through analytic calculation, where the partition function exhibits the Z_N symmetry even though the action breaks it explicitly. In this thesis, we consider a one-dimensional chain of fermionic/bosonic matter fields which are in the fundamental representation of the $SU(N)$ gauge group [51]. The lattice action can be derived from a one-dimensional continuum theory. We mention here that, there are several one-dimensional models considered in the literature [52–56] for different purposes over the years. The one-dimensional gauge chain can also be obtained from the $3 + 1$ lattice actions by restricting to terms that break the Z_N symmetry explicitly. Coincidentally, in these terms which break the Z_N symmetry, matter fields corresponding to different spatial sites do not couple. The terms can be arranged as a collection of non-interacting one-dimensional chains extending in the temporal direction. Hence the partition function can be written as the product of the partition functions of these one-dimensional chains. It is shown that the matter fields, in the partition function, can be integrated out exactly for any arbitrary N_τ , even when the temporal length of the chain is held fixed. From these calculations, the free energy for the Polyakov loop is obtained. The results show that, in the case of the Higgs (bosonic) field, the explicit breaking of Z_N rapidly decreases with N_τ vanishing in the “continuum” limit. In the case of fermions, the explicit breaking initially decreases rapidly with N_τ but approaches a non-zero limiting value. The non-perturbative lattice MC simulations, as well as integrable analytical models, show that the Z_N symmetry is realised in the presence of bosonic matter fields, in the continuum limit. From these results, however, it is not clear what is the reason for this realisation.

The non-invariance of the action under Z_N gauge transformation which is not periodic in temporal directions does not necessarily imply the explicit breaking of Z_N symmetry. The presence of Z_N symmetry or its explicit breaking can only be inferred from the free energy of the Polyakov loop. In the free energy or the partition function calculations, two factors play important roles. They are the distribution of the action, which is also known as the density of states (DoS) and the Boltzmann factor. The latter clearly does not respect the

Z_N symmetry. So the realization of the Z_N symmetry must come from the DoS and its dominance over the Boltzmann factor. Computing the DoS in $SU(N)$ +Higgs theory is a difficult task as the configuration space is infinite [18]. In this situation, the Z_2 +Higgs theory in four dimensions provides a suitable alternative. Since the field variables take values ± 1 , it is possible to calculate the DoS with some simplifications.

The Z_2 +Higgs theory has been extensively studied in literature [8, 9, 57–61]. The phase diagram of this theory is found to be similar to that of $SU(N)$ +Higgs theories in 3 and 4–dimensions [16, 17]. Though in this theory, there is no analogue of the beta-functions of $SU(N)$ +Higgs theories, and the temperature is controlled by the couplings of the theory [62]. The similarity with the $SU(N)$ +Higgs theories arises when periodic/anti-periodic boundary condition is imposed on the Higgs field, in any one of the four dimensions. As a consequence gauge transformations which are not periodic in this “temporal” direction are not allowed and the Z_2 symmetry is explicitly broken similar to the explicit breaking of Z_N symmetry in $SU(N)$ +Higgs theories. It is important to note the difference in the role of N_τ between Z_2 +Higgs and $SU(N)$ +Higgs theories. Though in both cases increase in N_τ introduces additional degrees of freedom, in $SU(N)$ +Higgs theory to study Z_N symmetry at fixed temperature the couplings need to be tuned.

In the Z_2 +Higgs theory, the Z_2 symmetry of the Polyakov loop and the nature of CD transition are studied by varying the number of lattice points, N_τ , along the temporal direction. The computations are mostly done on the Higgs symmetric side of the Higgs transition line. Our results show that the Z_2 symmetry is realised for large N_τ . Also, the behaviour of the CD transition is found to be similar to the pure gauge case apart from the location of the critical point. To understand the role of N_τ , a $0 + 1$ dimensional model is considered by keeping the temporal component of the gauge Higgs interaction corresponding to a single spatial coordinate.

For the one-dimensional model, the Polyakov loop can take values ± 1 . For each of these cases, the free energy can be calculated exactly. The free energy calculations show the

emergence of Z_2 symmetry in the large N_τ limit for arbitrary interaction coupling. Further, the Monte Carlo results for the distribution of the interaction term, in $3 + 1$ dimensions, are reproduced well by exact $0 + 1$ dimensional DoS with an additional Boltzmann factor, though with a different value of the coupling strength. The DoS for both values of the Polyakov loop sharply peaked at zero. For large N_τ both of them can be approximated by a single gaussian, with the same peak height and width, suggesting Z_2 symmetry. Now, since the peak height grows with N_τ , the DoS will dominate the thermodynamics in the $N_\tau \rightarrow \infty$, leading to vanishingly small Z_2 explicit symmetry breaking.

Chapter 2

Z_N symmetry in $SU(N)$ gauge theories

In this chapter, we describe the Z_N symmetry in $SU(N)$ gauge theories, in Euclidean space. The matter fields, fermionic fields and the bosonic Higgs fields are in the fundamental representation of the $SU(N)$ gauge group. The $SU(N)$ generators are in the fundamental representation. In the following, we describe how the Z_N arises in Euclidean action and its explicit breaking due to matter fields.

2.1 Z_N symmetry in pure $SU(N)$ gauge theories

The path-integral form of the partition function for pure $SU(N)$ gauge theory at finite temperature for the gauge field $A_\mu(x)$ is given by

$$\mathcal{Z} = \int [DA_\mu] e^{-S[A_\mu]} . \quad (2.1)$$

Here x is a four-vector x_μ with $\mu = 1, 2, 3, 4$, representing a point in Euclidean space. The gauge field $A_\mu(x) = T^a A_\mu^a(x)$, where T^a 's are the generators of $SU(N)$ gauge group with $a = 1, 2, \dots, N^2 - 1$. The generators are traceless matrices and satisfy the following

properties

$$\text{Tr}(T_a T_b) = \frac{1}{2} \delta_{ab}, \quad [T_a, T_b] = i f_{abc} T_c. \quad (2.2)$$

The generators are taken to be in the fundamental representation of the $SU(N)$, i.e. $N \times N$ dimensional. In the adjoint representation, i.e. $(N^2 - 1) \times (N^2 - 1)$ matrices, the Z_N symmetry does not arise and the Polyakov loop is not a good order parameter for the CD transition [63].

The Euclidean action, $S[A_\mu]$, in Eq. 2.1 is given by

$$S[A_\mu] = \int_V d^3x \int_0^\beta d\tau \left[\frac{1}{2} \text{Tr} \left(F_{\mu\nu}(\vec{x}, \tau) F_{\mu\nu}(\vec{x}, \tau) \right) \right]. \quad (2.3)$$

Here $\beta = \frac{1}{T}$, T is the temperature and g is the gauge coupling strength. In terms of the gauge fields A_μ , the non-abelian gauge field strength $F_{\mu\nu}$ is written as, $F_{\mu\nu} = \partial_\mu A_\nu - \partial_\nu A_\mu + ig[A_\mu, A_\nu]$. The path integration in Eq. 2.1 is carried out over gauge field that are periodic along the temporal direction, i.e. $A_\mu(\vec{x}, \tau = 0) = A_\mu(\vec{x}, \tau = \beta)$. At finite temperatures, all gauge transformations are allowed as long as they preserve the periodicity of the gauge fields in the temporal direction. The action, Eq. 2.3 is invariant under the following gauge transformation of gauge fields

$$A_\mu(\vec{x}, \tau) \longrightarrow A'_\mu(\vec{x}, \tau) = V(\vec{x}, \tau) A_\mu(\vec{x}, \tau) V^{-1}(\vec{x}, \tau) - \frac{i}{g} V(\vec{x}, \tau) \partial_\mu V^{-1}(\vec{x}, \tau), \quad (2.4)$$

where $V(\vec{x}, \tau) \in SU(N)$. The field strength tensor transforms as

$$F_{\mu\nu}(\vec{x}, \tau) \rightarrow F'_{\mu\nu}(\vec{x}, \tau) = V(\vec{x}, \tau) F_{\mu\nu}(\vec{x}, \tau) V^\dagger(\vec{x}, \tau). \quad (2.5)$$

The periodicity of the gauge transformed fields is preserved, even if $V(\vec{x}, \tau)$ is not periodic in τ but satisfies

$$V(\vec{x}, \tau = 0) = z V(\vec{x}, \tau = \beta), \quad \text{with } z \in Z_N \subset SU(N). \quad (2.6)$$

Here $z \in Z_N = \mathbb{1} \exp(\frac{2\pi i n}{N})$ with $n = 0, 1, 2, \dots, N - 1$. $\mathbb{1}$ is a $N \times N$ identity matrix. All the gauge transformations satisfying Eq.2.6 can be represented by the element z . The term Z_N symmetry refers to the fact that all allowed gauge transformations of the Euclidean gauge action are classified by center Z_N of the gauge group $SU(N)$. The Polyakov loop (L) which is the path-ordered product of links in the temporal direction, i.e.

$$L(\vec{x}) = \frac{1}{N} \text{Tr} \left[\text{P} \left\{ \exp \left(-ig \int_0^\beta A_0(\vec{x}, \tau) d\tau \right) \right\} \right], \quad (2.7)$$

transforms as $L \rightarrow zL$ under a gauge transformations Eq. 2.4 with the boundary condition as given in Eq. 2.6. So the Polyakov loop is invariant when the gauge transformations are periodic, i.e. $z = \mathbb{1}$. This transformation of the Polyakov loop is similar to that of magnetization under the Z_2 transformation in the Ising model [2, 32, 36]. As mentioned previously, in pure $SU(N)$ gauge theory, the thermal average of the Polyakov loop vanishes in the confined phase. In the deconfined phase, the Polyakov loop acquires a nonzero thermal average value. Thus it plays the role of an order parameter for the CD phase transition, and the Z_N symmetry is spontaneously broken in the deconfined phase. As a result of spontaneous symmetry breaking, there are N degenerate states in the deconfined phase characterized by the elements of Z_N . Note that L is the trace of a $SU(N)$ matrix. For $N = 2$ the range of values L can take is $[-1, 1]$. For $N > 2$ it can take any value in a n -polygon (with curved sides) in the complex plane whose vertices are given by $\exp(\frac{2\pi i n}{N})$ with $n = 0, 1, 2, \dots, N - 1$.

If F is the free energy of an isolated static fermion or boson, then the thermal average value of the Polyakov loop is [64, 65]

$$\langle |L| \rangle \sim e^{-F}. \quad (2.8)$$

In the confinement phase the free energy is infinite and the $\langle |L| \rangle = 0$. In the deconfinement phase the free energy becomes finite and $\langle |L| \rangle \neq 0$.

2.2 Z_N symmetry in $SU(N)$ gauge theories in the presence of matter fields in the fundamental representation

In the following, we describe the Z_N symmetry when the matter fields are present in the Euclidean action. Like the gauge fields, the matter fields in the Euclidean space are required to satisfy particular boundary conditions depending on the spin. This turns out to be in conflict with the Z_N symmetry when the matter fields are in the fundamental representation. Note that this problem does not arise in the presence of adjoint matter fields.

2.2.1 Z_N symmetry in $SU(N)$ gauge theories with Higgs

In the presence of the Higgs field Φ , in the fundamental representation, the Euclidean $SU(N)$ +Higgs action is given by

$$S[A_\mu, \Phi, \Phi^\dagger] = S[A_\mu] + \int_V d^3x \int_0^\beta d\tau \left[\frac{1}{2} (D_\mu \Phi)^\dagger (D_\mu \Phi) + \frac{m_H^2}{2} \Phi^\dagger \Phi + \frac{\lambda_H}{4!} (\Phi^\dagger \Phi)^2 \right]. \quad (2.9)$$

The Φ field is a $N \times 1$ column matrix with complex elements. Here the covariant derivative $D_\mu \Phi = \partial_\mu \Phi + igA_\mu \Phi$. m_H is the Higgs mass and λ_H is the Higgs quartic coupling. The total partition function of this theory at finite temperature is given by

$$\mathcal{Z} = \int [DA_\mu][D\Phi][D\Phi^\dagger] e^{-S[A_\mu, \Phi, \Phi^\dagger]}. \quad (2.10)$$

The bosonic field Φ is required to be periodic in the temporal direction, i.e.

$$\Phi(\vec{x}, 0) = \Phi(\vec{x}, \beta). \quad (2.11)$$

Under the $SU(N)$ gauge transformation, the Φ fields in the fundamental representation transform as

$$\Phi(\vec{x}, \tau) \longrightarrow \Phi'(\vec{x}, \tau) = V(\vec{x}, \tau)\Phi(\vec{x}, \tau) . \quad (2.12)$$

The requirement that the gauge transformed field Φ' also satisfies periodic boundary condition forces the gauge transformations to be periodic. Under a non-trivial Z_N gauge transformation, with $V(\vec{x}, \tau = 0) = zV(\vec{x}, \tau = \beta)$, the transformed gauge fields A'_μ satisfies periodic boundary condition in the temporal direction, i.e.

$$A'_\mu(\vec{x}, 0) = A'_\mu(\vec{x}, \beta) . \quad (2.13)$$

But the gauge transformed matter fields Φ' on the other hand satisfy the following temporal boundary condition

$$\Phi'(\vec{x}, 0) = z\Phi'(\vec{x}, \beta) . \quad (2.14)$$

For $z \neq \mathbb{1}$, the Φ' do not satisfy the required boundary condition in Eq. 2.11. Φ' field can not contribute to the partition function. However, one can consider the Z_N transformation acting only on the gauge fields. This will lead to $L \rightarrow zL$. Since the Z_N gauge transformations now have acted only on the gauge fields, the action will be different, i.e. $S(L) \neq S(zL)$. Hence the Z_N symmetry is broken explicitly. Note that, since $z \in SU(N)$, gauge transformations such as in Eq. 2.6, can be written as

$$V(\vec{x}, \tau) = g(\tau)V_p(\vec{x}, \tau), \text{ with } g(\tau = 0) = zg(\tau = \beta) , \quad (2.15)$$

and $V_p(\vec{x}, \tau)$ is periodic $\tau = \beta$. Hence, to see the effect of Z_N gauge transformations, one needs to consider gauge transformations which are functions $g(\tau)$ with the above properties. To see, which terms of the action are affected, let us consider $g(0) = zg(\beta)$ with $z \in Z_N$. This transformation is gauge equivalent to $g(\tau) = \exp[i\alpha(\tau)]$, with $\alpha(\tau) = (2\pi n/N)\theta(\tau - \beta)$. This gauge transformation will affect only the terms in which temporal gauge fields are involved, i.e. $|D_0\Phi|^2$. So at the leading order, the explicit breaking of Z_N

arises due to temporal gradient terms. The other terms in the action influence the explicit breaking at higher order, which may be significant in the Higgs broken phase.

2.2.2 Z_N symmetry in $SU(N)$ gauge theories with fermion

The action for a minimally coupled $SU(N)$ gauge theory of fermions in 3 + 1 Euclidean space is given by

$$S[A_\mu, \Psi, \bar{\Psi}] = S[A_\mu] + \int_V d^3x \int_0^\beta d\tau [\bar{\Psi}(\not{D} + m_f)\Psi] \quad (2.16)$$

The fermion field Ψ is also a $N \times 1$ column matrix with complex elements. Here $\not{D}\Psi = (\not{\partial} + ig\mathcal{A})\Psi$. The γ -matrices are the Euclidean versions of the (Minkowski) γ -matrices and they are 4×4 matrices in Dirac space. The Euclidean γ -matrices follow the anti-commutation relations as

$$\{\gamma_\mu, \gamma_\nu\} = 2\delta_{\mu\nu}\mathbb{1} \quad \text{with } \mu, \nu = 1, 2, 3, 4. \quad (2.17)$$

The fermion fields Ψ are in the fundamental representation, and m_f is the mass of Ψ fields. The corresponding partition function takes the form

$$\mathcal{Z} = \int [DA_\mu][D\Psi][D\bar{\Psi}] e^{-S[A_\mu, \Psi, \bar{\Psi}]} . \quad (2.18)$$

The Ψ fields contributing to the partition function satisfy the anti-periodic boundary condition in the temporal direction, i.e.

$$\Psi(\vec{x}, 0) = -\Psi(\vec{x}, \beta) . \quad (2.19)$$

These fields transform under a gauge transformation $V \in \text{SU}(N)$ as

$$\Psi(\vec{x}, \tau) \longrightarrow \Psi'(\vec{x}, \tau) = V(\vec{x}, \tau)\Psi(\vec{x}, \tau) . \quad (2.20)$$

Hence the hermitian conjugate of it can be written as

$$\bar{\Psi}(\vec{x}, \tau) \longrightarrow \bar{\Psi}'(\vec{x}, \tau) = \bar{\Psi}(\vec{x}, \tau)V^\dagger(\vec{x}, \tau) . \quad (2.21)$$

The action is invariant if

$$S[A_\mu, \Psi, \bar{\Psi}] = S[A'_\mu, \Psi', \bar{\Psi}'] . \quad (2.22)$$

The gauge transformed action gives

$$S[A'_\mu, \Psi', \bar{\Psi}'] = S[A'_\mu] + \int_V d^3x \int_0^\beta d\tau \left[\bar{\Psi}V^\dagger \left(\gamma_\mu(\partial_\mu + igA'_\mu) + m_f \right) V\Psi \right] . \quad (2.23)$$

The gauge transformed fields Ψ' also required to be anti-periodic. A non-trivial Z_N gauge transformation, with $V(\vec{x}, \tau = 0) = zV(\vec{x}, \tau = \beta)$ and $z \neq -\mathbb{1}$, would lead to Ψ' with

$$\Psi'(\vec{x}, 0) = z\Psi'(\vec{x}, \beta) . \quad (2.24)$$

Such fields can not contribute to the partition function as described in the case of Higgs and the Z_N symmetry is broken explicitly.

Explicit breaking of Z_N , i.e. $S(L) \neq S(zL)$, does not necessarily imply that it will also be broken at the level of partition function averages. To get an estimate of the explicit symmetry breaking we need to consider the partition function average of observables that are sensitive to Z_N symmetry such as Polyakov loop, gauge Higgs interaction, etc. It is impossible to compute these observables near the CD transition using perturbative calculations where non-perturbative effects are expected to dominate. Though the perturbative calculations have been successful in studying the Z_N symmetry in gauge theories at high temperatures away from the transition region. These studies are not reliable as both the

gauge coupling and the fluctuations increases as the temperature approaches T_c . Hence this problem is not analytically tractable in 3+1 dimensions. We mention here that some 0 + 1 dimensional models can be studied analytically as reported in the later part of this thesis. In 3 + 1 dimensions, the issue of Z_N symmetry can only be studied using non-perturbative means. Previously, in the non-perturbative Monte Carlo(MC) simulations of SU(2)+Higgs theory, the partition function averages show Z_2 symmetry near the CD transition, in the continuum limit. In the present work, we extend this work to SU(3)+Higgs.

Chapter 3

Confinement deconfinement transition and Z_3 symmetry in SU(3)+Higgs theory

In this chapter, we discuss the effects of bosonic matter fields, the Higgs, on Z_3 symmetry and the CD transition in SU(3)+Higgs theory. The Higgs is considered to be in the fundamental representation of the SU(3) gauge group. We carry out Monte Carlo simulations of the partition function and compute partition function averages of the observables that are sensitive to Z_3 symmetry e.g. Polyakov loop, gauge-Higgs interaction action, etc. To study the cut-off dependence on the effect of Higgs on Z_3 symmetry and the CD transition, several values of N_τ are considered.

3.1 Numerical simulations of the CD transition and the Z_3 symmetry

The Euclidean action in presence of Higgs fields is given by

$$S[A_\mu, \Phi, \Phi^\dagger] = \int_V d^3x \int_0^\beta d\tau \left[\frac{1}{2} \text{Tr}(F_{\mu\nu} F_{\mu\nu}) + \frac{1}{2} (D_\mu \Phi)^\dagger (D_\mu \Phi) + \frac{m_H^2}{2} \Phi^\dagger \Phi + \frac{\lambda_H}{4!} (\Phi^\dagger \Phi)^2 \right]. \quad (3.1)$$

To carry out the Monte Carlo simulation, we consider a Euclidean space with spatial volume L^3 and inverse of temperature, $1/T$, as temporal extent. m_H is the bare Higgs mass and λ_H is the Higgs quartic coupling. This 3+1 dimensional Euclidean space is discretized into $N_s^3 \times N_\tau$ points. In terms of the lattice constant a , $N_s = (L/a)$ and $N_\tau = (1/Ta)$. The Higgs field Φ_n and gauge field $A_\mu(n)$ live at site n . $n \equiv (\vec{n}, n_4) \equiv (n_1, n_2, n_3, n_4)$ with $1 \leq (n_1, n_2, n_3) \leq N_s$ and $1 \leq n_4 \leq N_\tau$. The transition from the continuum to the lattice is basically effected by making the following substitutions:

$$\begin{aligned} x &\rightarrow na \\ \int d^4x &\rightarrow a^4 \sum_n \\ \Phi(x) &\rightarrow \Phi(n) \\ A_\mu(x) &\rightarrow A_\mu(n). \end{aligned} \quad (3.2)$$

Instead of the discretized gauge field $A_\mu(n)$, the lattice action is written in terms of gauge link $U_{n,\mu} = e^{igaA_\mu(n)}$, where g is the gauge coupling constant. The gauge link connects the lattice points n and $n + \hat{\mu}$. Here $\hat{\mu}$ is a unit vector in the μ -th direction, with $(\mu = 1, 2, 3, 4)$. Under a gauge transformation $V_n \in \text{SU}(N)$, the gauge links transform as

$$U_{n,\mu} = V_n U_{n,\mu} V_{n+\mu}^{-1}. \quad (3.3)$$

The gauge field strength can be written in terms of the plaquette U_P , which is path ordered product of links $U_{n,\hat{\mu}}$ along an elementary square, i.e.

$$U_P = U_{n,\hat{\mu}} U_{n+\hat{\mu},\hat{\nu}} U_{n+\hat{\mu}+\hat{\nu}}^\dagger U_{n,\hat{\nu}}^\dagger . \quad (3.4)$$

The sketch of an elementary plaquette U_P is shown in Fig. 3.1. This is a gauge invariant

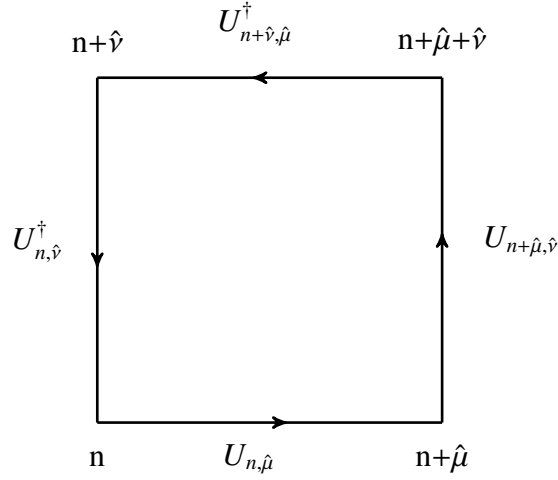


Figure 3.1: Sketch of an elementary plaquette U_P .

object. From Eq. 3.3, it can be easily seen that trace of a path-ordered product of links along closed loops is gauge invariant. From Eq. 3.4 U_P can be written in terms of field strength tensor as

$$U_P = e^{ia^2 g F_{\mu\nu}} . \quad (3.5)$$

For small lattice spacing, a , the exponential function can be expanded as follows

$$U_P = 1 + ia^2 g F_{\mu\nu}(n) - \frac{a^4 g^2}{2} [F_{\mu\nu}(n)]^2 - i \frac{a^6 g^3}{6} [F_{\mu\nu}(n)]^3 + \dots \quad (3.6)$$

The corresponding hermitian conjugate of U_P is

$$U_P^\dagger = 1 - ia^2 g F_{\mu\nu}(n) - \frac{a^4 g^2}{2} [F_{\mu\nu}(n)]^2 + i \frac{a^6 g^3}{6} [F_{\mu\nu}(n)]^3 + \dots \quad (3.7)$$

The terms with higher power of a can be neglected. Adding Eqs. 3.6 and 3.7 we have

$$\left[F_{\mu\nu}(n)\right]^2 \simeq \frac{1}{a^4 g^2} \left[2 - (U_P + U_P^\dagger)\right], \quad (3.8)$$

$$\text{Tr} \left[F_{\mu\nu}(n)\right]^2 = \frac{1}{a^4 g^2} \text{Tr} \left[2 - (U_P + U_P^\dagger)\right]. \quad (3.9)$$

The pure gauge Euclidean lattice action can be written as

$$S(U) = a^4 \frac{1}{2} \sum_n \text{Tr} \left[F_{\mu\nu}(n)\right]^2 = \beta_g \sum_p \left[1 - \frac{1}{2N} \text{Tr} (U_P + U_P^\dagger)\right], \quad (3.10)$$

where $\beta_g = 2N/g^2$. The covariant derivative on the lattice is given by

$$D_\mu \Phi(n) = \partial_\mu \Phi(n) + \frac{1 - U_{n,\hat{\mu}}}{a} \Phi(n), \quad (3.11)$$

where $\hat{\mu}$ is a vector of length, a , pointing along the μ -th direction. The 4-dimensional Laplacian, \square , is substituted by the lattice Laplacian, $\hat{\square}$, i.e.

$$\square \Phi(x) \rightarrow \frac{1}{a^2} \hat{\square} \Phi(n), \quad (3.12)$$

where

$$\hat{\square} \Phi(na) = \sum_\mu [\Phi(n + \hat{\mu}) + \Phi(n - \hat{\mu}) - 2\Phi(n)]. \quad (3.13)$$

Using all the above definitions of continuum operators and variables on the lattice, the corresponding total Euclidean action can be written as

$$\begin{aligned} S(U, \Phi) = & \beta_g \sum_p \left[1 - \frac{1}{2N} \text{Tr} (U_P + U_P^\dagger)\right] + \frac{8a^2}{2} \sum_n \text{Tr} (\Phi_n^\dagger \Phi_n) \\ & - a^2 \sum_{n,\mu} \text{Re} \text{Tr} (\Phi_{n+\mu}^\dagger U_{n,\mu} \Phi_n) - \frac{m_H^2 a^4}{2} \sum_n \text{Tr} (\Phi_n^\dagger \Phi_n) + \frac{\lambda_H a^4}{2} \sum_n \text{Tr} (\Phi_n^\dagger \Phi_n)^2. \end{aligned} \quad (3.14)$$

It is convenient to write the lattice action in terms of dimensionless variables, parameters etc. We use the following scaling of Φ , λ_H and the Higgs mass m_H [66] as

$$\Phi(x) \rightarrow \frac{\sqrt{\kappa}\Phi_n}{a}, \quad \lambda_H \rightarrow \frac{\lambda}{\kappa^2}, \quad m_H^2 \rightarrow \frac{(1 - 2\lambda - 8\kappa)}{a^2\kappa}, \quad (3.15)$$

In terms of the dimensionless field variables and parameters the total discretized lattice action can be written as

$$\begin{aligned} S(U, \Phi) = & \beta_g \sum_P \left[1 - \frac{1}{2N} \text{Tr}(U_P + U_P^\dagger) \right] - \kappa \sum_{n,\mu} \text{Re} \text{Tr}(\Phi_{n+\mu}^\dagger U_{n,\mu} \Phi_n) \\ & + \frac{1}{2} \sum_n \text{Tr}(\Phi_n^\dagger \Phi_n) + \lambda \sum_n \left(\frac{1}{2} \text{Tr}(\Phi_n^\dagger \Phi_n) - 1 \right)^2. \end{aligned} \quad (3.16)$$

For the present study we take, $N = 3$, $\lambda = 0$ and $m_H = 0$, and the resulting action can be written as [5, 66]

$$S = \beta_g \sum_P \left[1 - \frac{1}{2N} \text{Tr}(U_P + U_P^\dagger) \right] - \kappa \sum_{n,\mu} \text{Re}(\Phi_{n+\mu}^\dagger U_{n,\mu} \Phi_n) + \frac{1}{2} \sum_n (\Phi_n^\dagger \Phi_n). \quad (3.17)$$

$\kappa = 1/8$, for which, the system is found to be in the Higgs symmetric phase around the CD transition point. The gauge-Higgs interaction, the second term in Eq. 3.17, can be

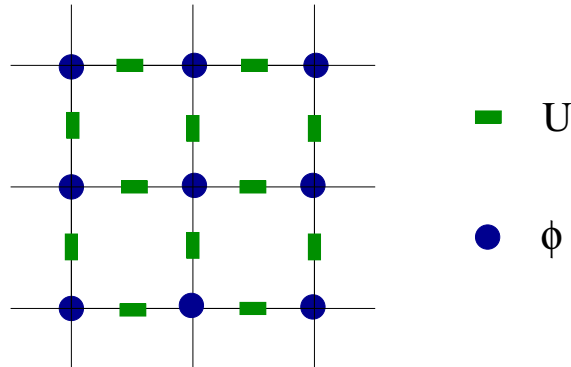


Figure 3.2: Position of gauge links U and Higgs fields Φ on the lattice.

graphically represented by Fig. 3.2. On the discrete lattice, the Polyakov loop is defined

as the path order product of gauge links along the temporal direction, i.e.

$$L(\vec{n}) = \prod_{n_4=1}^{N_\tau} U_{(\vec{n}, n_4), \hat{4}}. \quad (3.18)$$

The volume average of the Polyakov loop (L) is given by

$$L = \frac{1}{N_s^3} \sum_{\vec{n}} L(\vec{n}). \quad (3.19)$$

Under the gauge transformations, the Polyakov loop transforms as

$$L(\vec{n}) \rightarrow zL(\vec{n}). \quad (3.20)$$

The pure gauge part of the action is always invariant under the gauge transformations. But as mentioned above, the Φ fields cannot be transformed under nonperiodic gauge transformations, so the second term does not remain invariant under this transformation and the Z_3 symmetry is broken explicitly. As discussed in the previous chapter, only the terms involving the temporal links in the gauge-Higgs interaction terms break the Z_3 symmetry. The strength of the explicit breaking can be obtained by numerical simulations of the partition function and calculating averages of Z_3 sensitive observables, such as the Polyakov loop.

The numerical simulations of the above action in Eq. 3.17 results in a sequence of statistically independent configurations of $(U_{n,\mu}, \Phi_n)$ as follows. Using the Monte Carlo methods, an initial configuration of $\{U_{n,\mu}, \Phi_n\}$ is updated according to the probability distribution, $\exp(-S)$. To update a given link $U_{n,\mu}$, the rest of the fields coupled to it are treated as heat-bath. A new choice for the link is generated using the standard heat-bath method [10, 11], which we describe in the following.

For SU(3) link variables, there is no direct heat-bath algorithm. However, a pseudo-heat-bath algorithm can be formulated by updating the different SU(2) subgroups of SU(3) so

then the recursion relation can be obtained as

$$U^{(q)} = A_q U^{q-1}, \quad U^{(p)} = U'. \quad (3.24)$$

Note that our SU(3) pure gauge action is of the Wilson-action type, i.e.

$$S(U) \simeq -\frac{\beta_g}{N} \text{Re Tr}(UV), \quad (3.25)$$

where V is the sum of staples connected to the link U and $V \notin \text{SU}(3)$. It is a general 3×3 complex matrix. Now each multiplication with A_q gives rise to a heat bath distribution of the SU(2) group as described below.

$$S(A_q U) = -\frac{\beta_g}{N} \text{Re Tr}(A_q UV) = -\frac{\beta_g}{N} \text{Re Tr}(a_q w_q) + \text{terms independent of } a_q, \quad (3.26)$$

with $w_q = \begin{pmatrix} W_{ii} & W_{ij} \\ W_{ji} & W_{jj} \end{pmatrix}$, where $W = UV$. Here $a_q = a_0 + i\vec{a} \cdot \vec{\sigma}$ with $a_0^2 + |\vec{a}|^2 = 1$. The vector $\vec{a} = (a_1, a_2, a_3)$ and σ 's are the Pauli matrices. w_q now takes over the role of the SU(2)-staple as described in Eq. 3.28.

To proceed further as given in reference [67,68], we consider the following Wilson action to update the SU(2) subgroup of the link variable

$$S = \beta_g \sum_P \left[1 - \frac{1}{2} \text{Re Tr } U_P \right]. \quad (3.27)$$

The plaquette U_P contains the link variable $U \in \text{SU}(2)$ and the staple V . The probability of a link U is

$$dP(U) \propto dU \exp \left\{ \frac{\beta_g}{2} \text{Re Tr}(UV) \right\}, \quad (3.28)$$

where $V = \sum_{i=1}^6 V_i$ is the sum of the 6 staples connected to the link U . The link variable

U is an $SU(2)$ group element and can be parametrized as

$$U = \alpha_0 + i\vec{\alpha} \cdot \vec{\sigma}, \quad \vec{\alpha} = (\alpha_1, \alpha_2, \alpha_3), \quad (3.29)$$

The unitarity condition implies that $\alpha_0^2 + |\vec{\alpha}|^2 = 1$. The invariant group measure in terms of this parametrization is

$$dU = \frac{1}{2\pi^2} \delta(\alpha^2 - 1) d^4\alpha. \quad (3.30)$$

Now if $\hat{U} \in SU(2)$ then $\hat{U} = V/\sqrt{\det V} = V/c$, where $c = \sqrt{\det V}$. Since dU is an invariant measure we can write

$$\begin{aligned} dP(U\hat{U}^{-1}) &\propto dU \exp\left\{\frac{\beta_g}{2} \text{Re Tr}(U\hat{U}^{-1})\right\} \\ &= dU \exp\left\{\frac{\beta_g}{2} c \text{Re Tr } U\right\}. \end{aligned} \quad (3.31)$$

As $\text{Tr } U = 2\alpha_0$, the probability $dP(U)$ depends on α_0 . Thus we have to generate a U such that

$$dP(U) = dU \exp(\beta_g c \alpha_0). \quad (3.32)$$

Once α_0 is chosen, the vector $\vec{\alpha}$ can take any value on the surface of a sphere whose radius is $\sqrt{1 - \alpha_0^2}$. Thus α_0 needs to be generated in the interval $[-1, 1]$ with a probability

$$P(\alpha_0) \propto \sqrt{1 - \alpha_0^2} \exp(\beta_g c \alpha_0). \quad (3.33)$$

To generate α_0 with the above probability, the Creutz method is used [67]. In this method the factor $\exp(\beta_g c \alpha_0)$ generates α_0 , then the generated α_0 is accepted or rejected with the other factor $\sqrt{1 - \alpha_0^2}$. Now if the distribution of α_0 is peaked close to one, which is where the prefactor $\sqrt{1 - \alpha_0^2}$ is small, then the rejection rate becomes very large. To improve this, an alternative method has been introduced by Kennedy and Pendleton in ref [11]. In the following, we describe the standard updating procedure for the Higgs field [69].

To update a component of Φ_n , effective action is written down by collecting all terms in the

action with the particular component [69]. As it turns out for $m_H = 0$ the effective action is Gaussian. The width of the gaussian is a constant and does not depend on the nearest neighbour fields which act as heat-bath. The updating process is repeated for all the links and site variables. Since a new configuration is generated from an old one, the two are correlated. To reduce this correlation, we have calculated the autocorrelation of the Polyakov loop as $C(i) = \sum_{\tau} (\langle L(\tau)L(\tau+i) \rangle - \langle L(\tau) \rangle^2)$, where $L(\tau)$ and $L(\tau+i)$ correspond to the measured value of L for the τ -th and $(\tau+i)$ -th configurations in the Monte Carlo history. We extract the slope of $h = -\log [C(i)]$. The entire field configuration of the lattice is updated h times before a new configuration is accepted in the Monte Carlo history. The partition function averages are obtained by averaging observables over this history. The observables computed, to study the CD transition and explicit breaking of Z_3 , are the average of the Polyakov loop ($\langle |L| \rangle$) and its distributions $H(L)$, $H(\text{Arg}(L))$, the gauge-Higgs interaction term ($S_K = \text{Re} \sum_{n,\mu} (\Phi_{n+\mu}^\dagger U_{n,\mu} \Phi_n)$) and the plaquette ($S_g = \sum_p U_p$). The simulations were carried out for several values of $N_\tau = 2, 3, 4, 8, 12$, to study the continuum limit. The simulations of pure SU(3) were also carried out to observe changes effected by the presence of the Higgs field. We set $N_s \geq 4N_\tau$ for all the simulations.

3.2 The CD transition *vs* N_τ

The previous studies have shown that, in pure SU(3) gauge theory the nature of CD transition is first order [2, 34, 35, 70–82] and it does not depend on N_τ . The nature of this

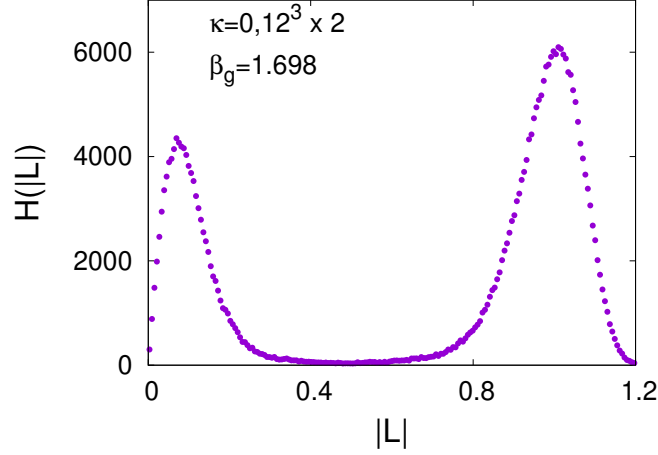


Figure 3.3: $H(|L|)$ for $N_\tau = 2$ at $\beta_g = 1.698$ and $\kappa = 0$.

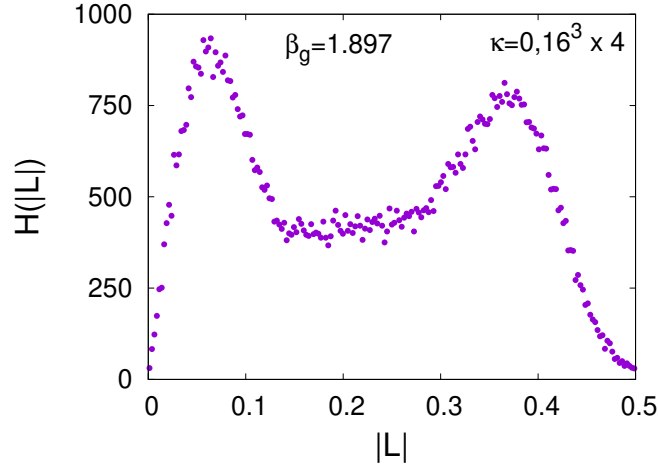


Figure 3.4: $H(|L|)$ for $N_\tau = 4$ at $\beta_g = 1.897$ and $\kappa = 0$.

transition is easily identified by $|L|$, its fluctuations, and the histograms of $|L|$, etc. In our simulations $N_s = 4N_\tau$ in most cases except when we consider finite-size scaling analysis. In Fig. 3.3 we show the histogram of Polyakov loop $H(|L|)$ for $N_\tau = 2$ at $\beta_g = 1.698$. In Fig. 3.4, the same is plotted for $N_\tau = 4$ at $\beta_g = 1.897$. Since the transition is first order and the β_g values are near the transition point, the histogram shows two peaks. The peak corresponding to the smaller(higher) value of $|L|$ corresponds to the confined(deconfined)

phase.

In order to study the nature of CD phase transition for pure SU(3) gauge theory, the average of absolute value of the Polyakov loop (L) vs β_g for $N_\tau = 2$ and 4 is plotted in Figs. 3.5 and 3.6 respectively. The simulation results for pure SU(3) agree with previous

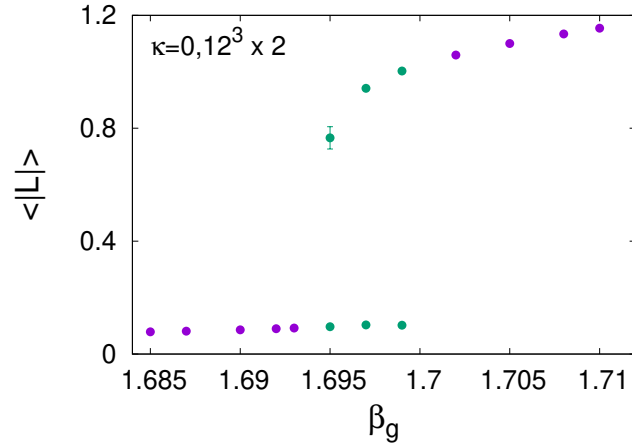


Figure 3.5: $\langle |L| \rangle$ vs β_g for $N_\tau = 2$.

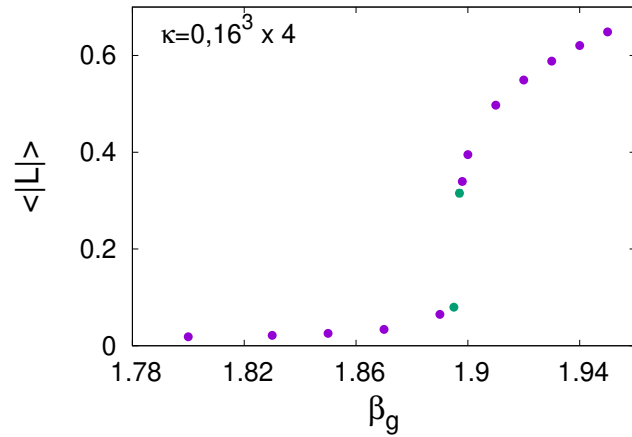


Figure 3.6: $\langle |L| \rangle$ vs β_g for $N_\tau = 4$.

results [74, 76]. The nature of the CD transition is found to be independent of N_τ as well. As in previous studies [73–75], the transition region shifts to higher values with N_τ . There is a range of β_g for which there are two values of $|L|$. These correspond to the two peaks of $H(|L|)$. In the simulations for small lattice sizes, both the confined and deconfined phases are sampled near the transition point (β_{gc}). In this case, $\langle |L| \rangle$ will lie somewhere between

the confined and deconfined values. As a result of this, $\langle |L| \rangle$ vs β_g may seem continuous. In the figures, we indicate the β_g values, by green color, for which both states are sampled. The scatter plots of the real and imaginary parts of the Polyakov loop are shown in Figs. 3.7–3.9 for $N_\tau = 2$ for different values of β_g . For $\beta_g = 1.692$, the scatter plot is Z_3 -symmetrically distributed around zero which gives $\langle |L| \rangle = 0$, i.e. the system is in the confined phase. At $\beta_g = 1.698$, there is a coexistence of both confined and deconfined

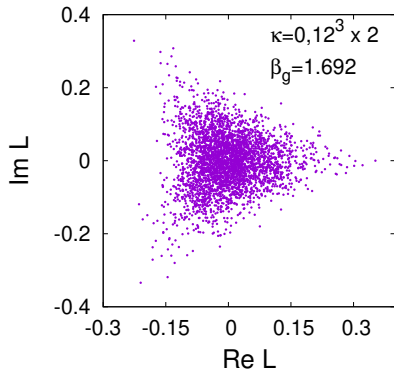


Figure 3.7: Confined phase.

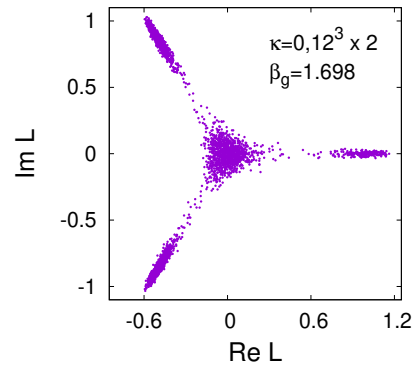


Figure 3.8: Near critical point.

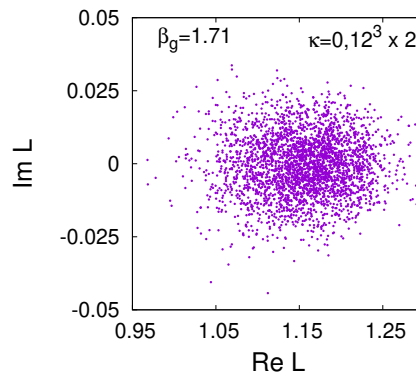


Figure 3.9: Deconfined phase.

phases. The three different states at $\theta = 0, 2\pi/3$ and $4\pi/3$, away from the central patch, are in the deconfined phase. For $\beta_g = 1.71$, there is only one state which lies in the deconfined phase for which $\langle |L| \rangle \neq 0$. For this β_g the different Z_3 states are not sampled. The Z_3 state sampled is biased by the initial configuration of the links. The coexistence of the confined and deconfined phases and the discontinuous jump in $\langle |L| \rangle$ show that the transition is first order. Similar results are obtained for higher N_τ as well.

To observe the effects of Higgs (Φ) as matter fields on the CD transition and the Z_3 symmetry, we compute the Polyakov loop average and its fluctuations for different values of β_g for $\kappa = 0.125$. Figs. 3.10 and 3.11, show results of β_g dependence of $\langle |L| \rangle$ and its fluctuations χ_L for $N_\tau = 2$.

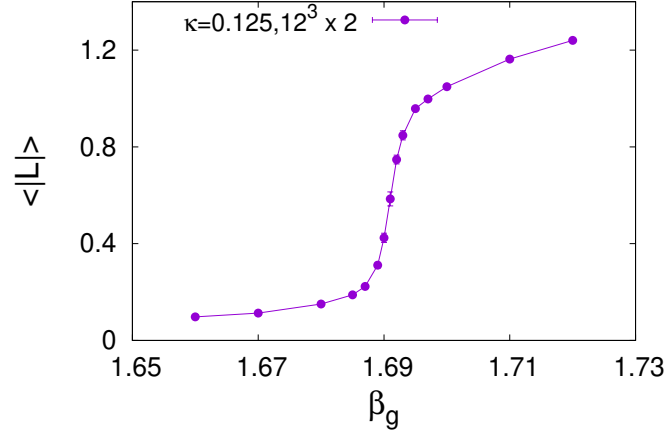


Figure 3.10: Polyakov loop vs β_g for $\kappa = 0.125$.

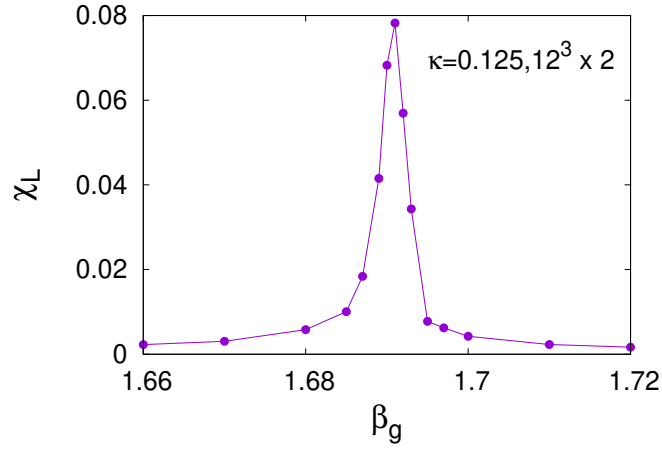


Figure 3.11: Susceptibility vs β_g for $\kappa = 0.125$.

As can be seen, $\langle |L| \rangle$ varies continuously suggesting a continuous transition. The corresponding fluctuations, χ_L , sharply peaked around $\beta_{gc} \sim 1.691$. However, determining whether the transition is a crossover or a second order, will require finite-size scaling analysis. This change in the nature of the transition from first order to continuous suggests that the Z_3 symmetry is getting affected by the presence of the Higgs fields at finite $N_\tau = 2$.

The Figs. 3.12 and 3.13 shows the histogram $H(|L|)$ for $N_\tau = 3$ and $N_\tau = 4$, at $\beta_g = 1.854$ and $\beta_g = 1.904$ respectively. We have taken, $N_s = 4N_\tau$. The two peaks in $H(|L|)$ suggest that the CD transition is first order.

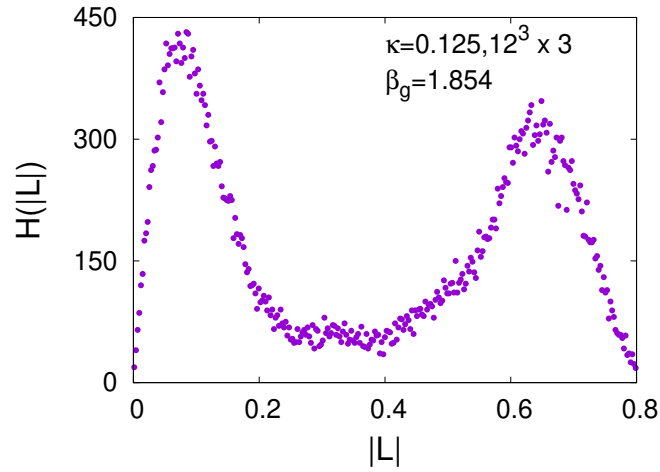


Figure 3.12: $H(|L|)$ for $N_\tau = 3$ at $\beta_g = 1.854$ and $\kappa = 0.125$.

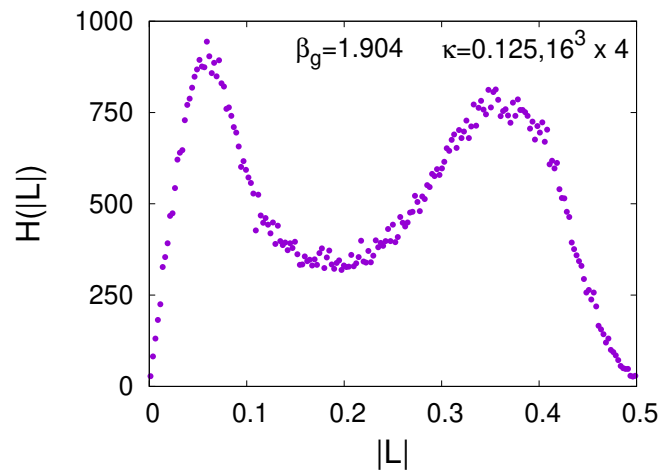


Figure 3.13: $H(|L|)$ for $N_\tau = 4$ at $\beta_g = 1.904$ and $\kappa = 0.125$.

We follow the same method as in the pure SU(3) case to calculate the Polyakov loop average $\langle |L| \rangle$. The results for $\langle |L| \rangle$ vs β_g are shown in Figs. 3.14 and 3.15 for $N_\tau = 3$ and 4 respectively. The results do not change qualitatively for higher N_s . The results from

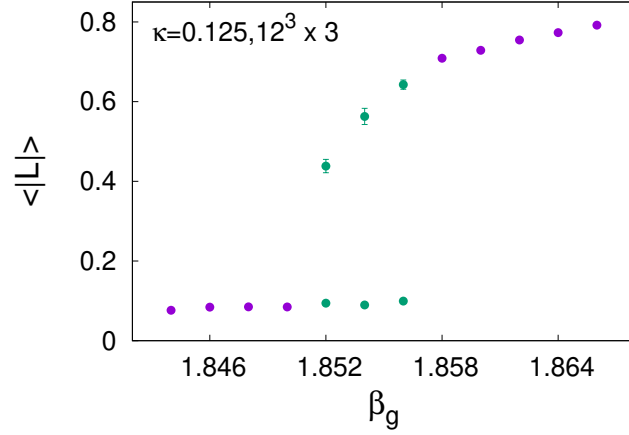


Figure 3.14: $\langle |L| \rangle$ vs β_g for $N_\tau = 3$.

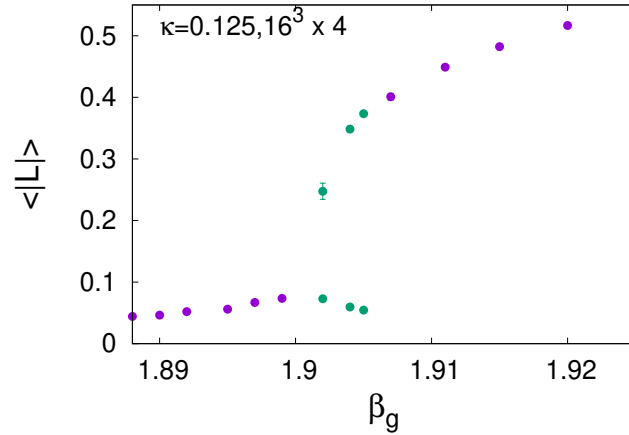


Figure 3.15: $\langle |L| \rangle$ vs β_g for $N_\tau = 4$.

$N_\tau = 2$ to $N_\tau = 4$ show that the nature of CD transition changes with N_τ . For higher N_τ the CD transition continues to be the first order. Since higher N_τ corresponds to a smaller cut-off, these results suggest that the CD transition is first order in the continuum limit. The first-order transition is also accompanied by the effective realization of Z_3 symmetry, as we discuss in the following section.

3.3 Z_3 symmetry vs N_τ

In this section, we present observables that are sensitive to the Z_3 symmetry, i.e. the distribution of the Polyakov loop in the complex plane, the average of the gauge-Higgs interaction S_K and the gauge action S_g etc. When there is Z_3 symmetry, the distribution should be invariant, as the transformation $L \rightarrow zL$ is made. Also, the difference in S_K between different Z_3 states in the deconfined state should vanish. Here, Z_3 states refer to peaks in the distribution of the Polyakov loop, away from the origin, in the complex L -plane. These states can also be seen in the scattered plot of L values from the Monte Carlo history, as patches for which the Polyakov loop phase (θ) is close to $0, 2\pi/3$ and $4\pi/3$, seen in Fig. 3.17.

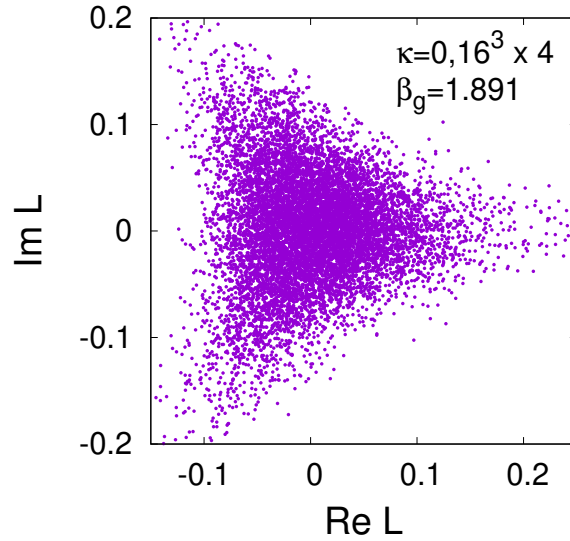


Figure 3.16: Distribution of L in the confined phase for $N_\tau = 4$.

The distributions of L for pure SU(3) are shown in Figs. 3.16 and 3.17 at $\beta_g = 1.891$ and $\beta_g = 1.92$ respectively. The distribution in Fig. 3.16 corresponds to the confined phase and in Fig. 3.17 corresponds to the deconfined phase. It can be seen that both distributions are almost Z_3 symmetric. A Z_3 rotation in the complex plane will result in identical figures.

In the deconfined phase, $\beta_g > \beta_{gc}$, the symmetry is spontaneously broken, which leads to Z_3 -states. The three patches in Fig. 3.17 correspond to the three Z_3 -states. Note that all the three states, for β_g away from β_{gc} , can not be sampled in a single MC run as the tunnelling rate between them is very small. To sample different Z_3 states we consider MC runs with different initial conditions. Though the Polyakov loop values differ, they have the same free energy.

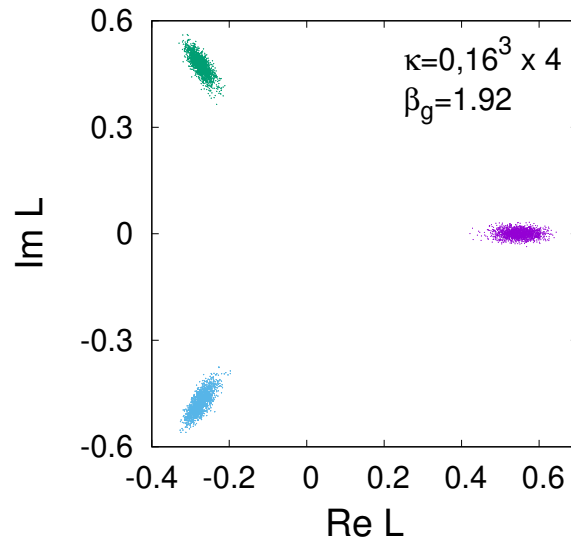


Figure 3.17: Distribution of L in the deconfined phase for $N_\tau = 4$.

In the presence of Higgs, we show the distribution $H(\theta)$ of the Polyakov loop phase (θ) in Fig. 3.18 at $\beta_{gc} = 1.691$ for $12^3 \times 2$ lattice. If there was Z_3 symmetry or if the Z_3 explicit breaking was small, then the distribution would have peaks near $\theta = 2\pi/3$ and $\theta = 4\pi/3$.

The figure clearly shows that there is only one peak in the distribution, signifying a

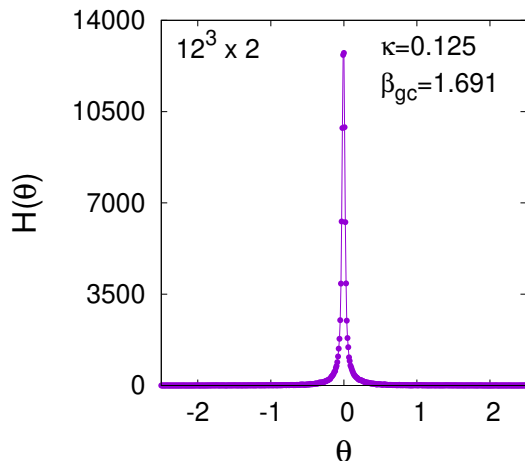


Figure 3.18: Distribution of phase of the Polyakov loop for $\langle |L| \rangle = 0.584874$.

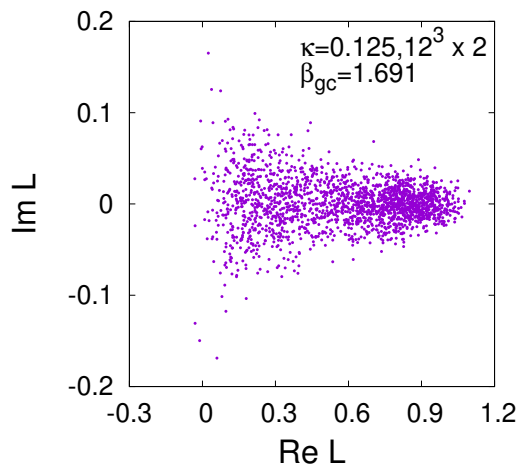


Figure 3.19: L on the complex plane for $12^3 \times 2$ lattice.

large explicit breaking of the Z_3 symmetry. The corresponding scattered plot of L on the complex plane is shown in Fig. 3.19 and it shows there is only one state at $\theta = 0$. Also, for other values of β_g near β_{gc} only one state appears which indicates that the Z_3 symmetry is broken explicitly. No change is observed for higher statics. Note that, for $N_\tau = 2$ the Z_3 states corresponding to $\theta = 2\pi/3, 4\pi/3$, arise for β_g away from the transition point,

i.e. deep in the deconfinement phase [46]. For $N_\tau = 4$, Fig. 3.20 shows $H(\theta)$ close to

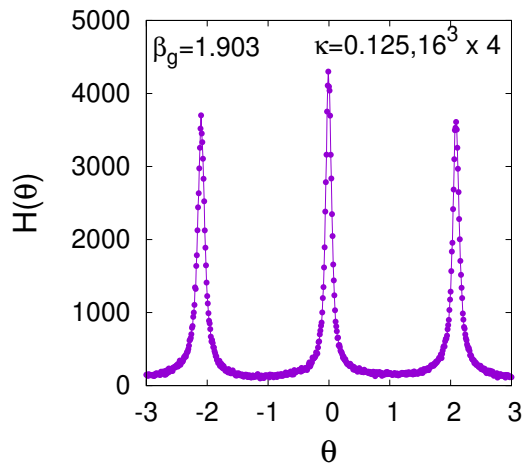


Figure 3.20: Distribution of phase of the Polyakov loop.

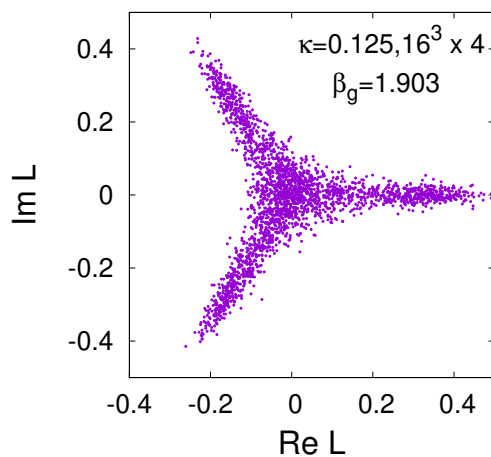


Figure 3.21: L on the complex plane for $16^3 \times 4$ lattice.

the critical point. There is a slight Z_3 asymmetry in $H(\theta)$, though peaks corresponding to $\theta = 2\pi/3, 4\pi/3$ are almost comparable to that of the peak at $\theta = 0$. In Fig. 3.21 the measured values of L , for same β_g , are plotted in the complex plane. The distribution of the scattered points is almost Z_3 symmetric. These results suggest that for larger N_τ the explicit breaking of Z_3 , near the transition point significantly decreases.

To compare the physical properties of the different Z_3 states, in the continuum limit, we compute observables such as $S_K = \text{Re} \sum_{n,\mu} (\Phi_{n+\mu}^\dagger U_{n,\mu} \Phi_n)$ and $S_g = \sum_p U_p$ between $\theta = 0$ and $\theta = 2\pi/3$ by varying N_τ . The β_g values, for each N_τ , are chosen such that they all correspond to the same physical temperature according to the one-loop beta-function [50]. Note that, for higher N_τ one loop beta-function will provide valid estimates of the temperature. In Figs. 3.22 and 3.23, the difference in S_K and S_g between $\theta = 0$ and $\theta = 2\pi/3$

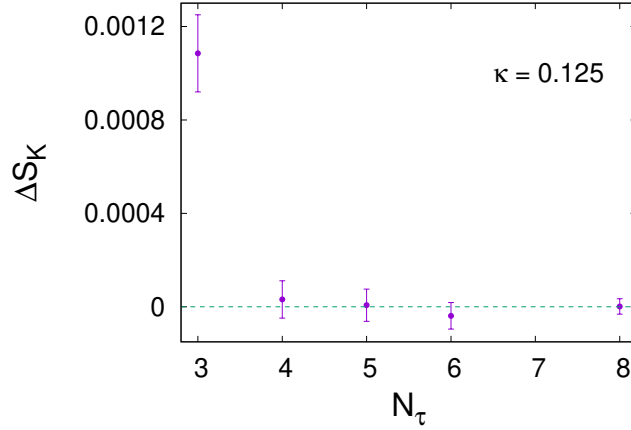


Figure 3.22: Difference of S_K between $\theta = 0$ and $2\pi/3$ in the deconfined phase.

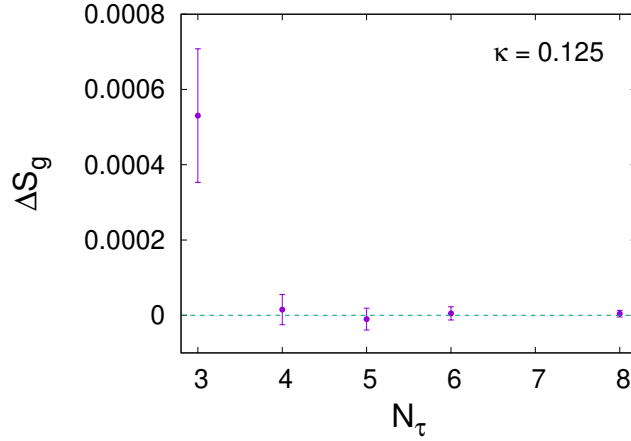


Figure 3.23: Difference of S_g between $\theta = 0$ and $2\pi/3$ in the deconfined phase.

vs N_τ are respectively plotted. These results correspond to the same physical temperature $T = 3.2314 \Lambda_L$ in the deconfined phase, where Λ_L is an integration constant with the dimension of a mass in the beta function. The results show that ΔS_K and ΔS_g correspond-

ing to $\theta = 0$ and $\theta = 2\pi/3$ decreases with N_τ and approaches vanishingly small value at a large N_τ limit. The free energy difference between them can be calculated by computing $\Delta S_g(m_H)$ and integrating it over m_H . Since $\Delta S_g(m_H = \infty) = 0$ and our results suggest that $\Delta S_g(m_H = 0)$ is vanishingly small for large N_τ , we expect $\Delta S_g = 0 \forall m_H$. This will result in a vanishingly small free energy difference between the Z_3 states in the continuum limit.

The above results suggest that the explicit breaking Z_3 symmetry will be vanishingly small in the continuum limit. To test whether the decrease in Z_3 explicit breaking with N_τ is due to a decrease in the interaction between the gauge and Higgs fields with N_τ , we compare the gauge Higgs interaction term (S_K) in the action, Eq. 3.17. Note that, a weaker interaction with increasing N_τ should lead to a decrease in S_K . Our results, in Fig. 3.24, show that S_K increases monotonically with N_τ . The increase slows down with N_τ , as it should saturate for larger N_τ , i.e. continuum limit. These results suggest that the Z_N symmetry in the continuum limit is not due to the Higgs mass exceeding the inverse of the lattice spacing and effectively falling through the lattice.

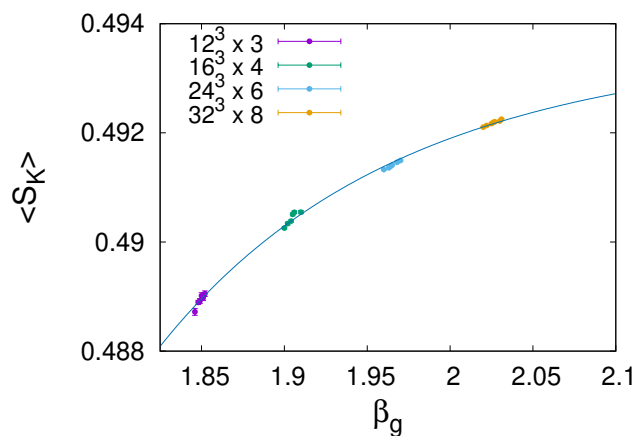


Figure 3.24: S_K for different N_τ near β_{gc} .

It will be helpful to obtain such results, where the partition function averages exhibit the Z_N symmetry even though the action breaks it explicitly, through analytical calculations. However, the exact calculation of the partition function in $(3 + 1)$ -dimensional theories is extremely difficult. In the next chapter, we consider a one-dimensional chain of

fermionic/bosonic matter fields which are in the fundamental representation of the $SU(N)$ gauge group. These two toy models are exactly integrable, i.e. the matter fields can be integrated out exactly. Thus, we are able to calculate the free energy as a function of the Polyakov loop for any arbitrary gauge field background.

Chapter 4

Gauged 1 – d chain of $SU(N)$ in presence of matter fields

In this chapter, we consider a one-dimensional lattice toy model of $SU(N)$ gauge theories in presence of matter fields. We work with a $0 + 1$ lattice action, which can be derived from one-dimensional continuum action. The one-dimensional chain can also be derived from the terms in $3 + 1$ dimensional action, which breaks the Z_N explicitly. Interestingly, the Z_N explicit breaking is caused by terms in the action involving temporal derivatives of matter fields. On the lattice, these terms at different spatial sites do not couple. Hence, the explicit breaking terms in $3 + 1$ are a collection of one-dimensional chains. The matter fields can be integrated out from the partition function of these chains, for any arbitrary background of gauge fields. This calculation results in free energy as a function of the Polyakov loop. The strength of the explicit breaking of Z_N can be obtained from this free energy.

4.1 Gauged 1 – d chain of SU(N) – Higgs

The SU(N)+Higgs action on the Euclidean lattice, for vanishing Higgs mass and quartic interactions, can be written as [5]

$$S = \beta_g \sum_p \left[1 - \frac{1}{2} \text{Tr} (U_p + U_p^\dagger) \right] - b \sum_{n,\hat{\mu}} (\Phi_n^\dagger U_{n,\hat{\mu}} \Phi_{n+\hat{\mu}} + h.c.) + a \sum_n \Phi_n^\dagger \Phi_n . \quad (4.1)$$

β_g is the gauge coupling constant, $a = \frac{1}{2}$ and the coupling $b = (m_b^2 + 8)^{-1}$, the Higgs mass m_b is expressed in lattice units [5]. The part of the action which breaks the Z_N symmetry explicitly is given by

$$S' = -b \sum_n (\Phi_n^\dagger U_{n,\hat{4}} \Phi_{n+\hat{4}} + h.c.) . \quad (4.2)$$

One can start from a continuum 1-dimensional toy model whose lattice discretization will result in the action in Eq. 4.2 [52–56]. As mentioned previously, the Φ fields in S' do not interact with nearest neighbours in the spatial direction. Therefore, we can rewrite the action as

$$S' = \sum_m S_m , \quad S_m = \sum_{\tau=1}^{N_\tau} -b (\Phi_{m+\tau\hat{4}}^\dagger U_{m+\tau\hat{4}} \Phi_{m+(\tau+1)\hat{4}} + h.c.) , \quad (4.3)$$

where $m = (n_1, n_2, n_3)$ denotes the spatial sites and $\hat{4}$ denotes an unit vector along the temporal direction. S_m represents the action for the one-dimensional gauged chain, along the temporal direction, anchored at the spatial site m . Since the Φ field at different spatial sites do not couple, the partition function corresponding to the action of Eq. 4.2 can be written as

$$\mathcal{Z}(U_{(m,n_4),\hat{4}}) = \int \prod_{m,n_4} d\Phi_{m,n_4} \text{Exp} [-S'] = \left(\int \prod_{n_4} d\Phi_{n_4} \text{Exp} [-S_{m=1}] \right)^{N_s^3} . \quad (4.4)$$

We simplify the notations and write $S_{m=1}$ as

$$S = a \sum_{i=1}^{N_\tau} \Phi_i^\dagger \Phi_i - b \sum_{i=1}^{N_\tau} (\Phi_i^\dagger U_i \Phi_{i+1} + h.c.) . \quad (4.5)$$

For convenience, the subscripts of the field variables have been replaced by i . N_τ denotes the number of temporal sites. Φ satisfies periodic boundary condition, i.e. $\Phi_{N_\tau+1} = \Phi_1$.

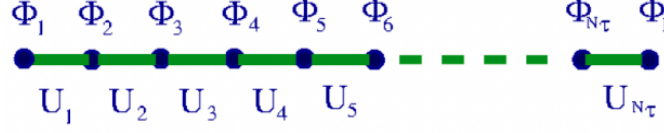


Figure 4.1: one-dimensional temporal chain.

The one-dimensional temporal chain, corresponding to the action of Eq. 4.5, is shown in Fig. 4.1. The Polyakov loop for the above chain

$$L = \frac{1}{N} \text{Tr} \left(\prod_{i=1}^{N_\tau} U_i \right), \quad (4.6)$$

transforms under Z_N transformation as $L \rightarrow zL$. The free energy $V(L)$, in units of temperature, is given by

$$V(L) = -\log(\mathcal{Z}_L), \quad (4.7)$$

where the partition function \mathcal{Z}_L is given by

$$\mathcal{Z}_L = \int \prod_{i=1}^{N_\tau} d\Phi_i^\dagger d\Phi_i \text{Exp}[-S]. \quad (4.8)$$

In order to derive the free energy $V(L)$, only the Φ_i fields in the partition function \mathcal{Z}_L are to be integrated out. To simplify the calculation we consider a gauge choice in which $U_i = \mathbb{1}$ for $i = 1, 2, \dots, N_\tau - 1$ and $U_{N_\tau} = U$. Note that this gauge choice preserves the Polyakov loop ($L = \text{Tr}(U)/N$).

For convenience the action in Eq. 4.5 is written as $S = S_1 + S_2$ as in the following

$$\begin{aligned} S_1 &= a\Phi_1^\dagger\Phi_1 - b(\Phi_{N_\tau}^\dagger U\Phi_1 + h.c.) \\ S_2 &= a \sum_{i=2}^{N_\tau} \Phi_i^\dagger\Phi_i - b \sum_{i=1}^{N_\tau-1} (\Phi_i^\dagger\Phi_{i+1} + h.c.). \end{aligned} \quad (4.9)$$

The Higgs field being in the fundamental representation of the $SU(N)$ gauge group at the i -th site can be written as

$$\Phi_i = \begin{pmatrix} \phi_i^1 \\ \phi_i^2 \\ \vdots \\ \phi_i^N \end{pmatrix}, \quad (4.10)$$

with $\phi_i^1, \phi_i^2, \dots, \phi_i^N$ are all complex. At first, the fields Φ_2 to $\Phi_{N_\tau-1}$ are integrated out sequentially using Gaussian integration, i.e.

$$\mathcal{Z} = \int \prod_{i=2}^{N_\tau-1} d\Phi_i^\dagger d\Phi_i \text{Exp}[-S_2]. \quad (4.11)$$

Afterwards, the remaining integration of Φ_1 and Φ_{N_τ} can be carried out to obtain the partition function

$$\mathcal{Z}_L = \int d\Phi_1^\dagger d\Phi_1 d\Phi_{N_\tau}^\dagger d\Phi_{N_\tau} (\mathcal{Z} \times \text{Exp}[-S_1]). \quad (4.12)$$

The integration of Φ_1 and Φ_{N_τ} requires evaluation of the determinant of a matrix of size $4N \times 4N$. The integrations of Φ_2 to $\Phi_{N_\tau-1}$ greatly simplify the problem, otherwise one would have to deal with evaluating a matrix whose size depends on N_τ .

In the integration of \mathcal{Z} in Eq. 4.11, due to the gauge choice mentioned above, the different components, i.e. ϕ_i , as well as the real and imaginary parts of any ϕ_i 's do not mix.

Therefore it can be written as

$$\mathcal{Z} = \prod_{r=1}^{2N} \mathcal{I}(\Phi_{1,r}, \Phi_{N_\tau,r}), \quad (4.13)$$

where $\Phi_{1,r}$ and $\Phi_{N_\tau,r}$ are the r -th component of Φ_1 and Φ_{N_τ} respectively. $\mathcal{I}(\Phi_{1,r}, \Phi_{N_\tau,r})$ is obtained by integrating out r -th component of Φ_2 to $\Phi_{N_\tau-1}$. The integration result will be a function of r -th component of Φ_1 and Φ_{N_τ} . The function for other components can be replaced by corresponding components of Φ_1 and Φ_{N_τ} . Hence, in the following, we

ignore the subscript r and denote the r -th component by ϕ as

$$\mathcal{I}(\phi_1, \phi_{N_\tau}) = \int \prod_{i=2}^{N_\tau-1} d\phi_i \text{Exp}[-S'_2], \quad (4.14)$$

where

$$S'_2 = a \sum_{i=2}^{N_\tau-1} \phi_i^2 - 2b \sum_{i=1}^{N_\tau-1} \phi_i \phi_{i+1}. \quad (4.15)$$

The integration $\mathcal{I}(\phi_1, \phi_{N_\tau})$, in Eq. 4.14, can also be written as

$$\mathcal{I}(\phi_1, \phi_{N_\tau}) = \int \prod_{i=3}^{N_\tau-1} d\phi_i e^{-S'_3} \int d\phi_2 \text{Exp}[-a\phi_2^2 + 2\phi_2(b\phi_1 + b\phi_3)]. \quad (4.16)$$

S'_3 is obtained by taking out terms from S'_2 which are dependent on ϕ_2 . After ϕ_2 is integrated out

$$\mathcal{I}(\phi_1, \phi_{N_\tau}) = \int \prod_{i=3}^{N_\tau-1} d\phi_i e^{-S'_3} \sqrt{\frac{\pi}{a}} \text{Exp}\left[\frac{1}{a}(b\phi_1 + b\phi_3)^2\right], \quad (4.17)$$

which can also be written as

$$\begin{aligned} \mathcal{I}(\phi_1, \phi_{N_\tau}) &= \int \prod_{i=4}^{N_\tau-1} d\phi_i e^{-S'_4} \\ &\times \sqrt{\frac{\pi}{a}} \int d\phi_3 \text{Exp}\left[-\left(a - \frac{b^2}{a}\right)\phi_3^2 + 2\phi_3\left(\frac{b^2}{a}\phi_1 + b\phi_4\right) + \frac{b^2}{a}\phi_1^2\right]. \end{aligned} \quad (4.18)$$

Here again S'_4 is S'_2 without terms containing ϕ_2 and ϕ_3 . Given the forms of $\mathcal{I}(\phi_1, \phi_{N_\tau})$ in Eqs. 4.16 and 4.18 one can easily write down the form of $\mathcal{I}(\phi_1, \phi_{N_\tau})$ after integration of ϕ_{k-1} as

$$\begin{aligned} \mathcal{I}(\phi_1, \phi_{N_\tau}) &= \int d\phi_{k+1} \dots d\phi_{N_\tau-1} e^{-S'_{k+1}} \\ &\times I_k \int d\phi_k \text{Exp}\left[-A_k\phi_k^2 + 2\phi_k(B_k\phi_1 + b\phi_{k+1}) + E_k\phi_1^2\right]. \end{aligned} \quad (4.19)$$

Carrying out the ϕ_k integration will result in

$$\begin{aligned} \mathcal{I}(\phi_1, \phi_{N_\tau}) &= \int d\phi_{k+2} \dots d\phi_{N_\tau-1} e^{-S'_{k+2}} \\ &\times I_{k+1} \int d\phi_{k+1} \text{Exp} \left[-A_{k+1} \phi_{k+1}^2 + 2\phi_{k+1} (B_{k+1} \phi_1 + b\phi_{k+2}) + E_{k+1} \phi_1^2 \right]. \end{aligned} \quad (4.20)$$

From Eqs. 4.19 and 4.20, one can read off the following recursion relations

$$I_{k+1} = \sqrt{\frac{\pi}{A_k}}, \quad A_{k+1} = a - \frac{b^2}{A_k}, \quad B_{k+1} = \frac{bB_k}{A_k}, \quad E_{k+1} = E_k + \frac{B_k^2}{A_k}, \quad (4.21)$$

with $I_2 = 1$, $A_2 = a$, $B_2 = b$ and $E_2 = 0$. Using these recursion relations we can work out the integration, $\mathcal{I}(\phi_1, \phi_{N_\tau})$ completely. Using $\mathcal{I}(\phi_1, \phi_{N_\tau})$'s one can write the partition function as

$$\begin{aligned} \mathcal{Z}_L &= Q \int d\Phi_1^\dagger d\Phi_1 d\Phi_{N_\tau}^\dagger d\Phi_{N_\tau} \\ &\times \text{Exp} \left[-A_{N_\tau} \Phi_{N_\tau}^\dagger \Phi_{N_\tau} - C_{N_\tau} \Phi_1^\dagger \Phi_1 + \left(\Phi_{N_\tau}^\dagger (B_{N_\tau} \mathbb{1} + bU) \Phi_1 + h.c. \right) \right], \end{aligned} \quad (4.22)$$

where

$$Q = \prod_{k=2}^{N_\tau} I_k^n, \quad n = 2N. \quad (4.23)$$

n corresponds to the number of components of the Φ field. The coefficient $C_{N_\tau} = a - E_{N_\tau}$. After the integration of the remaining fields Φ_1 and Φ_{N_τ} , the partition function takes the form

$$\mathcal{Z}_L = Q \sqrt{\frac{\pi^8}{\text{Det}(M)}}. \quad (4.24)$$

M is $(4N \times 4N)$ given by

$$\begin{pmatrix} A_{N_\tau} & B_{N_\tau} + bU \\ B_{N_\tau} + bU^\dagger & C_{N_\tau} \end{pmatrix}.$$

The exact form of $\text{Det}(M)$ for arbitrary N is difficult to find. However, the sequential integration has greatly simplified the problem. For arbitrary N_τ we need to deal with a

matrix of size $4N \times 4N$. In the following we consider $N = 2$ and evaluate \mathcal{Z}_L explicitly for an arbitrary U , which can be parametrized as

$$U = \alpha_0 + i\alpha \cdot \sigma, \quad \alpha = (\alpha_1, \alpha_2, \alpha_3), \quad (4.25)$$

where σ_i 's are the Pauli matrices. The corresponding matrix M is given by

$$\begin{pmatrix} A_{N_\tau} & 0 & 0 & 0 & B_1 & b\alpha_3 & -b\alpha_2 & b\alpha_1 \\ 0 & A_{N_\tau} & 0 & 0 & -b\alpha_3 & B_1 & -b\alpha_1 & -b\alpha_2 \\ 0 & 0 & A_{N_\tau} & 0 & b\alpha_2 & b\alpha_1 & B_1 & -b\alpha_3 \\ 0 & 0 & 0 & A_{N_\tau} & -b\alpha_1 & b\alpha_2 & b\alpha_3 & B_1 \\ B_1 & -b\alpha_3 & b\alpha_2 & -b\alpha_1 & C_{N_\tau} & 0 & 0 & 0 \\ b\alpha_3 & B_1 & b\alpha_1 & b\alpha_2 & 0 & C_{N_\tau} & 0 & 0 \\ -b\alpha_2 & -b\alpha_1 & B_1 & b\alpha_3 & 0 & 0 & C_{N_\tau} & 0 \\ b\alpha_1 & -b\alpha_2 & -b\alpha_3 & B_1 & 0 & 0 & 0 & C_{N_\tau} \end{pmatrix},$$

where $B_1 = -(b\alpha_0 + B_{N_\tau})$. The determinant of M is given by

$$\text{Det } M = \left(B_{N_\tau}^2 - A_{N_\tau} C_{N_\tau} + 2bB_{N_\tau}\alpha_0 + b^2 \right)^4. \quad (4.26)$$

Z_2 rotation of the Polyakov loop changes $\alpha_0 \rightarrow -\alpha_0$. So in the determinant the explicit symmetry breaking term of Z_2 is $2bB_{N_\tau}\alpha_0$. It is observed that B_{N_τ} rapidly decreases, vanishing in the larger N_τ limit restoring the Z_2 symmetry. Even for higher N one can see the realization of Z_N symmetry as the off-diagonal elements of the matrix M turn out to be just U and U^\dagger due to the vanishing of B_{N_τ} . Effecting a Z_N transformation, ie $U \rightarrow zU$, the factor z in U will cancel with z^* in U^\dagger leaving the determinant unchanged.

From the above results, it can be shown that there is a realization of Z_N symmetry for fixed temperature T . The number of temporal sites N_τ and T are related by $T = 1/(a_l N_\tau)$, where a_l is the lattice spacing. Fixing T amounts to $a_l \propto 1/N_\tau$. a_l enters into the calculations through the parameter $b = (m_b^2 + 8)^{-1}$ which depends on the Higgs mass parameter,

m_b , expressed in lattice units. For a fixed Higgs physical mass, the corresponding mass

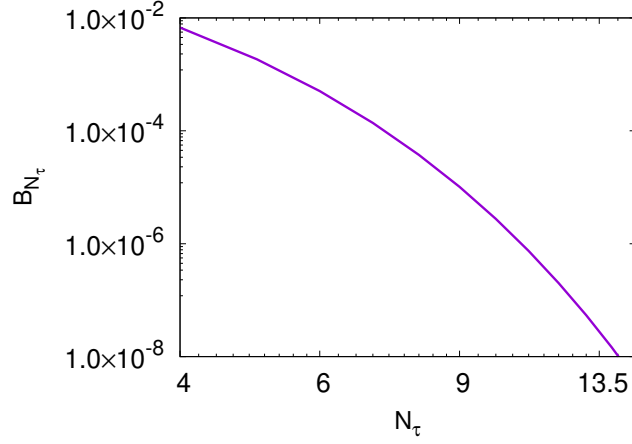


Figure 4.2: B_{N_τ} versus N_τ for Higgs mass parameter $m_b \propto 1/N_\tau$.

parameter in lattice units must decrease, i.e. $m_b \propto a_l$. Consequently, in the $N_\tau \rightarrow \infty$ limit the dimensionless parameter b increases to $b = 1/8$. This increase, however, does not affect the realisation of Z_N symmetry, since bB_{N_τ} in Eq. 4.26 vanishes in the $N_\tau \rightarrow \infty$ limit. Fig. 4.2 shows B_{N_τ} versus N_τ for $m_b \propto 1/N_\tau$. In the log-log scale, it is clear that B_{N_τ} decreases faster than exponential decay.

In the following, we consider the effects of staggered fermion fields on the Z_N symmetry.

4.2 Gauged 1 – d chain of $SU(N)$ – fermion

The lattice action for $SU(N)$ staggered fermions is given by [12]

$$S = \beta_g \sum_p \left[1 - \frac{1}{2} \text{Tr} (U_p + U_p^\dagger) \right] + 2m_f \sum_n \bar{\Psi}_n \Psi_n + \sum_{n,\mu} \eta_{n,\mu} \left[\bar{\Psi}_n U_{n,\mu} \Psi_{n+\mu} - \bar{\Psi}_n U_{n-\mu,\mu}^\dagger \Psi_{n-\mu} \right]. \quad (4.27)$$

Here the fermion mass m_f , as well as the fields Ψ , are expressed in lattice units. $\eta_{n,\mu}$ is the Kogut–Susskind (KS) phase and can take values ± 1 . It takes over the role of the γ_μ matrices. The one-dimensional gauged temporal chain, an analog of Eq. 4.5 in this case

turns out to be

$$S = 2m_f \sum_{i=1}^{N_\tau} \bar{\Psi}_i \Psi_i + \sum_{i=1}^{N_\tau-1} (\bar{\Psi}_i \Psi_{i+1} - \bar{\Psi}_{i+1} \Psi_i) - \bar{\Psi}_{N_\tau} U \Psi_1 + \bar{\Psi}_1 U^\dagger \Psi_{N_\tau}. \quad (4.28)$$

The change in the sign of the last two terms is due to the anti-periodicity of Ψ i.e. $\Psi_{N_\tau+1} = -\Psi_1$. Here we have considered the KS phase η to be +1 [13, 14], however, the results/conclusions do not depend on η . As in the previous section we work in the gauge in which all temporal links except the last one are set to identity. The last link is denoted by U . The corresponding Polyakov loop is $L = \text{Tr}(U)/N$. To find out the free energy $V(L)$, for a given configuration or value of L , we need to integrate out only the fermion fields. For convenience, like in the case of Higgs chain, we write $S = S_1 + S_2$ where

$$S_1 = 2m_f \bar{\Psi}_1 \Psi_1 - \bar{\Psi}_{N_\tau} U \Psi_1 + \bar{\Psi}_1 U^\dagger \Psi_{N_\tau}, \quad (4.29)$$

$$S_2 = 2m_f \sum_{i=2}^{N_\tau} \bar{\Psi}_i \Psi_i + \sum_{i=1}^{N_\tau-1} (\bar{\Psi}_i \Psi_{i+1} - \bar{\Psi}_{i+1} \Psi_i). \quad (4.30)$$

The fermion fields in the fundamental representation of the $SU(N)$ gauge group at the i -th site can be written as

$$\Psi_i = \begin{pmatrix} \psi_i^1 \\ \psi_i^2 \\ \vdots \\ \psi_i^N \end{pmatrix}, \quad \bar{\Psi}_i = (\bar{\psi}_i^1, \bar{\psi}_i^2, \dots, \bar{\psi}_i^N), \quad (4.31)$$

with $\psi_i^1, \psi_i^2, \dots, \psi_i^N$ are all complex.

In this case, we use Grassmann algebra to integrate out the fermion fields. The elements $\psi_1, \psi_2, \dots, \psi_n$ are said to be the generators of a Grassmann algebra when they anticommute

among each other, i.e.

$$\{\psi_i, \psi_j\} = \psi_i\psi_j + \psi_j\psi_i = 0, \quad i, j = 1, 2, \dots, n. \quad (4.32)$$

From Eq. 4.32 it follows that

$$\psi_i^2 = 0. \quad (4.33)$$

To do the integration over Grassmann variables, we now state the Grassmann rules for calculating integrals of the form

$$\int \prod_{i=1}^n d\psi_i f(\psi). \quad (4.34)$$

To calculate an arbitrary integral, the following conditions are satisfied by ψ_i

$$\begin{aligned} \int d\psi_i &= 0, \\ \int d\psi_i \psi_i &= 1. \end{aligned} \quad (4.35)$$

The integration measures $\{d\psi_i\}$ also anticommute among themselves, as well as with other ψ_j 's for all i, j

$$\{d\psi_i, d\psi_j\} = 0, \quad \{d\psi_i, \psi_j\} = 0. \quad (4.36)$$

In particular we consider a Grassmann algebra with $2n$ generators $\psi_i, \bar{\psi}_i$ with $i = 1, 2, \dots, n$.

All these $2n$ generators anticommute among each other, i.e.

$$\{\bar{\psi}_i, \psi_j\} = \{\bar{\psi}_i, \bar{\psi}_j\} = 0. \quad (4.37)$$

The corresponding integration measures also anticommute

$$\begin{aligned} \{d\bar{\psi}_i, d\psi_j\} &= \{d\bar{\psi}_i, d\bar{\psi}_j\} = 0, \\ \{d\bar{\psi}_i, \psi_j\} &= \{d\psi_i, \bar{\psi}_j\} = 0. \end{aligned} \quad (4.38)$$

In the following we initially integrate the fields $\Psi_2, \bar{\Psi}_2$ to $\Psi_{N_\tau-1}, \bar{\Psi}_{N_\tau-1}$ sequentially just as in the previous section. Afterwards $\Psi_1, \bar{\Psi}_1$ and $\Psi_{N_\tau}, \bar{\Psi}_{N_\tau}$ are integrated out to obtain the partition function

$$\mathcal{Z}_L = \int d\bar{\Psi}_1 d\Psi_1 d\bar{\Psi}_{N_\tau} d\Psi_{N_\tau} \text{Exp}[-S_1] \mathcal{Z}, \quad (4.39)$$

where \mathcal{Z} is given by

$$\mathcal{Z} = \int \prod_{i=2}^{N_\tau-1} d\bar{\Psi}_i d\Psi_i \text{Exp}[-S_2]. \quad (4.40)$$

Since S_2 is diagonal in color space we consider a particular color of Ψ_i and denote it by ψ_i . For this choice the relevant integral is

$$\mathcal{I}_\psi = \int \prod_{i=2}^{N_\tau-1} d\bar{\psi}_i d\psi_i \text{Exp}[-S_{2,\psi}]. \quad (4.41)$$

The part of the action which contain $\psi_2, \bar{\psi}_2$ is

$$\tilde{S}_2 = 2m_f \bar{\psi}_2 \psi_2 + \bar{\psi}_1 \psi_2 - \bar{\psi}_2 \psi_1 + \bar{\psi}_2 \psi_3 - \bar{\psi}_3 \psi_2. \quad (4.42)$$

To see the result of ψ_2 and $\bar{\psi}_2$ integration we need only to consider the following integral

$$\mathcal{I}_\psi^2 = \int d\bar{\psi}_2 d\psi_2 e^{-\tilde{S}_2}. \quad (4.43)$$

Since the terms in the exponential appear as quadratic in Grassmann variables, they commute among each other, i.e. $[S_{2,\psi}, \tilde{S}_2] = 0$. To proceed further, let us consider a function of the form

$$f(\psi, \bar{\psi}) = e^{-\sum_{i,j} \bar{\psi}_i A_{ij} \psi_j}, \quad (4.44)$$

which can also be written as

$$f(\psi, \bar{\psi}) = \prod_{i,j} e^{-\bar{\psi}_i A_{ij} \psi_j}. \quad (4.45)$$

Making use of Eq. 4.33

$$f(\psi, \bar{\psi}) = \prod_{i,j} (1 - \bar{\psi}_i A_{ij} \psi_j) . \quad (4.46)$$

After making use of the above properties the integration in Eq. 4.43 results in

$$\mathcal{I}_\psi^2 = 2m_f - \bar{\psi}_3 \psi_3 - \bar{\psi}_1 \psi_1 + \bar{\psi}_3 \psi_1 + \bar{\psi}_1 \psi_3 . \quad (4.47)$$

Now, we need to consider the action $S_{2,\psi} - \tilde{S}_2$. The terms in this action, which contain $\psi_3, \bar{\psi}_3$ are

$$\tilde{S}_3 = (2m_f \bar{\psi}_3 \psi_3 + \bar{\psi}_3 \psi_4 - \bar{\psi}_4 \psi_3) . \quad (4.48)$$

We now repeat the integration of $\psi_3, \bar{\psi}_3$ as done above, but the integrand now has to take into account the factor \mathcal{I}_ψ^2

$$\begin{aligned} \mathcal{I}_\psi^3 &= \int d\bar{\psi}_3 d\psi_3 e^{-\tilde{S}_3} \times \mathcal{I}_\psi^2 \\ &= \int d\bar{\psi}_3 d\psi_3 e^{-\tilde{S}_3} \times (2m_f - \bar{\psi}_3 \psi_3 - \bar{\psi}_1 \psi_1 + \bar{\psi}_3 \psi_1 + \bar{\psi}_1 \psi_3) \\ &= (1 + 4m_f^2 - 2m_f \bar{\psi}_1 \psi_1 - 2m_f \bar{\psi}_4 \psi_4 + \bar{\psi}_4 \psi_1 - \bar{\psi}_1 \psi_4 + \bar{\psi}_4 \psi_4 \bar{\psi}_1 \psi_1) . \end{aligned} \quad (4.49)$$

After integrating $\psi_2, \bar{\psi}_2$ and $\psi_3, \bar{\psi}_3$ the integral in Eq. 4.41 takes the form

$$\begin{aligned} \mathcal{I}_\psi &= \int \prod_{i=4}^{N_\tau-1} d\bar{\psi}_i d\psi_i \text{Exp}[-S_{2,\psi}^4] \\ &\times [1 + 4m_f^2 - 2m_f \bar{\psi}_1 \psi_1 - 2m_f \bar{\psi}_4 \psi_4 + \bar{\psi}_4 \psi_1 - \bar{\psi}_1 \psi_4 + \bar{\psi}_4 \psi_4 \bar{\psi}_1 \psi_1] . \end{aligned} \quad (4.50)$$

$S_{2,\psi}^4$ is obtained by dropping terms which depend on $\psi_2, \bar{\psi}_2$ and $\psi_3, \bar{\psi}_3$. The sequential integration ψ_4 up to $\psi_{N_\tau-1}$ and their conjugates straight forward and lead to

$$\mathcal{I}_\psi = A_{N_\tau} - B_{N_\tau} \bar{\psi}_1 \psi_1 - C_{N_\tau} \bar{\psi}_{N_\tau} \psi_{N_\tau} + \bar{\psi}_{N_\tau} \psi_1 + D_{N_\tau} \bar{\psi}_1 \psi_{N_\tau} + E_{N_\tau} \bar{\psi}_{N_\tau} \psi_{N_\tau} \bar{\psi}_1 \psi_1 , \quad (4.51)$$

where the coefficients A_{N_τ} to E_{N_τ} can be obtained by recursion as

$$\begin{aligned} A_{k+1} &= 2m_f A_k + C_k, & B_{k+1} &= 2m_f B_k + E_k, \\ C_{k+1} &= A_k, & D_{k+1} &= (-1)^k, & E_{k+1} &= B_k, \end{aligned} \quad (4.52)$$

with

$$A_4 = (1 + 4m_f^2), \quad B_4 = 2m_f, \quad C_4 = 2m_f, \quad E_4 = 1. \quad (4.53)$$

Taking the \mathcal{I} integrals into account we can write the partition function as

$$\begin{aligned} \mathcal{Z}_L &= \int d\bar{\Psi}_1 d\Psi_1 d\bar{\Psi}_{N_\tau} d\Psi_{N_\tau} \text{Exp} \left[\bar{\Psi}_{N_\tau} U \Psi_1 - \bar{\Psi}_1 U^\dagger \Psi_{N_\tau} \right] \\ &\times \prod_r \left(1 - 2m_f \bar{\psi}_1^r \psi_1^r - 2m_f \bar{\psi}_{N_\tau}^r \psi_{N_\tau}^r + 4m_f^2 \bar{\psi}_1^r \psi_1^r \bar{\psi}_{N_\tau}^r \psi_{N_\tau}^r \right) \\ &\times \left(A_{N_\tau} - B_{N_\tau} \bar{\psi}_1^r \psi_1^r - C_{N_\tau} \bar{\psi}_{N_\tau}^r \psi_{N_\tau}^r + \bar{\psi}_{N_\tau}^r \psi_1^r + D_{N_\tau} \bar{\psi}_1^r \psi_{N_\tau}^r + E_{N_\tau} \bar{\psi}_{N_\tau}^r \psi_{N_\tau}^r \bar{\psi}_1^r \psi_1^r \right). \end{aligned} \quad (4.54)$$

Note that ψ_i^r denotes the colour r of the field Ψ_i at the temporal site i . This expression can be simplified as

$$\begin{aligned} \mathcal{Z}_L &= \int d\bar{\Psi}_1 d\Psi_1 d\bar{\Psi}_{N_\tau} d\Psi_{N_\tau} \text{Exp} \left[\bar{\Psi}_{N_\tau} U \Psi_1 - \bar{\Psi}_1 U^\dagger \Psi_{N_\tau} \right] \\ &\times \prod_r \left(\tilde{A} - \tilde{B} \bar{\psi}_1^r \psi_1^r - \tilde{C} \bar{\psi}_{N_\tau}^r \psi_{N_\tau}^r + \bar{\psi}_{N_\tau}^r \psi_1^r + \tilde{D} \bar{\psi}_1^r \psi_{N_\tau}^r + \tilde{E} \bar{\psi}_{N_\tau}^r \psi_{N_\tau}^r \bar{\psi}_1^r \psi_1^r \right), \end{aligned} \quad (4.55)$$

where $\tilde{A} = A_{N_\tau}$, $\tilde{B} = (2m_f A_{N_\tau} + B_{N_\tau})$, $\tilde{C} = (2m_f A_{N_\tau} + C_{N_\tau})$, $\tilde{D} = D_{N_\tau}$ and $\tilde{E} = E_{N_\tau} + 2m_f C_{N_\tau} + 2m_f B_{N_\tau} + 4m_f^2 A_{N_\tau}$. For large m_f , in \mathcal{Z}_L the ratio of the leading and sub-leading term scales as $\sim m_f$. The sub-leading terms contain matrix elements of U . In the limit of $m_f \rightarrow \infty$, therefore the fermions decouple from the gluons and exact Z_N symmetry is recovered for any N_τ . For $N = 2$, the matrix form of U can be written as

$$\begin{pmatrix} U_{11} & U_{12} \\ -U_{12}^* & U_{11}^* \end{pmatrix}.$$

Ψ_1 and Ψ_{N_τ} in the exponential of Eq. 4.55 can be written as

$$\Psi_1 = \begin{pmatrix} \psi_1^1 \\ \psi_1^2 \end{pmatrix}, \quad \Psi_{N_\tau} = \begin{pmatrix} \psi_{N_\tau}^1 \\ \psi_{N_\tau}^2 \end{pmatrix}. \quad (4.56)$$

Hence the exponential factors can be written explicitly as

$$\begin{aligned} \bar{\Psi}_{N_\tau} U \Psi_1 &= \begin{pmatrix} \bar{\psi}_{N_\tau}^1 & \bar{\psi}_{N_\tau}^2 \end{pmatrix} \begin{pmatrix} U_{11} & U_{12} \\ -U_{12}^* & U_{11}^* \end{pmatrix} \begin{pmatrix} \psi_1^1 \\ \psi_1^2 \end{pmatrix} \\ &= \bar{\psi}_{N_\tau}^1 U_{11} \psi_1^1 + \bar{\psi}_{N_\tau}^1 U_{12} \psi_1^2 - \bar{\psi}_{N_\tau}^2 U_{12}^* \psi_1^1 + \bar{\psi}_{N_\tau}^2 U_{11}^* \psi_1^2, \end{aligned} \quad (4.57)$$

$$\begin{aligned} \bar{\Psi}_1 U^\dagger \Psi_{N_\tau} &= \begin{pmatrix} \bar{\psi}_1^1 & \bar{\psi}_1^2 \end{pmatrix} \begin{pmatrix} U_{11}^* & -U_{12} \\ U_{12}^* & U_{11} \end{pmatrix} \begin{pmatrix} \psi_{N_\tau}^1 \\ \psi_{N_\tau}^2 \end{pmatrix} \\ &= \bar{\psi}_1^1 U_{11}^* \psi_{N_\tau}^1 - \bar{\psi}_1^1 U_{12} \psi_{N_\tau}^2 + \bar{\psi}_1^2 U_{12}^* \psi_{N_\tau}^1 + \bar{\psi}_1^2 U_{11} \psi_{N_\tau}^2. \end{aligned} \quad (4.58)$$

In the integration of Eq. 4.55 only the factors with eight Grassmann variables $\bar{\psi}_1^1 \bar{\psi}_1^2 \psi_1^1 \psi_1^2 \bar{\psi}_{N_\tau}^1 \bar{\psi}_{N_\tau}^2 \psi_{N_\tau}^1 \psi_{N_\tau}^2$ will survive. Integration of the rest of the fields in Eq. 4.55 leads to

$$\begin{aligned} \mathcal{Z}_L &= \tilde{E}^2 + 2\tilde{E}\tilde{A}|U_{11}|^2 + \tilde{A}^2 + 2\tilde{B}\tilde{C}|U_{12}|^2 + 2\left[1 - \tilde{D} \operatorname{Re}(U_{11}^2)\right] \\ &\quad + (\tilde{E} + \tilde{A})(1 - \tilde{D})\operatorname{Tr}(U). \end{aligned} \quad (4.59)$$

The free energy for $N = 2$ is

$$\begin{aligned} V(L) &= -T \log(\mathcal{Z}_L) \\ &= -T \left\{ \log\left(\tilde{E}^2 + 2\tilde{E}\tilde{A}|U_{11}|^2 + \tilde{A}^2 + 2\tilde{B}\tilde{C}|U_{12}|^2 + 2\left[1 - \tilde{D} \operatorname{Re}(U_{11}^2)\right]\right) \right. \\ &\quad \left. + \log\left(1 + \frac{(\tilde{E} + \tilde{A})(1 - \tilde{D})\operatorname{Tr}(U)}{\tilde{E}^2 + 2\tilde{E}\tilde{A}|U_{11}|^2 + \tilde{A}^2 + 2\tilde{B}\tilde{C}|U_{12}|^2 + 2\left[1 - \tilde{D} \operatorname{Re}(U_{11}^2)\right]}\right) \right\}. \end{aligned} \quad (4.60)$$

As one can see from Eq. 4.59 that the Z_2 explicit breaking term is linear in $\tilde{E} + \tilde{A}$. For non zero m_f , in the free energy $V(L)$ the first four terms of \mathcal{Z}_L dominate over $\tilde{E} + \tilde{A}$.

Figs. 4.3 and 4.4 shows how the ratio $\frac{(\tilde{E}+\tilde{A})}{(\tilde{E}^2+\tilde{A}^2+2\tilde{E}\tilde{A}+2\tilde{B}\tilde{C})}$ varies with N_τ . If the lattice fermion mass parameter m_f is fixed, then the logarithm of that ratio decreases linearly with N_τ i.e. the second term in Eq. 4.60 vanishes at large N_τ . This implies that the Z_2 explicit breaking decreases with N_τ and vanishes at the $N_\tau \rightarrow \infty$ limit. But for $m_f \propto 1/N_\tau$, the Z_2 explicit breaking initially decreases rapidly but seems to approach a finite non zero limiting value at $N_\tau \rightarrow \infty$.

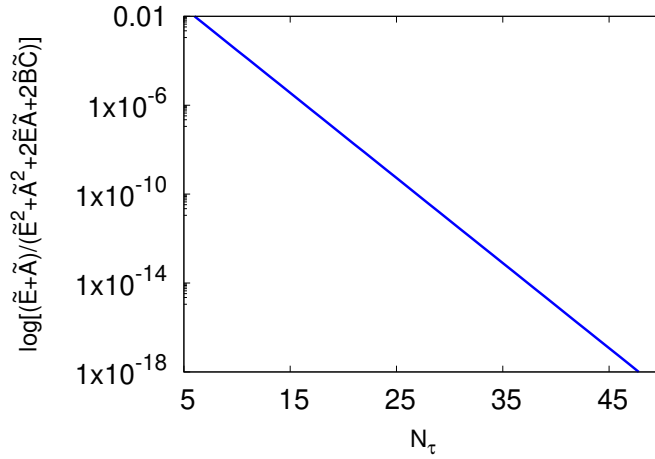


Figure 4.3: N_τ dependence for fermion mass parameter $m_f = \text{constant}$.

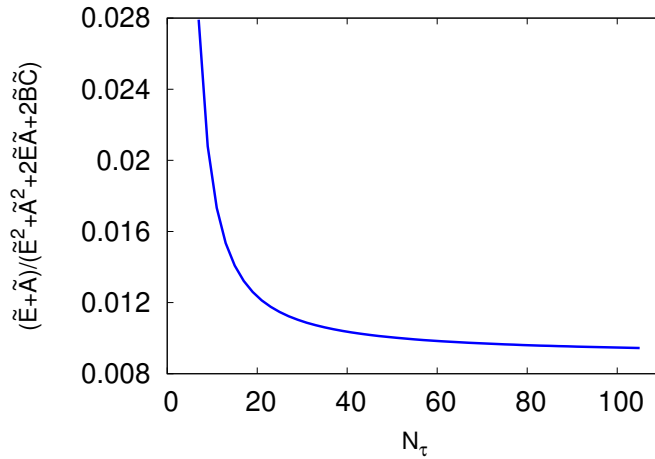


Figure 4.4: N_τ dependence for fermion mass parameter $m_f \propto 1/N_\tau$.

For higher N it is difficult to evaluate \mathcal{Z}_L for a general U . To proceed further we assume the U to be $U_{rs} = \lambda_r \delta_{rs}$. After the exponential in Eq. 4.55 is written as a polynomial

$$\begin{aligned} \text{Exp} \left[\bar{\Psi}_{N_\tau} U \Psi_1 - \bar{\Psi}_1 U^\dagger \Psi_{N_\tau} \right] &= e^{\bar{\Psi}_{N_\tau} U \Psi_1} e^{-\bar{\Psi}_1 U^\dagger \Psi_{N_\tau}} \\ &= \prod_r \left(1 + \lambda_r \bar{\psi}_{N_\tau}^r \psi_1^r \right) \left(1 - \lambda_r^* \bar{\psi}_1^r \psi_{N_\tau}^r \right) \\ &= \prod_r \left(1 + \lambda_r \bar{\psi}_{N_\tau}^r \psi_1^r - \lambda_r^* \bar{\psi}_1^r \psi_{N_\tau}^r + \bar{\psi}_{N_\tau}^r \psi_{N_\tau}^r \bar{\psi}_1^r \psi_1^r \right). \end{aligned} \quad (4.61)$$

The corresponding partition function for higher N is

$$\begin{aligned} \mathcal{Z}_L &= \int d\bar{\Psi}_1 d\Psi_1 d\bar{\Psi}_{N_\tau} d\Psi_{N_\tau} \prod_r \left(1 + \lambda_r \bar{\psi}_{N_\tau}^r \psi_1^r - \lambda_r^* \bar{\psi}_1^r \psi_{N_\tau}^r + \bar{\psi}_{N_\tau}^r \psi_{N_\tau}^r \bar{\psi}_1^r \psi_1^r \right) \\ &\quad \times \left(\tilde{A} - \tilde{B} \bar{\psi}_1^r \psi_1^r - \tilde{C} \bar{\psi}_{N_\tau}^r \psi_{N_\tau}^r + \bar{\psi}_{N_\tau}^r \psi_1^r + \tilde{D} \bar{\psi}_1^r \psi_{N_\tau}^r + \tilde{E} \bar{\psi}_{N_\tau}^r \psi_{N_\tau}^r \bar{\psi}_1^r \psi_1^r \right) \end{aligned} \quad (4.62)$$

$$\begin{aligned} &= \int d\bar{\Psi}_1 d\Psi_1 d\bar{\Psi}_{N_\tau} d\Psi_{N_\tau} \\ &\quad \times \prod_r \left(A - B \bar{\psi}_1^r \psi_1^r - C \bar{\psi}_{N_\tau}^r \psi_{N_\tau}^r + F_r \bar{\psi}_{N_\tau}^r \psi_1^r + D_r \bar{\psi}_1^r \psi_{N_\tau}^r + E_r \bar{\psi}_{N_\tau}^r \psi_{N_\tau}^r \bar{\psi}_1^r \psi_1^r \right), \end{aligned} \quad (4.63)$$

where $A = \tilde{A}$, $B = \tilde{B}$, $C = \tilde{C}$, $D_r = \tilde{D} - \lambda_r^* \tilde{A}$, $E_r = \tilde{E} - \lambda_r \tilde{D} + \lambda_r^* + \tilde{A}$ and $F_r = (1 + \lambda_r \tilde{A})$.

After the fields are integrated out we get the following result for the partition function:

$$\mathcal{Z}_L = \prod_r E_r. \quad (4.64)$$

The corresponding free energy is

$$\begin{aligned} V(L) &= -T \log(\mathcal{Z}_L) \\ &= -T \sum_r \left\{ \log(\tilde{E} + \tilde{A} - \lambda_r \tilde{D} + \lambda_r^*) \right\} \\ &= -T \sum_r \left\{ \log(\tilde{E} + \tilde{A}) + \log\left(1 - \frac{\lambda_r \tilde{D} - \lambda_r^*}{\tilde{E} + \tilde{A}}\right) \right\}. \end{aligned} \quad (4.65)$$

The second term in Eq. 4.65 breaks the Z_N symmetry explicitly. For a fixed lattice fermion mass parameter m_f , i.e. if the lattice spacing is fixed, then $\tilde{E} + \tilde{A}$ diverges in the limit $N_\tau \rightarrow \infty$. The second term vanishes in this limit. These results show that at zero temperature

the explicit breaking in this model will be vanishingly small. Fig. 4.5 shows how the logarithm of \tilde{A} and \tilde{E} varies with N_τ . It increases linearly and diverges in the $N_\tau \rightarrow \infty$ limit.

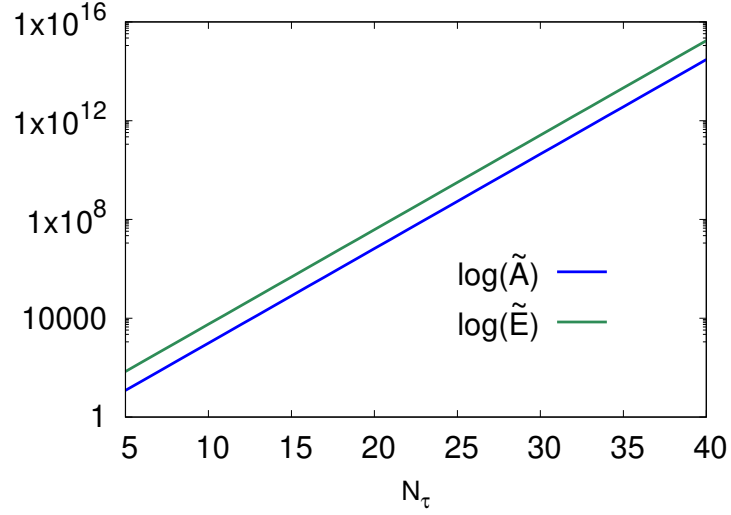


Figure 4.5: \tilde{A} and \tilde{E} versus N_τ for fermion mass parameter $m_f = \text{constant}$.

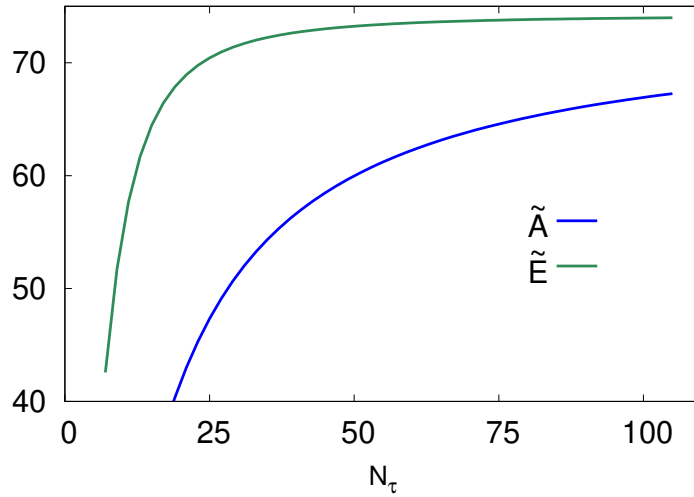


Figure 4.6: \tilde{A} and \tilde{E} versus N_τ for fermion mass parameter $m_f \propto 1/N_\tau$.

To study the explicit breaking of Z_N at a fixed nonzero temperature and physical fermion mass, the behavior of \tilde{E} and \tilde{A} must be studied in the limit $N_\tau \rightarrow \infty$ while scaling the fermion mass parameter in lattice units as $m_f \propto 1/N_\tau$. Unlike in the case of bosons, it is

not possible to carry this out analytically as the polynomial coefficients in \tilde{E} and \tilde{A} change with N_τ . However, we are able to numerically check that \tilde{E} and \tilde{A} increase rapidly with N_τ initially, but seem to approach a finite limiting value for $N_\tau \rightarrow \infty$. For $m_f \propto 1/N_\tau$, Fig. 4.6 shows the N_τ dependence \tilde{E} and \tilde{A} . These results suggest that for the one-dimensional fermion chain, the explicit breaking of Z_N vanishes only at zero temperature.

To understand the reason behind the realization of Z_N symmetry in $SU(N)$ +Higgs theory in the continuum limit, in the next chapter we discuss a simple model of Z_2 +Higgs theory in both 3+1 and 0+1 dimensions.

Chapter 5

Study of Z_2 symmetry, CD transition and density of states in Z_2 +Higgs theory

In the previous chapters, we have seen in examples of gauge theories in the presence of the Higgs field, that there is Z_N symmetry in partition function averages even though the action is not Z_N invariant. This is unlike in the Ising model, wherein in the presence of a symmetry-breaking external field, the partition function averages do not possess Z_2 symmetry. It is, therefore, important to understand the underlying reason for the Z_N symmetry. In $SU(N)$ +Higgs theory the explicit Z_N breaking is unconventional, as it is caused by a dynamical field. A dynamical field is associated with entropy, which may affect the Z_N symmetry. Conventionally in a partition function, there are two important factors, i.e. entropy and the Boltzmann factor. The latter is just the negative exponential of the action so breaks the Z_N symmetry. So it may be the entropy, in other words, the density of states (DoS) is responsible for the Z_N symmetry. To test this we consider the Z_2 +Higgs theory in this chapter. The fact that both the links and the Higgs fields take values ± 1 , makes it possible for a quantitative estimate of the DoS. Note that the Z_2 +Higgs theory does not have a continuum limit, hence, the temporal direction is not the same as the inverse of temperature. However, the model action processes Z_2 symmetry and the effect

of a large number of temporal sites can be studied. In this chapter, we also describe a one-dimensional model along the lines of models considered in the last chapter.

5.1 Z_2 symmetry in Z_2 +Higgs gauge theory

The action for the Z_2 +Higgs theory in four dimensional lattice ($N_s^3 \times N_\tau$) is given by

$$S = -\beta_g \sum_P U_P - \kappa \sum_{n,\hat{\mu}} \Phi_{n+\hat{\mu}} U_{n,\hat{\mu}} \Phi_n . \quad (5.1)$$

Here β_g is the gauge coupling strength. The plaquette U_P which is path ordered product of the links along an elementary square on the $\mu - \nu$ plane, i.e.

$$U_P = U_{n,\hat{\mu}} U_{n+\hat{\mu},\hat{\nu}} U_{n+\hat{\nu},\hat{\mu}} U_{n,\hat{\nu}} . \quad (5.2)$$

κ is the gauge Higgs interaction strength. Both $U_{n,\hat{\mu}}$ and Φ_n take values ± 1 .

The pure gauge part of the action, the first term in Eq. 5.1, is invariant under the Z_2 gauge transformations

$$U_{n,\hat{\mu}} \rightarrow V_n U_{n,\hat{\mu}} V_{n+\hat{\mu}}^{-1} , \quad (5.3)$$

where $V_n = \pm 1 \in Z_2$. The V_n 's satisfy the following boundary condition,

$$V(\vec{n}, n_4 = 1) = z V(\vec{n}, n_4 = N_\tau) . \quad (5.4)$$

$z = \pm 1 \in Z_2$. So the gauge transformations can be classified by the group Z_2 . For $z = -1$ the gauge transformations are anti-periodic in the temporal direction.

The Polyakov loop is defined as the product of links along the temporal direction, i.e.

$$L(\vec{n}) = \prod_{n_4=1}^{N_\tau} U_{(\vec{n},n_4),\hat{4}} , \quad (5.5)$$

transforms non-trivially under Z_2 gauge transformations [2]. It is easy to see that, in a gauge transformation, the Polyakov loop transforms as

$$L(\vec{n}) \rightarrow zL(\vec{n}) . \quad (5.6)$$

This transformation property of the Polyakov loop under Z_2 (or Z_N in general) gauge transformation is similar to that of magnetization in the Ising model. So the Polyakov loop, $L(\vec{n})$ is Z_2 gauge invariant as long as the transformation is periodic i.e. $z = +1$ but changes sign when the transformation is anti-periodic. The partition function in the pure gauge case ($\kappa = 0$) is given by

$$\mathcal{Z} = \int DU e^{-S} . \quad (5.7)$$

Since the action for $\kappa = 0$ is invariant under Z_2 gauge transformations, any configuration and its gauge rotated counterpart will contribute equally to the partition function. Therefore the distribution of the Polyakov loop exhibits Z_2 symmetry in this case. Equivalently the free energy of the Polyakov loop will have Z_2 symmetry.

The presence of the Higgs field changes the space of allowed gauge transformations. The reason is that the Higgs field is required to be periodic in the temporal direction. Under a gauge transformation, Φ_n transforms as

$$\Phi_n \rightarrow V_n \Phi_n . \quad (5.8)$$

Now the periodic boundary condition of Φ would be spoiled if non-periodic gauge transformations, characterized by $z = -1$ are allowed. In this case, given a configuration, one can define a Z_2 counterpart in which only the gauge links are Z_2 rotated. Obviously, these pair of configurations will not contribute equally to the partition function for $\kappa \neq 0$. So according to the Boltzmann factor, $\sum_{\vec{n}} L(\vec{n})$ and $-\sum_{\vec{n}} L(\vec{n})$ are non degenerate. This situation is similar to the presence of an external field in the Ising model. However, the status of Z_2 symmetry in the free energy can be answered only after integrating out the Higgs

field for a given $L(\vec{n})$ and its Z_2 rotated configurations.

The Polyakov loop and Ising spins are similar in how they transform under respective transformations. However, there is an important difference between them. This becomes clear when one compares $L(\vec{n})$ and an Ising spin at a spatial point $\vec{n} = \{n_1, n_2, n_3\}$. A given value of $L(\vec{n})$ is associated with an entropy factor. This is because there are many different combinations of $U_{(\vec{n}, n_4), \hat{4}}$ and $\Phi_{\vec{n}, n_4}$ are possible for a given value of $L(\vec{n})$. Larger the N_τ , larger is the corresponding entropy. This aspect of the Polyakov loop needs to be taken into account to understand the explicit breaking or realization of Z_2 symmetry. In the following, we discuss the algorithm of the Monte Carlo simulations [83], present simulation results for the phase diagram in the $\beta_g - \kappa$ plane, distribution of the Polyakov loop, and CD transition in the Higgs symmetric phase, etc.

5.2 Numerical technique and Monte Carlo simulation results

In the Monte Carlo simulations, the Metropolis algorithm is used for sampling the statistically significant configurations [15]. To update a particular gauge link $U_{n,\mu}$, we consider the change in the action by flipping it. If the action decreases then the flipped gauge link is accepted for the new configuration. If the action increases by ΔS then the new link is accepted with probability $\text{Exp}(-\Delta S)$. The same procedure is adopted for Φ_n . The process of updating is carried out over all n and μ in multiple sweeps. Configurations separated by 10 sweeps are used in our analysis, which brings down the autocorrelation between successive configurations to an acceptable level. For these simulations, $N_\tau = 4 - 24$ and $N_s = 16 - 84$ with $N_s/N_\tau = 4$ lattices have been considered [84]. Note that the choice of this ratio is used to mimic the calculations of $SU(N)$ gauge theories. N_s needs to be significantly larger than the correlation length.

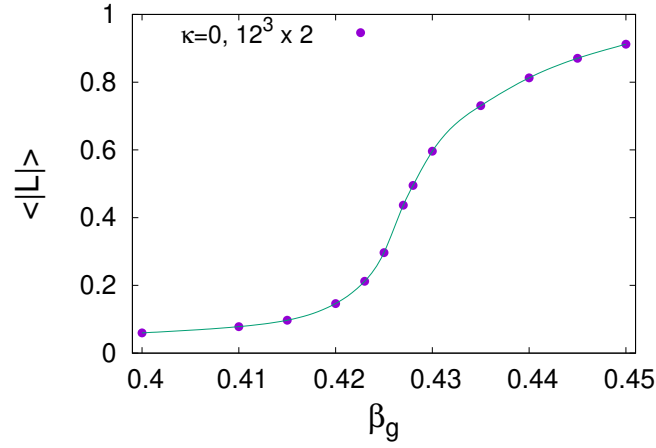


Figure 5.1: The average of the Polyakov loop vs β_g for $N_\tau = 2$.

The pure gauge simulations are initially performed to understand the nature of the CD transition and Z_2 symmetry of the Polyakov loop. The simulations were repeated in the presence of Φ to study its effects. The pure gauge transition has been studied previously in the mean-field approximations [57], which finds the transition is first order in four dimensions. Also using duality transformations it can be shown that the critical $\beta_g \sim 0.4407$ for $\kappa = 0$ [58]. These results are supported by Monte Carlo simulations of smaller lattices [8]. The simulations carried out in this work are also consistent with these results. Fig. 5.1 shows plot of the average of the Polyakov loop versus β_g for $N_\tau = 2$. The Polyakov loop varies smoothly around the critical point, indicating a crossover transition.

In Figs. 5.2 and 5.3 the average of the Polyakov loop is plotted vs β_g for $N_\tau = 4, 8$. There is a range in β_g for which clearly separated peaks in the distribution of the Polyakov loop have been observed. We take the average of the Polyakov loop values corresponding to each peak separately. Therefore we have two points in the figure for a given β_g .

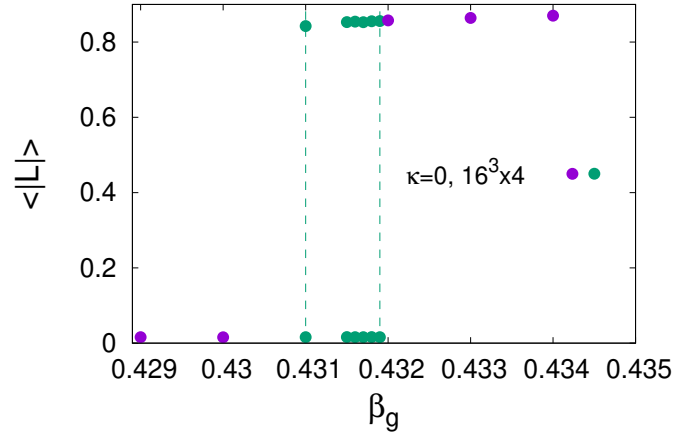


Figure 5.2: The average of the Polyakov loop vs β_g for $N_\tau = 4$.

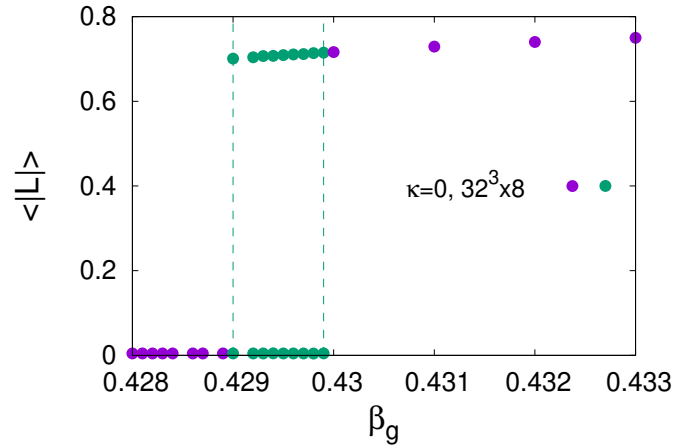


Figure 5.3: The average of the Polyakov loop vs β_g for $N_\tau = 8$.

The two peaks are shown in the Monte Carlo history of the Polyakov loop in Figs. 5.4 and 5.5. Here $\beta_g = 0.4316$ ($N_\tau = 4$) and 0.4295 ($N_\tau = 8$) lies in the transition region as shown by the green line. There is a coexistence of confined and deconfined phases for this value of β_g .

The two peaks also suggest that the transition is first order. For larger lattice sizes the range of β_g over which two states are observed increases [50]. This is expected as

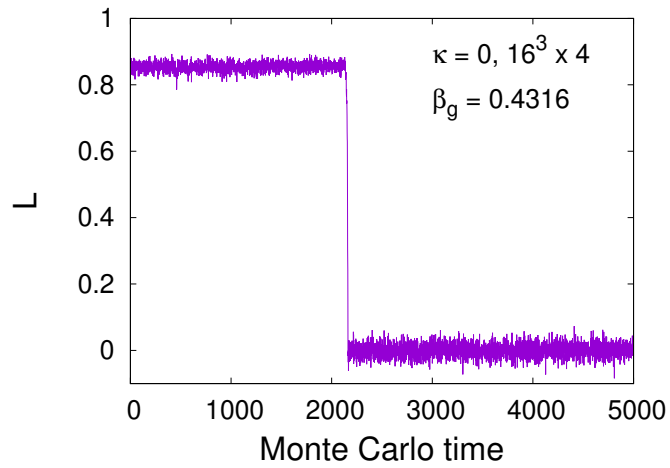


Figure 5.4: Monte Carlo history of Polyakov loop for $N_\tau = 4$.

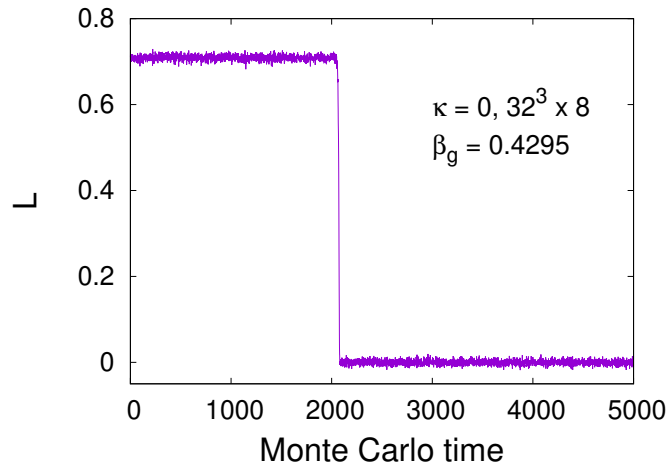


Figure 5.5: Monte Carlo history of Polyakov loop for $N_\tau = 8$.

the strength of fluctuations relatively decrease with volume (when correlation length is smaller than the spatial size of the system), making it difficult for the field to climb over the barrier and cross to the other side.

The effect of the Φ field on the CD transition and Z_2 symmetry is expected to depend on κ . To relate these two aspects of pure gauge theory to the phases of the Higgs field, simulations were performed to obtain the Higgs transition line.

For a given β_g , $\kappa > \kappa_c$ corresponds to the Higgs broken phase. In this phase the action term dominates. For $\kappa < \kappa_c$ the fluctuations of the Higgs rather than the action dominate the thermodynamic properties. This situation is similar to the Ising model at high temperatures. In Fig. 5.6 the Higgs transition line is plotted in the $\beta_g - \kappa$ plane.

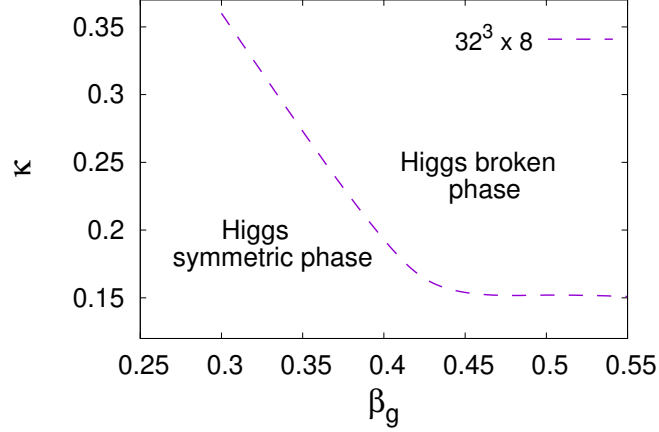


Figure 5.6: Phase diagram.

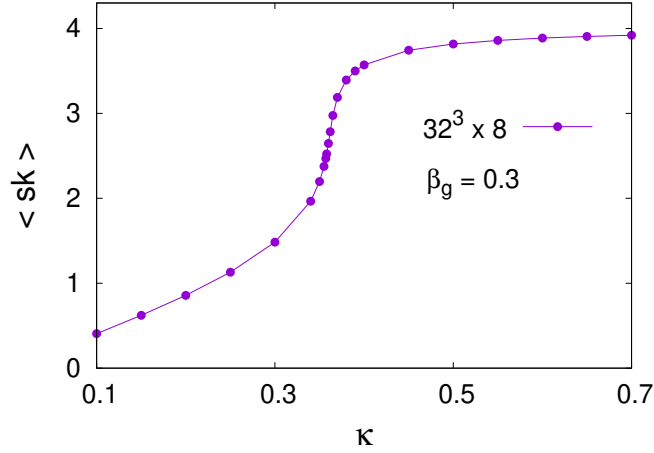


Figure 5.7: $\langle sk \rangle$ vs κ for $\beta_g = 0.3$.

The location of the phase boundary is obtained by studying the κ dependence of the interaction term $sk = \sum_{n,\hat{\mu}} \Phi_{n+\hat{\mu}} U_{n,\hat{\mu}} \Phi_n$ and its fluctuations for different values of β_g . In our simulations, the Higgs transition is found to be first order for the intermediate range of β_g and crossover for both small and large β_g , as observed in previous studies [16, 17]. For large β_g , critical κ_c remains flat and increases with decrease in β_g in the small β_g regime. In our simulations the critical values (β_{gc}, κ_c) were found to vary mildly with N_τ . The

corresponding $\langle sk \rangle$ vs κ plots are shown in Figs. 5.7–5.9 for $\beta_g = 0.3, 0.35$ and 0.45 . The transition is crossover for $\beta_g = 0.3$ and 0.45 , but it is first order for $\beta_g = 0.35$.

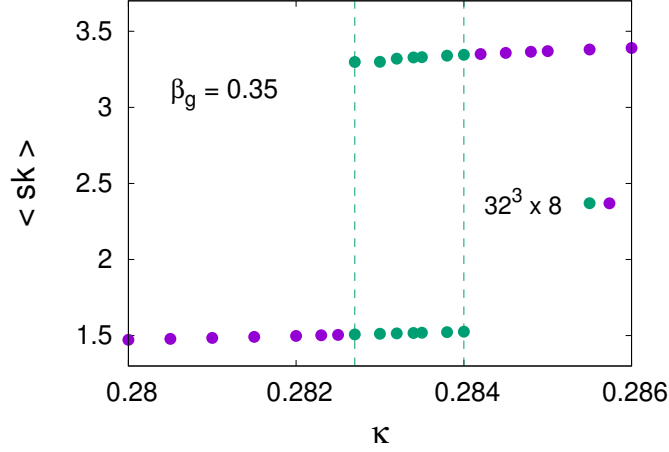


Figure 5.8: $\langle sk \rangle$ vs κ for $\beta_g = 0.35$.

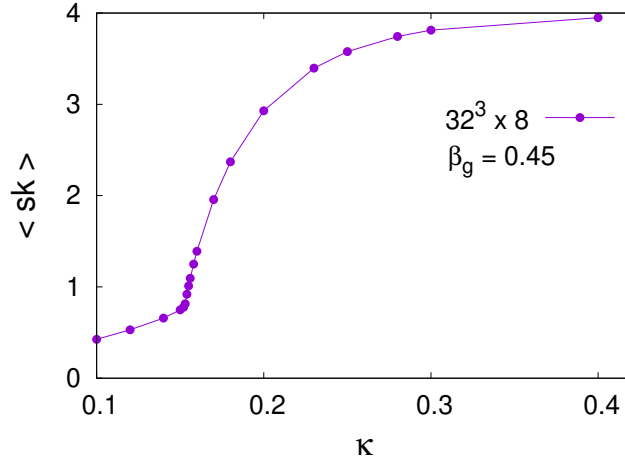


Figure 5.9: $\langle sk \rangle$ vs κ for $\beta_g = 0.45$.

The interaction term has a tendency to maximize $\Phi_{n+\hat{\mu}} U_{n,\hat{\mu}} \Phi_n$. In the large κ limit this will dominate over entropy and we expect $\Phi_{n+\hat{\mu}} U_{n,\hat{\mu}} \Phi_n \rightarrow 1$. In this limit, the Polyakov loop will approach unity. For a suitable gauge choice, the volume average of the Higgs field will approach one, indicating that the corresponding phase will be Higgs broken phase. For $L = -1$ the corresponding action will differ by an order of the size of the system, hence will be suppressed. This corresponds to the maximal explicit breaking of the Z_2 symmetry of the Polyakov loop. In the Higgs broken phase, i.e. large κ , the interaction

term dominates over the entropy. The action takes the largest value when all the temporal links are +1. So, in the Higgs phase, Z_2 symmetry is badly broken, also observed in our simulations. In the Higgs symmetric phase, i.e. smaller κ , it is the fluctuations of Higgs in other words the distribution of the interaction term dominate. In this phase, there is a possibility for the realization of Z_2 symmetry.

In Figs. 5.10–5.12 we show CD transition in the Higgs symmetric phase ($\kappa = .13$). For comparison, $\kappa = 0$ results also have been included. For $N_\tau = 2$ the transition becomes weaker when Higgs fields are included. For $N_\tau = 4, 8$ the CD transition is first order even in the presence of Φ , though the transition point shifts to lower values of β_g .

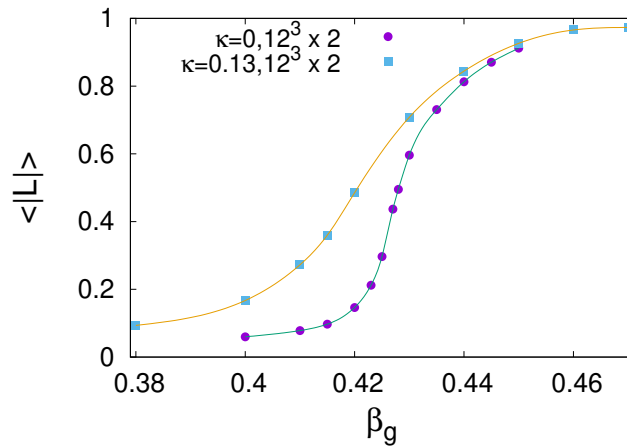


Figure 5.10: The average of the Polyakov loop vs β_g for $N_\tau = 2$.

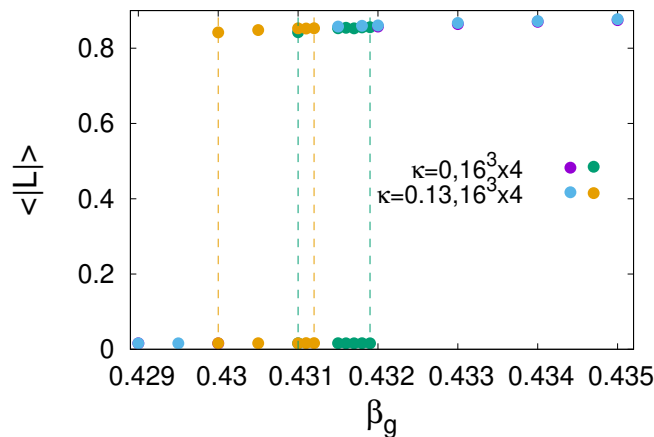


Figure 5.11: The average of the Polyakov loop vs β_g for $N_\tau = 4$.

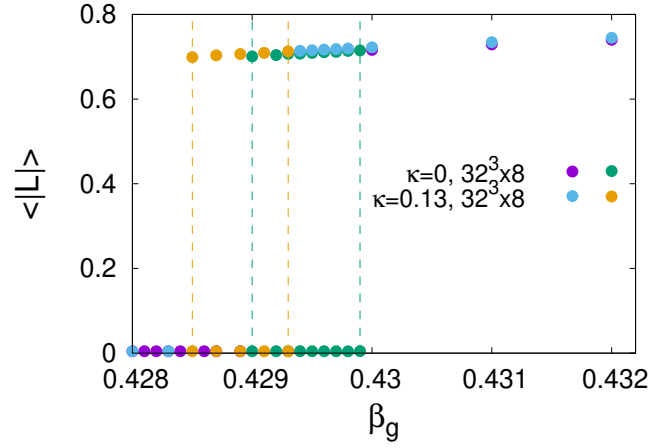


Figure 5.12: The average of the Polyakov loop vs β_g for $N_\tau = 8$.

To check the N_τ dependence of the Z_2 symmetry at $\kappa = .13$, the histograms of the Polyakov loop are computed both in the confined and the deconfined phases for $N_\tau = 2, 3$, and 8. In the deconfined phase, $L < 0$ data is Z_2 rotated and then compared with $L > 0$ data. We plot $H(|L|)$ but present $L > 0$ and $L < 0$ sectors as separate data. The distributions/histograms are shown in Figs. 5.13–5.18. For $N_\tau = 2$ the histograms clearly show there is no Z_2 symmetry. On the deconfinement side, there is no Z_2 symmetry as the two Polyakov loop sectors do not overlap. For $N_\tau = 3$ the two peaks corresponding to the two sectors are approaching each other. For $N_\tau = 8$, the histogram of the Polyakov loop for two Z_2 sectors agrees well with each other, which suggests a small explicit breaking of Z_2 .

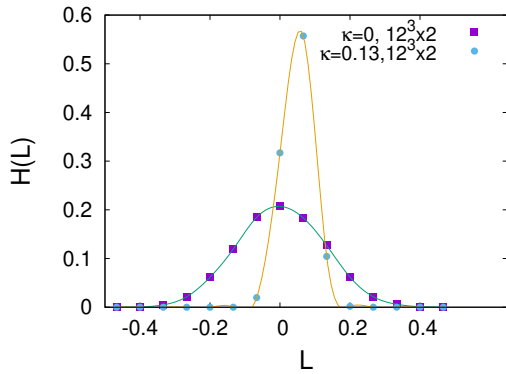


Figure 5.13: Histogram of L in the confined phase.

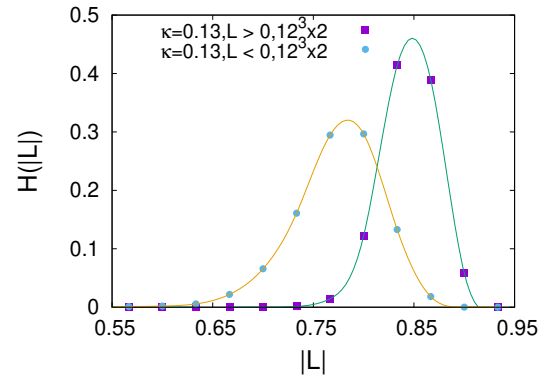


Figure 5.14: Histogram of L in the deconfined phase.

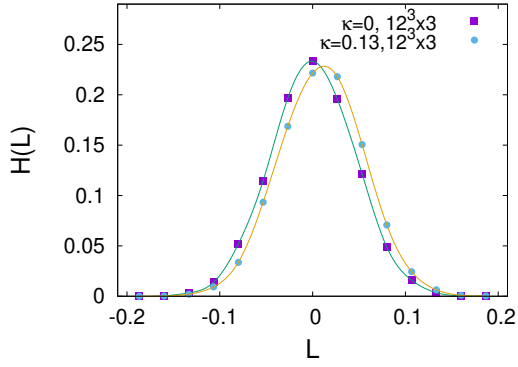


Figure 5.15: Histogram of L in the confined phase.

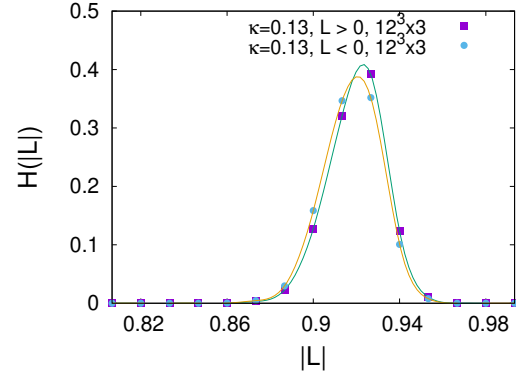


Figure 5.16: Histogram of L in the deconfined phase.

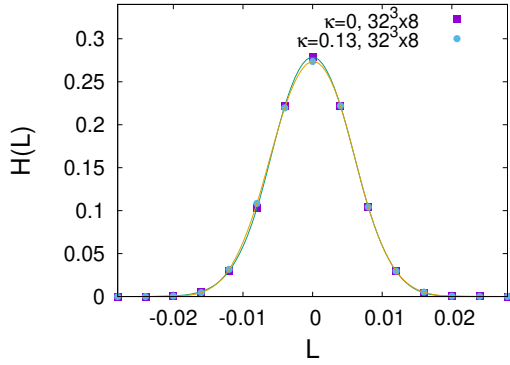


Figure 5.17: Histogram of L in the confined phase.

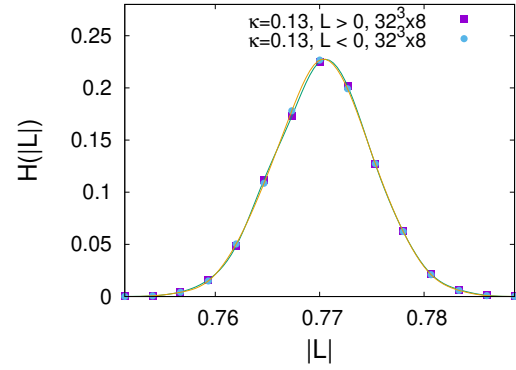


Figure 5.18: Histogram of L in the deconfined phase.

The κ dependence of the Z_2 symmetry is studied by computing the thermal average of the temporal part of the interaction, i.e. $sk_4 = \sum_n \Phi_n U_{n,\hat{4}} \Phi_{n+\hat{4}}^\dagger$ and the corresponding susceptibility χ_{sk_4} . These simulations are carried out in the deconfined phase, as there are two Z_2 states corresponding to each sector of the Polyakov loop. The results for $(\langle sk_4 \rangle, \chi_{sk_4})$ are shown in Figs. 5.19–5.22. The difference in $(\langle sk_4 \rangle, \chi_{sk_4})$ between the two sectors is vanishingly small below, $\kappa = \kappa_s(N_\tau)$. κ_s is found to increase with N_τ . For the largest considered, $N_\tau = 24$, the two sectors agree in $(\langle sk_4 \rangle, \chi_{sk_4})$ up to the Higgs transition point $\kappa = \kappa_c$. When the Higgs transition is first order the Z_2 symmetry is observed for $\kappa > \kappa_c$, in the Higgs symmetric phase. Note that for $\kappa > \kappa_c$ the Higgs symmetric phase is meta-stable.

It is clear from our 3 + 1 dimensional simulations that the Z_2 symmetry is realized in

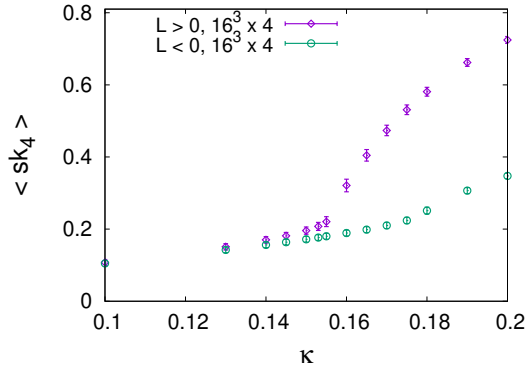


Figure 5.19: sk_4 average vs κ for $\beta_g = 0.435$ on $16^3 \times 4$ lattice.

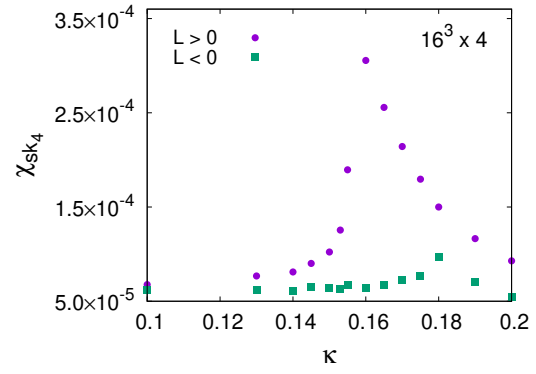


Figure 5.20: sk_4 fluctuation vs κ for $\beta_g = 0.435$ on $16^3 \times 4$ lattice.

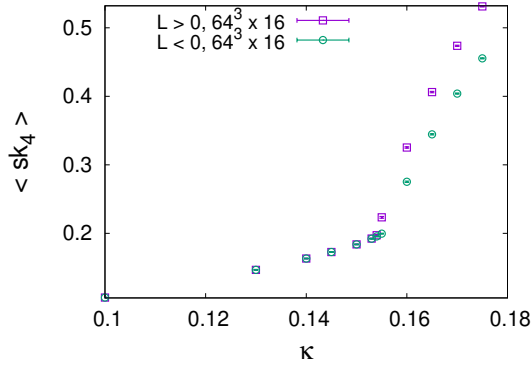


Figure 5.21: sk_4 average vs κ for $\beta_g = 0.435$ on $64^3 \times 16$ lattice.

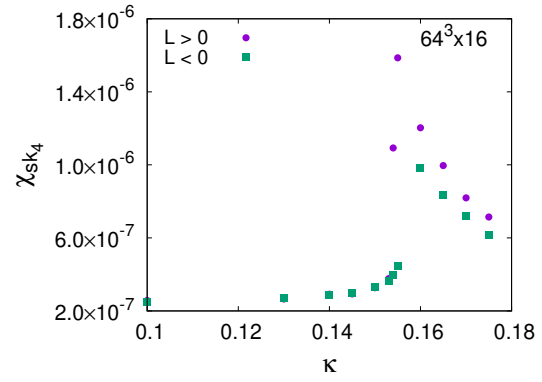


Figure 5.22: sk_4 fluctuation vs κ for $\beta_g = 0.435$ on $64^3 \times 16$ lattice.

the Higgs symmetric phase for large N_τ , i.e. the partition function averages of physical observables exhibit the Z_2 symmetry. For large N_τ , below $\beta_{gc}(N_\tau)$ thermal average of the Polyakov loop $\langle L \rangle = 0$. Note that $\langle L \rangle \propto \text{Exp}(-F/T)$, where F is the free energy between static charges. This suggests that for $\beta_g \leq \beta_{gc}(N_\tau)$ static charges are confined. Previously confinement was observed only in the $\beta_g \rightarrow 0$ limit [9]. It would be interesting to study the confinement aspects of the Z_N symmetry realization in $SU(N)$ gauge theories for larger N_τ .

To understand the realization of Z_2 symmetry in the current theory, we consider a 0 + 1 dimensional model keeping only the temporal component of the interaction term corresponding to a single spatial coordinate in the following section.

5.3 The partition function and density of states in 0 + 1 dimensions

The temporal component of the gauge Higgs interaction corresponding to a particular spatial site can be written as

$$S = -\kappa sk_4, \quad sk_4 = \sum_{n=1}^{N_\tau} \Phi_n U_n \Phi_{n+1}. \quad (5.9)$$

n denotes the temporal lattice site, i.e. $1 \leq n \leq N_\tau$. Φ_n satisfies the periodic boundary condition $\Phi_{N_\tau+1} = \Phi_1$. Since the action will not be invariant if a $z = -1$ gauge transformation is made on U_i 's, the action breaks the Z_2 symmetry explicitly. For this model, the Polyakov loop can take values ± 1 . To see the N_τ dependence of the Z_2 symmetry we calculate the free energy $V(L, N_\tau)$. To simplify the calculations we set $U_i = 1$, for $i = 1, 2, \dots, N_\tau - 1$ and $U_{N_\tau} = L$. All other configurations of U_i corresponding to a given value of L are gauge equivalent. Now the partition function for $L = 1$ is nothing but that of the one-dimensional Ising chain. For $L = -1$ the only difference is that the coupling between Φ_{N_τ} and Φ_1 is anti-ferromagnetic.

The action for $L = +1$ is

$$S(L = 1) = -\kappa (\Phi_1 \Phi_2 + \Phi_2 \Phi_3 + \dots + \Phi_{N_\tau-1} \Phi_{N_\tau} + \Phi_{N_\tau} \Phi_1). \quad (5.10)$$

The corresponding partition function is given by

$$\mathcal{Z}(L = 1) = \sum_{\Phi_1=-1}^{+1} \sum_{\Phi_2=-1}^{+1} \dots \sum_{\Phi_{N_\tau}=-1}^{+1} \text{Exp} \left[\kappa \sum_{i=1}^{N_\tau} \Phi_i \Phi_{i+1} \right]. \quad (5.11)$$

The partition function can be expressed in terms of matrices. This is a product of 2×2 matrices. To see this, let the matrix P be defined such that its matrix elements are given

by

$$\langle \Phi | P | \Phi' \rangle = e^{(\kappa \Phi \Phi')}, \quad (5.12)$$

where Φ and Φ' may independently take on the values ± 1 . Here is a list of all the matrix elements:

$$\begin{aligned} \langle +1 | P | +1 \rangle &= e^\kappa \\ \langle -1 | P | -1 \rangle &= e^\kappa \\ \langle +1 | P | -1 \rangle &= \langle -1 | P | +1 \rangle = e^{-\kappa}. \end{aligned} \quad (5.13)$$

Thus an explicit representation of the transfer matrix P is given by

$$P = \begin{pmatrix} e^\kappa & e^{-\kappa} \\ e^{-\kappa} & e^\kappa \end{pmatrix}.$$

With these definitions, we can write the partition function in the form

$$\begin{aligned} \mathcal{Z}(L=1) &= \sum_{\Phi_1=-1}^{+1} \sum_{\Phi_2=-1}^{+1} \dots \sum_{\Phi_{N_\tau}=-1}^{+1} \langle \Phi_1 | P | \Phi_2 \rangle \langle \Phi_2 | P | \Phi_3 \rangle \dots \langle \Phi_{N_\tau} | P | \Phi_1 \rangle \\ &= \sum_{\Phi_1=-1}^{+1} \langle \Phi_1 | P^{N_\tau} | \Phi_1 \rangle \\ &= \text{Tr } P^{N_\tau} \\ &= \lambda_1^{N_\tau} + \lambda_2^{N_\tau}. \end{aligned} \quad (5.14)$$

The two eigen values of the P matrix are $\lambda_1 = e^\kappa + e^{-\kappa}$ and $\lambda_2 = e^\kappa - e^{-\kappa}$ with $\lambda_1 \geq \lambda_2$.

The free energy corresponding to the partition function is given by

$$\begin{aligned} V(L=1) &= -T \log [\mathcal{Z}(L=1)] \\ &= -T \log (\lambda_1^{N_\tau} + \lambda_2^{N_\tau}) \\ &= -T \log \left\{ \lambda_1^{N_\tau} \left[1 + \left(\frac{\lambda_2}{\lambda_1} \right)^{N_\tau} \right] \right\} \end{aligned}$$

$$= -T \left\{ \log \lambda_1^{N_\tau} + \log \left[1 + \left(\frac{\lambda_2}{\lambda_1} \right)^{N_\tau} \right] \right\}. \quad (5.15)$$

Since the ratio $\frac{\lambda_2}{\lambda_1} < 1$, so at $N_\tau \rightarrow \infty$ limit the free energy becomes

$$V(L = 1) = -TN_\tau \log(\lambda_1). \quad (5.16)$$

The action for $L = -1$ is

$$S(L = -1) = -\kappa(\Phi_1 \Phi_2 + \Phi_2 \Phi_3 + \dots + \Phi_{N_\tau-1} \Phi_{N_\tau} - \Phi_{N_\tau} \Phi_1). \quad (5.17)$$

The corresponding partition function for $L = -1$ turns out to be

$$\mathcal{Z}(L = -1) = \lambda_1^{N_\tau} - \lambda_2^{N_\tau}. \quad (5.18)$$

For each choice of L , the partition function can be calculated exactly, i.e.

$$\mathcal{Z}(L = 1) = \lambda_1^{N_\tau} + \lambda_2^{N_\tau}, \quad \mathcal{Z}(L = -1) = \lambda_1^{N_\tau} - \lambda_2^{N_\tau}. \quad (5.19)$$

The corresponding free energies at large N_τ are given by,

$$V(L = 1) = V(L = -1) = -TN_\tau \log(\lambda_1). \quad (5.20)$$

This results show that there is Z_2 symmetry in $0 + 1$ dimensions in the limit of $N_\tau \rightarrow \infty$.

As noted previously, the restoration of the Z_2 symmetry (vanishingly small explicit breaking) must come from the Z_2 symmetry of the entropy or the DoS. For $L = 1$ the sequence of allowed value of sk_4 is $\{N_\tau, N_\tau - 4, \dots \geq -N_\tau\}$. On the other hand for $L = -1$ the corresponding sequence is $\{N_\tau - 2, N_\tau - 6, \dots \geq 2 - N_\tau\}$.

The DoS or $\rho(sk_4)$ for $N_\tau = 4, 8, 12$ and 16 are shown in Figs. 5.23–5.26. For small N_τ there are clear difference for $L = \pm 1$. The difference persists for the largest as well as smallest values of sk_4 . For even N_τ , $\rho(sk_4) = 2N_\tau!/(N_\tau - q)!q!$ where $q = 0, 2, \dots, N_\tau$ for $L = 1$ and $q = 1, 3, \dots, N_\tau - 1$ for $L = -1$. For odd N_τ , $\rho(sk_4) = 2N_\tau!/(N_\tau - q)!q!$ where $q = 1, 3, \dots, N_\tau$ for $L = 1$ and $q = 0, 2, \dots, N_\tau - 1$ for $L = -1$.

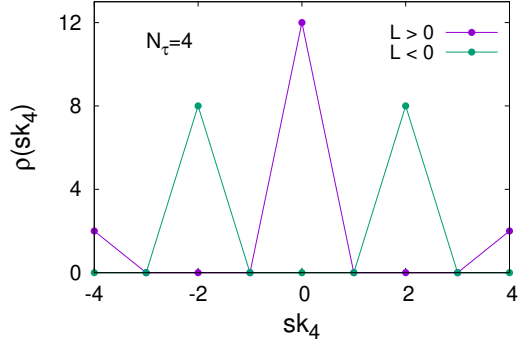


Figure 5.23: $\rho(sk_4)$ for $\kappa = 0$ in 0+1 dimensions.

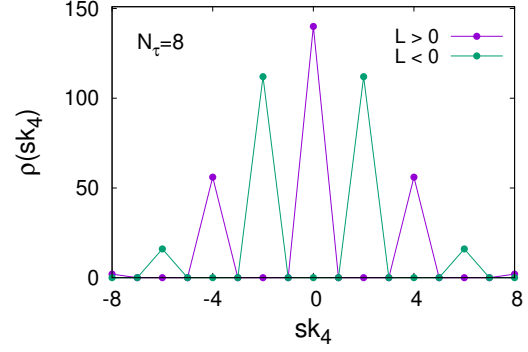


Figure 5.24: $\rho(sk_4)$ for $\kappa = 0$ in 0+1 dimensions.

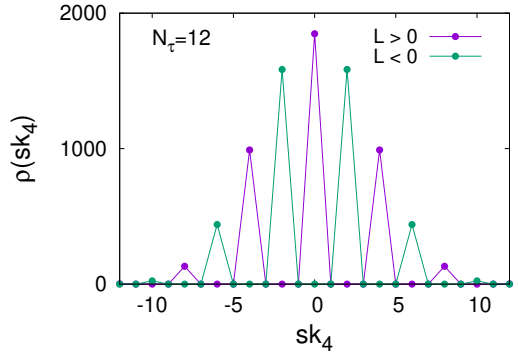


Figure 5.25: $\rho(sk_4)$ for $\kappa = 0$ in 0+1 dimensions.

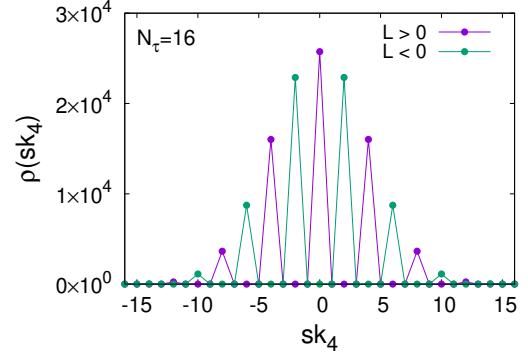


Figure 5.26: $\rho(sk_4)$ for $\kappa = 0$ in 0+1 dimensions.

For large N_τ , $\rho(sk_4)$'s for both $L = \pm 1$ approach a Gaussian centred at $sk_4 = 0$, with $\sqrt{N_\tau}$ as standard deviation. The logarithm of the peak height is given by $\simeq \log N_\tau! - 2\log(N_\tau/2)! + \log 2$ for N_τ even. For $N_\tau = 2n + 1$ the same can be approximated by $\log N_\tau! - \log(n^2 + n) + \log 2$. The thermodynamics in the $N_\tau \rightarrow \infty$ limit will be dominated by peak height and distribution of $\rho(sk_4)$ around the peak, which is Z_2 symmetric, for all finite κ . These results show that the origin of the Z_2 symmetry in Z_2 +Higgs theory is due to the dominance of the DoS. Interestingly this situation is similar to one dimensional

Ising chain where entropy dominates for any nonzero temperature.

In order to take into account the effect of nearest neighbour coupling along the spatial direction we consider 1 + 1 dimensional model with $N_s = 2$ and vary N_τ . In this case the Polyakov loop can take value $L = 0, \pm 2$. The exact calculation of $\rho(sk)$ get increasingly difficult with N_τ . One can however consider generating configurations randomly by giving equal probability for each allowed value of a given variable. The results for the distribution of the total action for $N_\tau = 4$ and $N_\tau = 16$ are shown in Figs. 5.27 and 5.28. As one can see that for higher N_τ , $\rho(sk)$ around the peak (at $sk = 0$) do not depend on L .

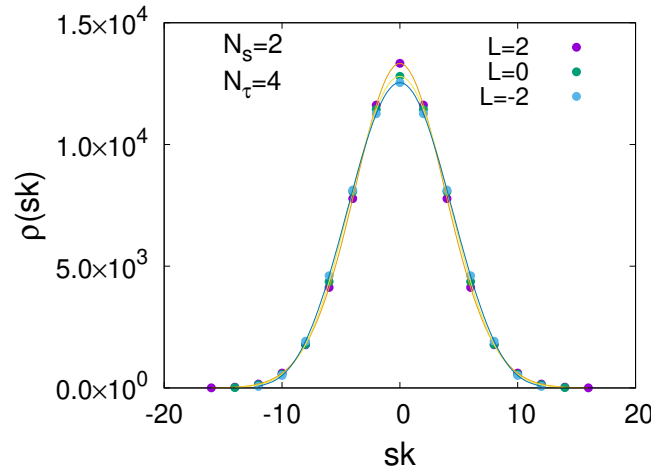


Figure 5.27: $\rho(sk)$ for $\kappa = 0$ in 0+1 dimensions.

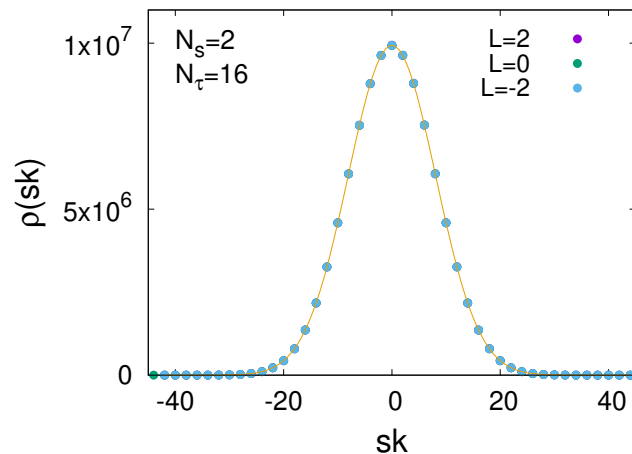


Figure 5.28: $\rho(sk)$ for $\kappa = 0$ in 0+1 dimensions.

To find out how well the $\rho(sk_4)$ describes the Monte Carlo simulations of the four-dimensional

partition function, the thermal average of the distribution function $H(sk_4)$ of sk_4 has been computed. For each configuration, $H(sk_4)$ is given by the number of spatial sites with a given value of sk_4 . Note that the distribution of sk_4 takes into account the Boltzmann factor which shifts the peak of $\rho(sk_4)$ to the right. Fig. 5.29 shows the distribution $H(sk_4)$ for $N_\tau = 4$ at $\kappa = 0.1$ and $\beta_g = 0.435$. The values correspond to the deconfined and Higgs symmetric phase. There is a large difference in $H(sk_4)$ for the two Polyakov loop sectors, i.e. the Z_2 symmetry is broken explicitly. Since $\langle L \rangle \neq 1$, L at the lattice sites can take $+1$ or -1 values. For $\langle L \rangle > 0$ ($\langle L \rangle < 0$), there will a finite fraction of the spatial site, for which $L = -1$ ($L = +1$). Consequently, a plot of $H(sk_4)$ has two envelopes. The lower envelope

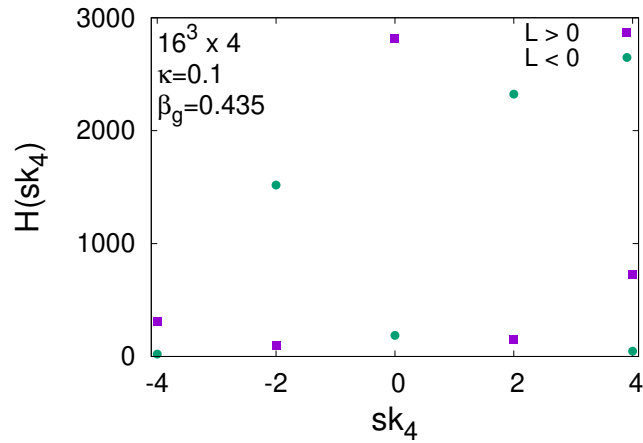


Figure 5.29: $H(sk_4)$ for $\kappa = 0.1$, $\beta_g = 0.435$ for 3 + 1 dimension.

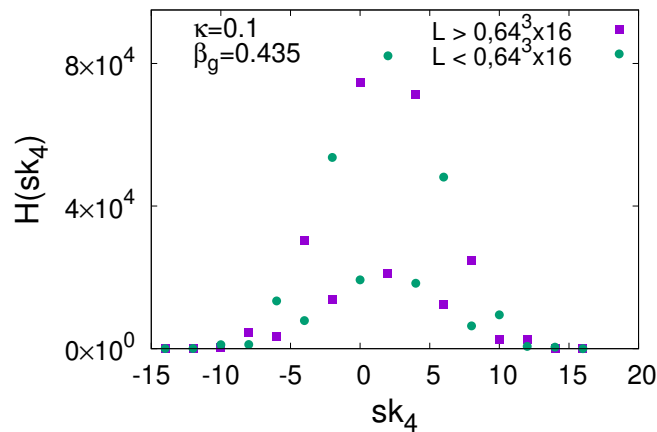


Figure 5.30: $H(sk_4)$ for $\kappa = 0.1$, $\beta_g = 0.435$ for 3 + 1 dimension.

in $H(sk_4)$ corresponds to the smaller fraction of lattice sites with $L = -1$ ($L = +1$) when

$\langle L \rangle > 0$ ($\langle L \rangle < 0$). In Fig. 5.30, for $N_\tau = 16$ the results clearly show that $H(sk_4)$ for both the Polyakov loop sectors can be approximately described by a single function in other words the presence of Z_2 symmetry. The thermal average of the Polyakov loop for the two sectors are found to be $\langle L \rangle = 0.5896 \pm 0.002$ and -0.5897 ± 0.00199 .

In Fig. 5.31, we try to fit the 3 + 1 dimensional simulation result with 0 + 1 dimensional DoS by including an extra Boltzmann factor, i.e. $\exp(\kappa' sk_4)$. The resulting fit agrees very well with $H(sk_4)$. We expect that the 0 + 1 results can describe the 3 + 1 Monte Carlo simulations in most of the phase diagrams except for critical points. Note here, $H(sk_4)$ values from 3 + 1 simulations correspond to $\kappa = 0.1$. However, to fit DoS one needs a $\kappa = 0.106$ which is higher. This is due to the fact that in 3 + 1 dimensions sk_4 at a given spatial point interacts with sk_4 at the nearest neighbor sites. The above results suggest that, the 3+1 dimensional results can be reproduced from 0+1 dimensional results by using $H(sk_4) \propto \rho(sk_4) \exp(\kappa' sk_4)$. Here $H(sk_4)$ is the DoS in 3+1 dimension and $\rho(sk_4)$ is the DoS in 0+1 dimension. Considering a mean-field approximation one can compute the free energy difference between $L = 1$ and $L = -1$ at $\kappa = \kappa'$ for the 3 + 1 dimensional system at $\kappa = 0.1$, which turns out to be 10^{-10} .

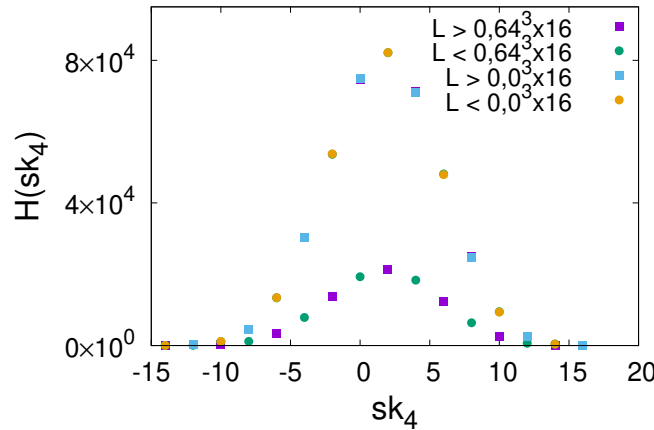


Figure 5.31: $H(sk_4)$ fitted with 0 + 1 density of states with a Boltzmann factor.

Chapter 6

Conclusion

In this thesis, we have studied the Z_N symmetry in $SU(N)$ gauge theories in the presence of matter fields. The matter fields considered here are in the fundamental representation of the $SU(N)$ gauge group. The presence of matter fields leads to the explicit breaking of Z_N symmetry at the level of action. The strength of this explicit breaking depends on the parameters of the theory. The calculation of the explicit symmetry breaking requires that the matter fields are integrated out. This is done using non-perturbative lattice simulations, in the phase diagrams close to the CD transition. In previous numerical studies of $SU(2)$ +Higgs theories in 3+1 dimensions, it was observed that the presence of matter fields breaks the Z_2 symmetry explicitly for small N_τ . The numerical results also suggest that at the large N_τ limit the Z_2 symmetry is restored in the Higgs symmetric phase i.e. the explicit symmetry breaking is vanishingly small in the continuum limit [5]. In this thesis, we have extended that work for $SU(3)$ +Higgs. To understand the effect of Higgs as matter fields we have studied the CD transition and Z_3 symmetry in $SU(3)$ +Higgs theory for a vanishing bare mass and quartic coupling of the Higgs field. The Monte Carlo simulation results show that the nature of the CD transition, as well as the explicit breaking of Z_3 , varies with N_τ . Most of the simulations that have been done are around the CD transition point. For $N_\tau = 2$ the Polyakov loop varies continuously across the transition. However,

determining whether the transition is a crossover or a second order, will require finite-size scaling analysis. The distribution of the Polyakov loop does not exhibit Z_3 symmetry, suggesting large explicit breaking. In comparison, for $N_\tau = 2$, the pure gauge CD transition is first order. This shows that for $N_\tau = 2$, the first order CD transition turns to a continuous in the presence of Higgs. For $N_\tau = 3$, even in the presence of Higgs, the transition is the first order. The distribution of the Polyakov loop near the transition point does have peaks corresponding to all the Z_3 sectors. However, the peak heights are found to be different. This suggests that the explicit breaking is there but small compared to the $N_\tau = 2$ case. The results for $N_\tau = 4$ is similar to $N_\tau = 3$. The distributions of the Polyakov loop show partial Z_3 symmetry, with the difference in the peak height of Z_3 sectors being small compared to $N_\tau = 3$. This pattern that CD transition is first order and monotonic decrease in the explicit breaking continuous for higher N_τ considered in our simulations. To make a quantitative assessment of explicit breaking we compute the difference of the gauge-Higgs interaction as well as that of the pure gauge action. Our results show that the difference in both observables decreases and approaches a vanishingly small value at large N_τ . The vanishing difference in gauge actions in the large N_τ limit will lead to the same free energy for all the Z_3 states. These results suggest that the CD transition is first order and the explicit breaking of Z_3 is vanishingly small in the continuum limit. Perturbative calculations show that deep inside the deconfinement there Z_3 is explicitly breaking. It is possible that the realization of Z_3 is limited to the region close to the transition point. It will be interesting to explore Z_3 for large β_g values and compare them with perturbative results. We have observed that the action does not possess the Z_3 symmetry but the partition function averages turn out to be Z_3 symmetric. We believe that the entropy has the Z_3 symmetry and dominates over the Boltzmann factor in the continuum limit, which leads to the realization of Z_3 symmetry. We mention here that for non-zero Higgs mass, the results will be similar to the present study. In the future, we plan to study the implications of non-zero λ . It is highly desirable to obtain such results through analytic calculations where the partition function exhibits the Z_N symmetry even though the action breaks it

explicitly.

In order to observe this, we have studied the explicit breaking of Z_N symmetry in a model of a one-dimensional gauged chain of bosons and fermions [51]. Here we have tried to do an analytic calculation to obtain the free energy for $SU(N)$ gauge theories in presence of matter fields. The matter fields are integrated out, in the partition function, which results in an analytic form of the Polyakov loop free energy. The action for the gauged chains can be obtained by considering the terms of the corresponding 3 + 1 gauge theories which break the Z_N symmetry explicitly. The same can also be obtained by, the spatial links being set to unity and matter fields uniform in the spatial direction. In this simplification, most of the terms of the original action drop out except for the ones which break the Z_N symmetry. Also, the problem reduces to a collection of a non-interacting, 1-dimensional chain of gauged bosons/fermions making analytical calculations possible. To derive the free energy $V(L)$ for the Polyakov loop L , the partition function is evaluated for a given background of temporal gauge links. The calculations become simple in the gauge where all the temporal links are set to unity except the last one. Subsequently, the matter fields are integrated out sequentially except for the two fields connected to the last gauge link. The integration of the last two fields results in the determinant of a finite-sized matrix for the Higgs case, even for any arbitrary N_τ . For fermions, the integration of the last two fields is simpler. The process of sequential integration leads to well-defined recursion relations and greatly simplifies the calculation of a determinant of a matrix of arbitrary size ($\sim N_\tau N$) by reducing it to size $\sim 2N$. In the Higgs case, the Z_N symmetry is realized in the partition function for $N_\tau \rightarrow \infty$, both at zero and non-zero temperatures. Consequently, the Polyakov loop free energy exhibits the Z_N symmetry. For fermions, the explicit breaking initially decreases rapidly with N_τ . However it approaches a non-zero limiting value for $N_\tau \rightarrow \infty$. The dependence of explicit breaking on N_τ , in these results, can be attributed to the dominance of the density of the states over the action.

To understand the realization of Z_N symmetry we have numerically studied the simple

model of Z_2 +Higgs in both 3+1 and 0+1 dimensions [18]. In the 3+1 dimension, the CD transition is the first order for pure Z_2 gauge theory for $N_\tau \geq 3$. For smaller values of gauge-Higgs interaction coupling (κ), the transition is still first order in nature. It is observed that the Z_2 symmetry is explicitly broken in presence of Higgs fields for small N_τ . The numerical results show that for large N_τ , the Z_2 symmetry is realized in the Higgs symmetric phase within statistical errors. To understand the mechanism of emergence of the Z_2 symmetry a simplified one-dimensional model of Z_2 +Higgs is considered by keeping only the temporal interaction terms at a given spatial site. The partition function and the corresponding free energy for each of the two Polyakov loop sectors are exactly calculated. It is shown that the free energy difference between the two Polyakov loop sectors vanishes in the large N_τ limit, which leads to Z_2 symmetry purely due to the dominance of entropy. The DoS for finite N_τ is calculated, where the asymmetry between the different Polyakov loop sectors rapidly decreases with N_τ . So the DoS dominate the thermodynamics at the large N_τ limit resulting in the realization of Z_2 (or in general Z_N) symmetry. The effect of nearest neighbor interaction along the spatial directions in a simple model shows the persistence of Z_2 symmetry in the DoS. Further, it is shown that the 3+1 Monte Carlo simulations can be reproduced using the DoS of the one-dimensional model after including a simple Boltzmann factor. For a better understanding of the effects of Z_2 or Z_N realization on the confinement, the interaction between static charges needs to be studied in $SU(N)$ gauge theories in view of the results reported in this thesis, which we plan to do in the future. The realization of Z_N symmetry due to the dominance of DoS, its effect on the CD transition, and the Z_N states in the deconfined phase will play an important role in the study of the early Universe. Our results suggest that for a better understanding of Z_N symmetry and related physical phenomena in $SU(N)$ gauge theory of fermion, near the CD transition requires non-perturbative simulations with smaller lattice cut-off than the results that are presently available.

Bibliography

- [1] N. Weiss, “The Effective Potential for the Order Parameter of Gauge Theories at Finite Temperature,” *Phys. Rev. D* **24** (1981) 475.
- [2] B. Svetitsky and L. G. Yaffe, “Critical Behavior at Finite Temperature Confinement Transitions,” *Nucl. Phys. B* **210** (1982) 423–447.
- [3] N. Weiss, “The Wilson Line in Finite Temperature Gauge Theories,” *Phys. Rev. D* **25** (1982) 2667.
- [4] M. Biswal, S. Digal, and P. S. Saumia, “Dynamical Restoration of Z_N Symmetry in $SU(N)$ + Higgs Theories,” *Nucl. Phys. B* **910** (2016) 30–39, [arXiv:1511.08295 \[hep-lat\]](#).
- [5] M. Biswal, M. Deka, S. Digal, and P. S. Saumia, “Confinement-deconfinement transition in $SU(2)$ Higgs theory,” *Phys. Rev. D* **96** no. 1, (2017) 014503, [arXiv:1610.08265 \[hep-lat\]](#).
- [6] Y. Guo and Q. Du, “Two-loop perturbative corrections to the constrained effective potential in thermal QCD,” *JHEP* **05** (2019) 042, [arXiv:1810.13090 \[hep-ph\]](#).
- [7] U. M. Heller and F. Karsch, “Finite Temperature $SU(2)$ Lattice Gauge Theory With Dynamical Fermions,” *Nucl. Phys. B* **258** (1985) 29–45.
- [8] M. Creutz, “Phase Diagrams for Coupled Spin Gauge Systems,” *Phys. Rev. D* **21** (1980) 1006.

- [9] E. H. Fradkin and S. H. Shenker, “Phase Diagrams of Lattice Gauge Theories with Higgs Fields,” *Phys. Rev. D* **19** (1979) 3682–3697.
- [10] N. Cabibbo and E. Marinari, “A New Method for Updating SU(N) Matrices in Computer Simulations of Gauge Theories,” *Phys. Lett. B* **119** (1982) 387–390.
- [11] A. D. Kennedy and B. J. Pendleton, “Improved Heat Bath Method for Monte Carlo Calculations in Lattice Gauge Theories,” *Phys. Lett. B* **156** (1985) 393–399.
- [12] G. W. Kilcup and S. R. Sharpe, “A Tool Kit for Staggered Fermions,” *Nucl. Phys. B* **283** (1987) 493–550.
- [13] H. Kluberg-Stern, A. Morel, O. Napoly, and B. Petersson, “Flavors of Lagrangian Susskind Fermions,” *Nucl. Phys. B* **220** (1983) 447–470.
- [14] L. Susskind, “Lattice Fermions,” *Phys. Rev. D* **16** (1977) 3031–3039.
- [15] W. K. Hastings, “Monte Carlo Sampling Methods Using Markov Chains and Their Applications,” *Biometrika* **57** (1970) 97–109.
- [16] G. A. Jongeward and J. D. Stack, “MONTE CARLO CALCULATIONS ON Z(2) GAUGE - HIGGS THEORIES,” *Phys. Rev. D* **21** (1980) 3360.
- [17] M. Creutz, L. Jacobs, and C. Rebbi, “Monte Carlo Computations in Lattice Gauge Theories,” *Phys. Rept.* **95** (1983) 201–282.
- [18] M. Biswal, S. Digal, V. Mamale, and S. Shaikh, “Confinement-deconfinement transition and Z2 symmetry in Z2+Higgs theory,” *Mod. Phys. Lett. A* **36** no. 30, (2021) 2150218, [arXiv:2102.11091](https://arxiv.org/abs/2102.11091) [hep-lat].
- [19] S. Sarkar, H. Satz, and B. Sinha, eds., *The physics of the quark-gluon plasma*, vol. 785. 2010.
- [20] H. Satz, “The Quark-Gluon Plasma: A Short Introduction,” *Nucl. Phys. A* **862-863** (2011) 4–12, [arXiv:1101.3937](https://arxiv.org/abs/1101.3937) [hep-ph].

- [21] H. Bohr and H. B. Nielsen, “Hadron Production from a Boiling Quark Soup,” *Nucl. Phys. B* **128** (1977) 275–293.
- [22] R. Hagedorn, “Statistical thermodynamics of strong interactions at high-energies,” *Nuovo Cim. Suppl.* **3** (1965) 147–186.
- [23] U. M. Heller, “Deconfinement in SU(2) Gauge Theory With Fermions of Intermediate Mass,” *Phys. Lett. B* **163** (1985) 203–206.
- [24] J. B. Kogut, J. Polonyi, H. W. Wyld, and D. K. Sinclair, “Thermodynamics of SU(2) Gauge Theory With Dynamical Light Fermions,” *Phys. Rev. D* **31** (1985) 3307.
- [25] J. B. Kogut, J. Polonyi, H. W. Wyld, and D. K. Sinclair, “On the Thermodynamics and Scaling Behavior of SU(2) Gauge Theory With Fermion Feedback,” *Nucl. Phys. B* **265** (1986) 293–302.
- [26] O. Philipsen, “The QCD equation of state from the lattice,” *Prog. Part. Nucl. Phys.* **70** (2013) 55–107, [arXiv:1207.5999 \[hep-lat\]](#).
- [27] R. Gupta, “Equation of State from Lattice QCD Calculations,” *Nucl. Phys. A* **862-863** (2011) 111–117, [arXiv:1104.0267 \[hep-lat\]](#).
- [28] S. Sharma, “QCD Thermodynamics on the Lattice,” *Adv. High Energy Phys.* **2013** (2013) 452978, [arXiv:1403.2102 \[hep-lat\]](#).
- [29] P. H. Damgaard and U. M. Heller, “The Fundamental SU(2) Higgs Model at Finite Temperature,” *Nucl. Phys. B* **294** (1987) 253.
- [30] M. E. Shaposhnikov, “On nonperturbative effects at the high temperature electroweak phase transition,” *Phys. Lett. B* **316** (1993) 112–120, [arXiv:hep-ph/9306296](#).
- [31] J. Greensite and K. Matsuyama, “Symmetry, Confinement, and the Higgs Phase,” *Symmetry* **14** no. 1, (2022) 177, [arXiv:2112.06421 \[hep-lat\]](#).

- [32] L. D. McLerran and B. Svetitsky, “Quark Liberation at High Temperature: A Monte Carlo Study of SU(2) Gauge Theory,” *Phys. Rev. D* **24** (1981) 450.
- [33] L. D. McLerran and B. Svetitsky, “A Monte Carlo Study of SU(2) Yang-Mills Theory at Finite Temperature,” *Phys. Lett. B* **98** (1981) 195.
- [34] L. G. Yaffe and B. Svetitsky, “First Order Phase Transition in the SU(3) Gauge Theory at Finite Temperature,” *Phys. Rev. D* **26** (1982) 963.
- [35] T. Celik, J. Engels, and H. Satz, “The Order of the Deconfinement Transition in SU(3) Yang-Mills Theory,” *Phys. Lett. B* **125** (1983) 411–414.
- [36] B. Svetitsky, “Symmetry Aspects of Finite Temperature Confinement Transitions,” *Phys. Rept.* **132** (1986) 1–53.
- [37] D. J. Gross, R. D. Pisarski, and L. G. Yaffe, “QCD and Instantons at Finite Temperature,” *Rev. Mod. Phys.* **53** (1981) 43.
- [38] A. P. Balachandran and S. Dital, “Topological string defect formation during the chiral phase transition,” *Int. J. Mod. Phys. A* **17** (2002) 1149–1158, [arXiv:hep-ph/0108086](https://arxiv.org/abs/hep-ph/0108086).
- [39] U. S. Gupta, R. K. Mohapatra, A. M. Srivastava, and V. K. Tiwari, “Simulation of Z(3) walls and string production via bubble nucleation in a quark-hadron transition,” *Phys. Rev. D* **82** (2010) 074020, [arXiv:1007.5001](https://arxiv.org/abs/1007.5001) [hep-ph].
- [40] J. Ignatius, K. Kajantie, and K. Rummukainen, “Cosmological QCD Z(3) phase transition in the 10-TeV temperature range?,” *Phys. Rev. Lett.* **68** (1992) 737–740.
- [41] J. Kuti, J. Polonyi, and K. Szlachanyi, “Monte Carlo Study of SU(2) Gauge Theory at Finite Temperature,” *Phys. Lett. B* **98** (1981) 199.
- [42] F. Green and F. Karsch, “Mean Field Analysis of SU(N) Deconfining Transitions in the Presence of Dynamical Quarks,” *Nucl. Phys. B* **238** (1984) 297–306.

- [43] V. M. Belyaev, I. I. Kogan, G. W. Semenoff, and N. Weiss, “Z(N) domains in gauge theories with fermions at high temperature,” *Phys. Lett. B* **277** (1992) 331–336.
- [44] F. Karsch, E. Laermann, A. Peikert, C. Schmidt, and S. Stickan, “Flavor and quark mass dependence of QCD thermodynamics,” *Nucl. Phys. B Proc. Suppl.* **94** (2001) 411–414, [arXiv:hep-lat/0010040](#).
- [45] V. Dixit and M. C. Ogilvie, “Metastability in SU(N) gauge theories at high temperatures,” *Phys. Lett. B* **269** (1991) 353–356.
- [46] M. Deka, S. Digal, and A. P. Mishra, “Meta-stable States in Quark-Gluon Plasma,” *Phys. Rev. D* **85** (2012) 114505, [arXiv:1009.0739 \[hep-lat\]](#).
- [47] M. Biswal, S. Digal, and P. S. Saumia, “Z₃ metastable states in PNJL model,” *Phys. Rev. D* **102** no. 7, (2020) 074020, [arXiv:1907.07981 \[hep-ph\]](#).
- [48] M. Biswal, *Z_N Symmetry and confinement-deconfinement transition in SU(N)+ Higgs theory*. PhD thesis, IMSc, Chennai, 2018.
- [49] H. Satz, “Universal Deconfinement in SU(2) Gauge Theory With Dynamical Quarks,” *Phys. Lett. B* **157** (1985) 65–69.
- [50] P. H. Damgaard and U. M. Heller, “Deconfinement in the Fundamental SU(2) Higgs Model,” *Phys. Lett. B* **171** (1986) 442–448.
- [51] M. Biswal, S. Digal, V. Mamale, and S. Shaikh, “Z_N symmetry in SU(N) gauge theories,” *Int. J. Mod. Phys. A* **37** no. 09, (2022) 2250047, [arXiv:2102.12935 \[hep-lat\]](#).
- [52] A. D. Boozer, “Quantum field theory in (0 + 1) dimensions,” *Eur. J. Phys.* **28** (2007) 729–745.
- [53] J. Bloch, F. Bruckmann, and T. Wettig, “Subset method for one-dimensional QCD,” *JHEP* **10** (2013) 140, [arXiv:1307.1416 \[hep-lat\]](#).

- [54] G. W. Semenoff and N. Weiss, “Symmetry and observables in induced QCD,” in *11th International Hutsulian Workshop on Group Theoretical Methods in Physics*, pp. 215–238. 10, 1992. [arXiv:hep-th/9303056](#).
- [55] J. Pawłowski and A. Rothkopf, “Thermal dynamics on the lattice with exponentially improved accuracy,” *Phys. Lett. B* **778** (2018) 221–226, [arXiv:1610.09531 \[hep-lat\]](#).
- [56] G. V. Dunne, K.-M. Lee, and C.-h. Lu, “On the finite temperature Chern-Simons coefficient,” *Phys. Rev. Lett.* **78** (1997) 3434–3437, [arXiv:hep-th/9612194](#).
- [57] R. Balian, J. M. Drouffe, and C. Itzykson, “Gauge Fields on a Lattice. 1. General Outlook,” *Phys. Rev. D* **10** (1974) 3376.
- [58] R. Balian, J. M. Drouffe, and C. Itzykson, “Gauge Fields on a Lattice. 3. Strong Coupling Expansions and Transition Points,” *Phys. Rev. D* **11** (1975) 2104. [Erratum: *Phys.Rev.D* 19, 2514 (1979)].
- [59] D. J. E. Callaway and L. J. Carson, “The Abelian Higgs Model: A Monte Carlo Study,” *Phys. Rev. D* **25** (1982) 531–537.
- [60] G. Bhanot and B. A. Freedman, “Finite Size Scaling for the Three-dimensional Abelian Higgs Model,” *Nucl. Phys. B* **190** (1981) 357–364.
- [61] G. Bhanot and M. Creutz, “Ising gauge theory at negative temperatures and spin-glasses,” *Phys. Rev. B* **22** (Oct, 1980) 3370–3373. <https://link.aps.org/doi/10.1103/PhysRevB.22.3370>.
- [62] M. Caselle and M. Hasenbusch, “Deconfinement transition and dimensional crossover in the 3-D gauge Ising model,” *Nucl. Phys. B* **470** (1996) 435–453, [arXiv:hep-lat/9511015](#).

- [63] S. Datta and R. V. Gavai, “Phase diagram of SO(3) lattice gauge theory at finite temperature,” *Nucl. Phys. B Proc. Suppl.* **63** (1998) 451–453, [arXiv:hep-lat/9708016](#).
- [64] A. M. Polyakov, “Thermal Properties of Gauge Fields and Quark Liberation,” *Phys. Lett. B* **72** (1978) 477–480.
- [65] L. Susskind, “Lattice Models of Quark Confinement at High Temperature,” *Phys. Rev. D* **20** (1979) 2610–2618.
- [66] K. Kajantie, M. Laine, K. Rummukainen, and M. E. Shaposhnikov, “The Electroweak phase transition: A Nonperturbative analysis,” *Nucl. Phys. B* **466** (1996) 189–258, [arXiv:hep-lat/9510020](#).
- [67] M. Creutz, “Monte Carlo Study of Quantized SU(2) Gauge Theory,” *Phys. Rev. D* **21** (1980) 2308–2315.
- [68] W. Schroers, “Advanced algorithms for the simulation of gauge theories with dynamical fermionic degrees of freedom,” other thesis, 11, 2001.
- [69] B. Bunk, “Monte Carlo methods and results for the electro-weak phase transition,” *Nucl. Phys. B Proc. Suppl.* **42** (1995) 566–568.
- [70] F. Karsch, E. Laermann, and C. Schmidt, “The Chiral critical point in three-flavor QCD,” *Phys. Lett. B* **520** (2001) 41–49, [arXiv:hep-lat/0107020](#).
- [71] R. V. Gavai and F. Karsch, “The SU(3) Phase Transitions in the Presence of Light Dynamical Quarks,” *Nucl. Phys. B* **261** (1985) 273–284.
- [72] Y. Iwasaki, K. Kanaya, T. Yoshie, T. Hoshino, T. Shirakawa, Y. Oyanagi, S. Ichii, and T. Kawai, “Deconfining transition of SU(3) gauge theory on $N(t) = 4$ and 6 lattices,” *Phys. Rev. Lett.* **67** (1991) 3343–3346.
- [73] A. D. Kennedy, J. Kuti, S. Meyer, and B. J. Pendleton, “Where Is the Continuum in Lattice Quantum Chromodynamics?,” *Phys. Rev. Lett.* **54** (1985) 87.

- [74] S. A. Gottlieb, J. Kuti, D. Toussaint, A. D. Kennedy, S. Meyer, B. J. Pendleton, and R. L. Sugar, “The Deconfining Phase Transition and the Continuum Limit of Lattice Quantum Chromodynamics,” *Phys. Rev. Lett.* **55** (1985) 1958.
- [75] M. Fukugita, T. Kaneko, and A. Ukawa, “Correlation Function of the Polyakov String in SU(3) Lattice Gauge Theory at Finite Temperatures,” *Phys. Lett. B* **154** (1985) 185–189.
- [76] R. Falcone, R. Fiore, M. Gravina, and A. Papa, “Screening masses in the SU(3) pure gauge theory and universality,” *Nucl. Phys. B* **785** (2007) 19–33, [arXiv:0704.3882 \[hep-lat\]](https://arxiv.org/abs/0704.3882).
- [77] J. B. Kogut, H. Matsuoka, M. Stone, H. W. Wyld, S. H. Shenker, J. Shigemitsu, and D. K. Sinclair, “Quark and Gluon Latent Heats at the Deconfinement Phase Transition in SU(3) Gauge Theory,” *Phys. Rev. Lett.* **51** (1983) 869.
- [78] O. Kaczmarek, F. Karsch, E. Laermann, and M. Lutgemeier, “Heavy quark potentials in quenched QCD at high temperature,” *Phys. Rev. D* **62** (2000) 034021, [arXiv:hep-lat/9908010](https://arxiv.org/abs/hep-lat/9908010).
- [79] F. R. Brown, N. H. Christ, Y. F. Deng, M. S. Gao, and T. J. Woch, “Nature of the Deconfining Phase Transition in SU(3) Lattice Gauge Theory,” *Phys. Rev. Lett.* **61** (1988) 2058.
- [80] P. Hasenfratz, F. Karsch, and I. O. Stamatescu, “The SU(3) Deconfinement Phase Transition in the Presence of Quarks,” *Phys. Lett. B* **133** (1983) 221–226.
- [81] J. B. Kogut, M. Stone, H. W. Wyld, W. R. Gibbs, J. Shigemitsu, S. H. Shenker, and D. K. Sinclair, “Deconfinement and Chiral Symmetry Restoration at Finite Temperatures in SU(2) and SU(3) Gauge Theories,” *Phys. Rev. Lett.* **50** (1983) 393.

- [82] M. Fukugita and A. Ukawa, “Deconfining and Chiral Transitions of Finite Temperature Quantum Chromodynamics in the Presence of Dynamical Quark Loops,” *Phys. Rev. Lett.* **57** (1986) 503.
- [83] M. Creutz, L. Jacobs, and C. Rebbi, “Experiments with a Gauge Invariant Ising System,” *Phys. Rev. Lett.* **42** (1979) 1390.
- [84] J. Engels, F. Karsch, and H. Satz, “Finite Size Effects in Euclidean Lattice Thermodynamics for Noninteracting Bose and Fermi Systems,” *Nucl. Phys. B* **205** (1982) 239–252.